Università Politecnica delle Marche
Scuola di Dottorato di Ricerca in Scienze dell'Ingegneria
Curriculum in Ingegneria Civile, Ambientale, Edile e Architettura

---

Behavioural-based resilient solutions for a safer built environment in a seismic emergency

Ph.D. Dissertation of:

Michele Lucesoli

Advisor:

Prof. Enrico Quagliarini

Curriculum supervisor:

Prof. Francesco Fatone

XIX edition - new series

Università Politecnica delle Marche
Scuola di Dottorato di Ricerca in Scienze dell'Ingegneria
Curriculum in Ingegneria Civile, Ambientale, Edile e Architettura

---

Behavioural-based resilient solutions for a safer built environment in a seismic emergency

Ph.D. Dissertation of:

Michele Lucesoli

Advisor:

Prof. Enrico Quagliarini

Curriculum supervisor:

Prof. Francesco Fatone

XIX edition - new series

Università Politecnica delle Marche
Dipartimento di Ingegneria Civile, Edile e Architettura (DICEA)
Via Brecce Bianche — 60131 - Ancona, Italy

Fate presto

Acknowledgements

Fate presto - "Harry up to save those who are still alive, to help those who no longer have anything", was the title, in capital letters, three days after the earthquake of November 23, 1980, that shook the Irpinia in the south of Italy. Exactly forty years ago. The delay and the inadequate coordination of rescuers have contributed to produce thousands of dead in a torn land. This work is completely aimed at avoiding a similar situation in the future. The days immediately after the 2016 Central Italy earthquake (that produce 299 victims by striking Amatrice and other small villages also in my native region), I have started my master degree thesis with Professor Enrico Quagliarini who I would like to say thank you for having introduced me to the world of the research. Following his work, I have started the Ph.D. having also the opportunity to know all the team of our department to which I owe a lot. Especially, I would like to say thank you to my colleagues: Gabriele for his professional suggestions as my direct supervisor, and to Benedetta with who I have shared all the moments of this growth path. Apart from the university, I would also like to address my sincere thanks to my family, especially to my sister, and to Elisa that has always supported me and having faith in what I am doing.

Ancona, December 2020

Michele Lucesoli

Abstract

Guaranteeing the safety of populations within the built environment constitutes an essential aspect for the engineers. However, populations are more exposed to sudden-onset natural disasters if they are in the built environment, where they live, work, and gather. Among natural disasters, earthquake is one of the most hazardous due to the visible induced effects on the surroundings. Due to the impossibility to predict those events, the emergency planning before the disaster and its management in the aftermath embodies the preventive aspects on which this research is focused. Nowadays, risk-mitigating solutions were widely implemented by Civil Defence Bodies of different countries. However, the adopted strategies (e.g.: guiding people towards safe areas, provide them the first aid, improving buildings' strength) can result incoherent with the real emergency that may occur. Predicting environmental modifications (e.g.: damages) and human reactions (e.g.: evacuation choices) to such stimuli could allow intervening incisively on citizens' safety levels. The present thesis delineates a methodological framework able to collect, assess, and predict the effects of all the risk-influencing factors. Speditive methodologies for scenario creation are developed to derive data at the urban scale without consuming excessive resources and time. In this way, the built environment's physical vulnerabilities and human exposure-related factors are evaluated and simulated. Finally, a resilient metric to interpret the collected data is obtained to having knowledge of urban centre criticalities that could impede inhabitants' evacuation and, at the same time the rescue teams' intervention. On such basis, effective risk-reduction solutions are tested on a post-intervention scenario by iterating again the outlined process. The elaborated workflow can support public administrations in emergency plans redaction. Meanwhile, the collecting data process (where the adopted methodologies can be replaced) can be employed in simulation-based activities aimed at scenarios prediction. Although this study takes widely into account the human-based approach, future works should perform additional analysis investigating how a human being can be directly influenced by the introduced risk reduction solutions (e.g.: wayfinding signs presence, shaped obstacles to avoid congestions, rescuers intervention) in simulation environments.

Contents

List of figures

List of tables

Nomenclature

Symbol	Measure	Description
BE	-	Built Environment
R	-	Seismic risk, related to the number of people killed or injured, the damage to property and the impact on economic activity due to the occurrence of the disastrous event
V	-	Seismic vulnerability, related to the "weakness" of the element
H	-	Seismic hazard, related to the possibility of future seismic actions
E	-	Seismic exposure, related to the presence and the "value" of buildings and other objects and the possible consequences on human life
M_W	-	Earthquake moment magnitude
μ_D	-	Mean damage grade
I	-	Macroseismic intensity
Q	-	Ductility factor
$V_{L,Agg}; V_{F,Agg}$	-	Vulnerability indexes for aggregates (Agg) evaluated according to Equation 13 involving respectively the structural units vulnerability indexes from Lagomarsino and Giovinazzi 2006 and Ferreira Vicente Varum 2010
$V_{L,SU}; V_{F,SU}$	-	Vulnerability indexes for structural units (SU) evaluated respectively through Lagomarsino and Giovinazzi 2006 and Ferreira Vicente Varum 2010
$Area_{SU}$	m^2	Planar area of the structural unit (at ground level)
$Area_{Agg}$	m^2	Planar area of the aggregate (at ground level)
Vol_{SU}	m^3	The volume of the structural unit
Vol_{Agg}	m^3	The volume of the aggregate
$V_{L,Agg,Max}$	-	Aggregates vulnerability index evaluated through the higher vulnerability of structural units composing the aggregate
$V_{L,Agg,Ave}$	-	Aggregates vulnerability index evaluated through the average vulnerability of structural units composing the aggregate
$V_{L,Agg,Area}$	-	Aggregates vulnerability index evaluated according to Equation 10
$V_{L,Agg,Vol}$	-	Aggregates vulnerability index evaluated according to Equation 11

$\Delta_{A/V}$	(%)	Percent differences between $Area_{SU}/Area_{Agg}$ and Vol_{SU}/Vol_{Agg} ratios
d	-	Coefficient to increase vulnerability assessing different masonry typologies within the aggregate
q	-	Coefficient to increase vulnerability assessing the overall number of structural units that compose the aggregate
v_p	-	Single parameter vulnerability contribution of SISMA method by Mazzotti 2008
w_s	-	Assigned weight to each vulnerability parameter in SISMA method by Mazzotti 2008
V_s	-	Aggregates vulnerability index of SISMA method by Mazzotti 2008
R^2	-	Linear regression coefficient
ρ	-	Pearson correlation coefficient
MRL	-	Main regression line
$MIRF_{max}$	-	Monotonic increasing regression function on maximum values
$MIRF_{min}$	-	Monotonic increasing regression function on minimum values
a_g	m/s^2	Peak ground acceleration (PGA)
$I_{R,j}$	-	Street network Risk index for j-link
$I_{Rn,j}$	-	Normalized street network Risk index for j-link
Wi_k	-	Weigh related to the i-th parameter
Wc_k	-	Weigh related to the k-th factor
Sp_{ik}	-	Value conferred to the i-th parameter of the k-th factor
Sp_{ik}^{max}	-	Maximum attributable value to the i-th parameter of the k-th factor
V_b	-	Seismic vulnerability index of the considered building through the macroseismic method
b	-	Incidence of the building in the link, as the ratio between building and link lengths
L_b	m	Building length
$V_{link,j}$	-	Seismic vulnerability of the j-link
$V_{Nlink,j}$	-	Normalized seismic vulnerability of the j-link
RDS	-	Road Damage Scale [1]
Average Flow	Veic./h	Number of vehicles that travel across a section per unit time
L	m	Link length from node to node
L_{max}	m	Maximum link length in the analysed sample
W	m	Link width in terms of carriageway average extension
W_{max}	m	Maximum Link width in the analysed sample

A	m^2	Area of evaluated Square
A_{max}	m^2	The maximum Square area in the analysed sample
h	m	Mean building height
QX	[%]	Generated debris percentage outside a building
b	-	Stand for the considered building
W_b	m	Refers to the mean street width facing the building *b*
d_{ruins}	m	Evaluated effective debris depth on street
QX_1	[%]	Generated debris percentage outside a building according to the *debris estimation criterion 1*
V^*_1	-	Buildings vulnerability index modified employed in *debris estimation criterion 1*
V_{FP}	-	Buildings vulnerability index according to [2]
M_{ev}	-	Earthquake moment magnitude to assume as input
$M_{ev,max}$	-	Earthquake maximum moment magnitude expected in the studied region
QX_2	[%]	Generated debris percentage outside a building according to the *debris estimation criterion 2*
V^*_2	-	Buildings vulnerability index modified employed in *debris estimation criterion 1*
V_{GL}	-	Buildings vulnerability index according to [3]
B_{link}	-	It is the acronym for indicating the index proposed by [4]
$k95$	-	95th percentile of the cumulative distribution function of mean damage grades according to [3]
Mw	-	The registered moment magnitude of the Central Italy seismic event in 2016
I^*_{vf}	-	Façade walls vulnerability index (Tiago M. Ferreira, Vicente, and Varum 2014)
I_{vf}	-	Normalized façade walls vulnerability index
C_{vi}	-	The assigned score for each class for façade walls vulnerability index estimation
p_{vi}	-	An assigned weighting factor to vulnerability influencing parameters for façade walls vulnerability index estimation
i	-	Incidence of the building in the link, as the ratio between building and link lengths
EPES	-	Earthquake Pedestrians' Evacuation Simulator [6]
AA	-	Assembly Areas
SAA	-	Spontaneous Assembly Areas
I_{EMS-98}	-	Earthquake intensity according to the European Macroseismic Scale [7]
S_{AA}	-	Safety levels evaluation of Assembly Areas

$J_{p,s}$	-	Describes the percentage of pedestrians joining the considered assembly area
T	-	Pedestrians' difference-in-path ratio (the indicator of the link tortuosity)
$S_{link,AA}$	-	Safety level referred to a link arriving in a AA
O_{link}	-	Link occupancy index which includes pedestrian's area and ruins presence
A_{ruins}	m^2	Link area occupied by ruins and debris presence
$N_{av,link}$	-	The average number of pedestrians using the path
$\%\sigma_{N,sim}$	-	Correction factor on pedestrian's link usage
$dA_{ped,E-F}$	m^2	Average moving pedestrian's area (fixed at 1 m^2)
W_{link}	m	The average width of the link
L_{link}	m	The total length of the link
F_{link}	-	Interference between the evacuating pedestrians evaluating through the normalized flow along the link
LOS	$m^2/person$	Level of Service
A_{eff}	m^2	Link effective area removing the inaccessible area and the area occupied by ruins
N_p	-	Number of gathered pedestrians in a AA
$S_{area,SAA}$		The intrinsic safety level of a spontaneous assembly area
$A_{eff,SAA}$	m^2	The effective area of spontaneous assembly area removing the inaccessible area and the area occupied by ruins
W_{SAA}	m	Width of the SAA from one side to another
$W_{center,b}$	m	Distance from the geometrical SAA centre and the interfering building side
$d_{ruins,b}$	m	The average depth of ruins along the link
$N_{av,SAA}$	-	Average simulated number of pedestrians in SAA
n_{exits}	-	The number of possible accesses to the area
$S_{path,SAA}$	-	Represents the sum of all $S_{links,SAA}$ normalized for the number of links that compose the rescuers' access path
$S_{link,SAA}$	-	The safety level of a link employed to reach a spontaneous assembly area by rescuers
n_{link}	-	Number of links that compose the rescuers' access path
$A_{plan,tot}$	m^2	Link total area
$A_{plan,inc}$	m^2	Link inaccessible areas (e.g.: private courtyards)
$A_{eff,link}$	m^2	The effective area of links removing the inaccessible area and the area occupied by ruins
pos_{link}	-	Assumed positions of the considered link inside the rescuers' path
$n_{link,path}$	-	Total number of links composing the path

Chapter 1

1 Introduction

Recent natural disasters have rekindled the debate on inhabitant safety levels and the introduction of sustainable solutions to mitigate the risk and to make a more resilient Built Environment (BE). Sudden onset disasters such as earthquakes cannot be predicted, populations in their daily life cannot be forewarned, and the Built Environment, (especially the historic one) which host such individuals, can hide multiple criticalities. Such statements have the aim to highlight how the counting of victims and injuries can be dramatic in the aftermath of such unpredictable events, and above all, how this number can be reduced by intervening promptly in the first phase of the emergency. Safety planners with their employed tools currently do not take into consideration all those risk components that could drastically influence the evacuation process.

Currently, widely encouraged are preventive action and the need for maintenance of the BE elements, which mainly coincide with those vulnerable buildings where to direct refurbishments. Nevertheless, this is not enough, additional aspects could impede the evacuation of the survivors and the intervention of the rescue teams in the immediate aftermath of an event. The conditions of the urban street network for instance, after the earthquake, must be predicted in order to avoid impediments due to ruins obstructions (due to buildings collapse) and structural weaknesses of the infrastructure itself (e.g.: retaining walls, bridges, underground cavities). In recent decades many studies have developed several tools to inquire about factors influencing the seismic risk in historic urban centres. At the same time, different methodologies to assess the reliability of risk-reduction solutions are been proposed. However, these works should be aimed at keeping under control wide scenarios at the urban scale. To do that, desktop mapping services and remote survey tools should be pursued. The results should promote rapid and easy to use assessment methodologies by avoiding expensive and time-consuming field surveys. Nowadays, emergency management and safety planners have to face the evacuation process by considering not only the BE elements but also their users (i.e.: citizens) at the centred of their solutions preferring behavioural-based approaches. Hence, typical and specific human behaviours performed in emergency conditions can heavily influence the evacuation. Additionally, the eventual presence in the BE of individuals with scarce familiarity with places or affected by physical impairments slows down the dynamics process towards safe points (e.g.: assembly areas) especially in the case of overcrowded open spaces conditions.

On such basis, a complete and holistic workflow is here implemented to collect all the necessary data to create an urban emergency scenario the more similar to the reality. To this aim, simulation-based tools to detect the weaknesses of the Built Environment and the criticalities of the hosted population are employed. Finally, on such basis, resilient solutions to mitigate the risk and to improve the inhabitants' safety levels can be adequately proposed and tested.

1.1 Background

First of all, many studies [8–10] converge on the definition of the effective component that constitutes the risk. The formulation *R=HVE* provides the main risk components (i.e.: Hazard, Vulnerability and Exposure). Two of these (H and V), are widely discussed and analysed. The hazard is located at the centre of past studies regarding the physical entity of the natural events, the ways to measure their severity, and their effects on the environment. Although the hazard constitutes a fundamental element to take into account in this thesis, it will be not furtherly discussed. Vulnerability for instance, according to [11], is subdivided into *physical vulnerability*, as the vulnerability of the physical environment, and *social vulnerability* as experienced by people and their social, economic, and political systems. Social vulnerability is then subdivided into *individual vulnerability* (this study mainly focuses on) and *collective vulnerability* regarding the whole community. Finally, the exposure, in general, is focused on the human presence, on the number of people, on the historic and artistic heritage and to the presence of relating services [9].

Physical vulnerability in earthquakes mainly concerns the physical and structural features of the Built Environment. Different studies in literature based on the seismic vulnerabilities inquire about structures weak points, low quality of construction materials, and the resistance capacity to seismic actions of buildings and all the man-made structures and infrastructures (e.g.: urban streets, bridges, tunnels, retaining walls, and embankments) that compose the BE. Several approaches are been proposed in the literature: empirical, analytics, macroseismic etcetera [3,12,13]. They can be subdivided, for our scopes, in relation to the quantity of processed data having consequences obviously in the detailed levels of obtained results from the analysis. The present study is mainly focused on those approaches that require fewer data to collect and analyse and contextually, methods that permit a rapid application are preferred to inquire about emergency issues at a wide urban scale. Speed up the currently available processes to detect and assess BE elements' physical vulnerability is one of the main aims pursued in this work.

Social vulnerability, according to [14], can include human-related factors such as physical features of individuals, their psychological and behavioural aspects, since these elements compose the “set of characteristics and circumstances” of individuals and communities towards the damaging effects of the considered disaster hazard. People’s characteristics (e.g.: age, gender, disabilities, difficulties in motion [6], health fragility [15,16], culture, socioeconomic status of the household [17]) and people’s response to the hazard [18] (e.g.: susceptibility, disaster preparedness, coping capacity, which also refers to their behavioural aspects and their reactions) can influence positively or negatively their propensity to be threatened by disaster effects [19]. These elements can be evaluated for the whole disaster-prone community (*collective vulnerability*, e.g. evacuation and emergency management issues; social issues at the community scale) and the specific individual (*individual vulnerability*, e.g. behaviours, gender, age, health fragility, other features and motion quantities). In earthquakes, for instance, the exposure is strictly related to the presence of persons in a specific environment [20] defined as risky for human life (e.g.: the total number of people, eventual overcrowding conditions, and how many people are in proximity to the

seismogenic sources). Recent literature [21–23] has started to analyse the behavioural-related issue of the human being under certain stressful conditions of risk. A large number of them are aimed at developing simulation models able [6,24,25] to predict human motion features and the overall evacuation dynamic. Such models have to be based on data retrieved from empirical experiments or detected from real emergencies recorded around the world. However, some limits are related to the practical employments of such simulation outputs and how advantageous instructions to emergency planners can be derived.
Exposure is known as *the presence and number of people, property, livelihoods, systems or other elements in hazard areas (and so thereby subject to potential losses)*[1]. Moreover, the presence in stricken areas of industrial and manufacturing activities and commercial transportation systems could lead to economic losses and the interruption of productive capacity as a consequence of disastrous events[26]. However, such economic aspects are not encompassed in this thesis. In earthquakes, for instance, the exposure is strictly related to the presence of persons in a specific BE prone to such events [20] the occurring of additional situations can exacerbate the exposure (e.g.: high-density population areas, eventual presence of mass gathering events that contributes to giving origin to overcrowding conditions, and the proximity of such people to the risk sources). Exposure issues can also concern urban paths and areas when citizens pass through repetitively or when they remain there for a long time. Therefore, the concept of exposure can be connected to the number and human presence in the proximity of the risk source for a specific instant. However, limited are the studies focused on how to acquire such information in a rapid way. This necessity could be pursued by starting to inquire about the intended use of the BE elements that are strictly related to the citizens' occupation of the urban areas.

1.2 Work aim

This thesis is focused on those risk components, mainly vulnerability and exposure, related to seismic disasters in urban areas that have important consequences on the Built Environment and their inhabitants' life. In view of the above, widely debated literature studies that inquire such components and the existing methodologies to assess the vulnerability and citizens safety conditions currently present some limits. The work aim is to delineate a precise and complete workflow starting from the collection of all risk-influencing factors from a holistic point of view, from both a Built Environment and behavioural-based perspective. Then, the same workflow can guide safety planners through the simulation of different scenarios able to implement dynamically the combined effects of multi inputs. The presented work through the adoption of a safety levels assessment metric is able to construe the collected data and simulation outputs. Thanks to this, scenarios criticalities are evinced, specific interventions on the BE are predisposed, and evacuation strategies for occupants are proposed. By reiterating this workflow with the introduced solutions, planners are able to test their efficacy and reliability. These last series of mentioned steps can be considered the innovative and tangible contribution of this exhaustive work towards programmed emergency planning and evacuation management in adherence to the reality to make the environment where we live more resilient.

[1] https://www.preventionweb.net/risk/vulnerability last access 19/11/2020

1.3 Methodological framework

The main aim of this thesis, according to Section 1.2 is to delineate a well-determined workflow to be followed during the entire process. To do this, the PDCA (Plan, Do, Check, Act) approach (described in Figure 1) is adopted as a general operational framework, which has been used by previous works for disaster safety and emergency management evaluations [27–29]. The work proposed below is developed following such steps. The presented methodologies elaborated by the author can be singularly considered as supporting works for the final implementation of the workflow. Different case studies will be employed for testing each developed methodology, the methodological framework here presented will be then implemented in an additional case study at the end of the thesis. Indeed, the methodologies described below are aimed at obtaining data on urban scenarios prone to earthquakes and to assess the interactions between individuals and: (i) the urban scenarios, buildings, and related earthquake-induced modifications, especially in relation to the evacuation path conditions (e.g.: debris formation due to damaged buildings and street network vulnerability); (ii) the emergency management system, including evacuation plan aspects (e.g. positions of assembly areas); and (iii) other individuals. Synthetically the workflow can be resumed as follow:

- PLAN the action by creating scenarios for safety assessment analysis
- DO by performing evacuation simulation
- CHECK the safety levels by analysing simulation results
- ACT by proposing risk reduction solution

PLAN. The definition of possible emergency scenarios for urban centres should involve the characterization of the physical scenario. In order to speed up the urban scale application and the definition of different scenarios [30], the use of the more expedite collection, assessment, evaluation, and representation approaches is preferable. From the BE side, the developed methodologies in Sections 2.2.1 and 2.3.1 can support the data collection process to the scenarios creation task. The behavioural-based approach described in Section 3.2.1 allows to include exposure-related issues to quantifying human presence in the environment.
DO. The evaluation of safety levels for the exposed population in immediate aftermath conditions should be performed by adopting validated evacuation simulation models and related software tools [6,31,32], that should jointly analyse both the earthquake-induced scenario modifications and the evacuation process. Regarding the evacuation process, it should be evaluated from the analysis of the individuals' actions in earthquake-modified conditions that can be based on the considerations outlined in Section 3.1.
CHECK. After simulation implementation, the quantitative analysis of their results is performed through Key Performance Indicators (KPIs). KPIs are essentially based on a human-centric metrics standpoint [33,34] and combine main factors to evaluate the scenario criticalities for both building vulnerability and damages, population and rescuers' paths conditions in evacuation strategies and related safety levels. Such results can be represented through indexes for the overall urban fabric and represented through risk-maps to quickly localize specific risks for each urban component.
ACT. The final step of this workflow is to consider the risk-mitigation strategies by implementing them to the initial scenarios by creating a post-intervention scenario and so to close the PDCA cycle by going back to the very first stage of the process. Proposed strategies

come from literature and experimental evidences-based, for example, concerning: building retrofitting interventions; evacuation planning (i.e. the position of assembly areas, rescuers' access paths, evacuation path definition); preparedness and population awareness; and emergency management, including support to population (i.e. wayfinding signage implementation, the position of rescuers on the urban layout, etc.).

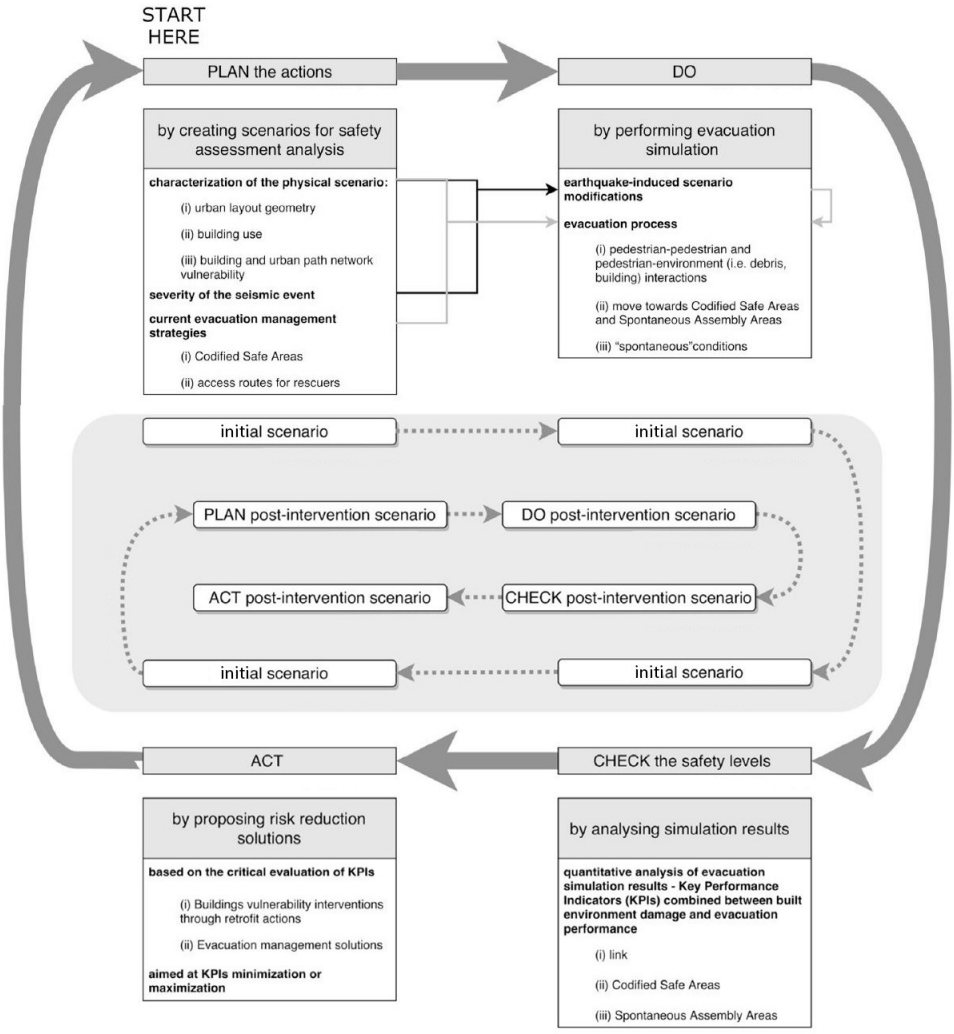

Figure 1 The proposed operational framework according to the PDCA cycle [27,28]; image source: [29] re-elaborated by the author

1.4 Phases

The work outlined below is organised in the following manner made by three main phases developed in the next three chapters (2, 3 and 4). After this first chapter (introduction), chapter 2 and chapter 3 collect a series of assessment and data collection methodologies subdivided into two main themes regarding the Built Environment (mainly buildings and open spaces) and the human presence in it. The work here performed constitutes the basis for the operational framework reproduced in the last chapter 4. The methodological sections and the results are here outlined in the following way: (M) stands for Methodology and (R) for Results.

1st Chapter. It contains the introduction, the background knowledge, and the presentation of the work aim that is expected in this thesis and the methodological framework to employed in the overall research activity;

2nd Chapter. A large part of the present work is widely focused on the "Plan" step according to Section 1.3 above. In detail, this chapter contains the development and testing of rapid and easy-to-use methodologies necessary to assess and collect all the data needed for the scenario creation task. Here, the physical vulnerability assessing methodologies are provided from a Built Environment point of view: Sections 2.2.1 (M) and 2.2.2 (R) regard buildings related aspects, while Sections 2.3.1 (M) and 2.3.2 (R) investigate the availability of the urban paths network;

3rd Chapter. Section 3.1 is deeply focused on human behaviours-related aspects influencing the emergency. While, in Sections 3.2 (M) and 3.3 (R) the Behavioural-based approach is presented. Sections 3.2.1 (M) and 3.3.1 (R) converge on individual vulnerability and exposure-related factors data collection.

4th Chapter. Sections 4.2 (M) and 4.3 (R), try to give tangible employment of all the information and data about the risk-influencing factors evaluated above in order to conclude de PDCA cycle by "Doing, Checking and Acting" in the view of emergency management and planning from a holistic and reliable perspective. The outputted metric is aimed at pursuing the objectives declared in Section 1.2 by taking advantages of the propaedeutic work of the second and third chapters.

Chapter 2

2 The Built Environment

2.1 A panoramic on the seismic risk evaluation of BE composing elements

Historical urban centres are nowadays fragile and complex systems to preserve from disastrous events. In such places, historical buildings can highly suffer from direct damages and losses (to the hosted artworks, source of attraction for tourists) and related safety issues for the hosted population (hence inhabitants and tourists), at the whole urban scale [35]. However, buildings are not the only elements to take into consideration. Indeed, the Built Environment (BE) can be defined as a network of (1) *buildings* (that could be *monumental*, with historic-artistic-cultural features e.g.: govern palaces, churches, monasteries, bell towers, obelisks, theatres, castles, triumphal arches and arch bridges, or *ordinary*, embodied by common dwellings or modern public facilities [36]), (2) *open spaces* (that are the main urban voids, such as squares) and (3) *urban paths* (facing buildings and connected open spaces, such as the urban streets, which can be used by evacuees and rescuers to move into the earthquake-damaged scenario) [37–40]. Mutual interactions among such elements and specific factors characterizing historic centres could lead to exacerbating the urban fabric complexity in emergency conditions [13,39]. A synthetic and not exhaustive list of such aspects is here provided: a) interactions between buildings placed in the same urban block or even composing the same aggregate; b) urban fabric characterization essentially based on the narrow and tangled street network; c) possible related streets blockage due to debris formation; d) streets instability because of soil conditions; e) interferences with inhabitants' and rescuers' mobility in the immediate aftermath.

From this overall perspective, inquiring the seismic vulnerability of buildings can assume a key role in emergency planning. Many methodologies have been developed in this direction with the aim to predict what are the possible earthquake-induced effects and damage at the full historical city centre scale. Among such methodologies [41,42], mechanical methods can provide accurate data on building features, vulnerability and possible damages (and mechanisms) [12], but, for wide-scale applications, they usually imply huge costs for surveys and specific analysis on buildings (mainly performed by high-trained technicians), and are very time-consuming [43]. Such an approach can easily collide with the scarce resources' availability for local government authorities. On the contrary, empirical methods (including the macroseismic ones) can be quickly adopted at the urban scale to quantify buildings' vulnerability [3,44,45]. Such methods are based on a rapid assessment of leading features of buildings. They preferably limit the investigation level to data that can be retrieved by using external inspections or buildings database analysis (i.e.: the lowest detail limit is represented by building typology [7]). Although, data from indoor surveys should be needed (e.g.: walls distance, thickness and connections, foundations levels and types) [3,44] the present thesis is

aimed at demonstrating how qualitative information can be collected without in situ surveys. By applying and testing a "remote approach" reliable data for vulnerability evaluation are obtained [46].
Vulnerability assessment methods can support emergency planning by tracing vulnerability maps [44,47]. Such maps embody the role of providing a quick representation of which areas could suffer more significant earthquake-induced problems related to building features. Usually, they can be also linked with the aim to list intervention strategies with different priority on specific buildings [39].
To do this with effective results, these maps should interest wide urban areas. However, a large part of the well-known and most reliable vulnerability assessment methodologies assume the single structural units[2] that compose the buildings aggregate[3] as the objectives of the analysis. Hence, transferring the inspection from single structural units to the whole aggregate without lacks in terms of vulnerability estimation could be considered a smart solution to speed up the evaluation process of the whole BE. A rapid model to convert the seismic vulnerability indexes of each structural unit (starting by the values obtained with this method [3]) into the seismic vulnerability index of the whole building aggregate is essential in this case [39]. Such rapid scale passage can reduce the requested of resources in money and time avoiding the application of additional methodologies inquiring aggregates vulnerability. Moreover, organizing information about vulnerability level at the scale of the aggregate could be useful to predict emergency path conditions in the aftermath of a disastrous event.

Earthquake-induced modifications to the urban fabric can influence the effective safety levels for the population moving along evacuation paths and the related possibility to reach safe areas (e.g.: no possibility to reach assembly points because evacuation paths could be blocked by debris) in which individuals could receive the first responders' support [28,48–50]. Debris formed from building collapse could be added to street pavement cracks or land failure by provoking additional risks for citizens' evacuation and rescuers' access to the damaged scenario [30,51–53]. According to a general risk assessment approach [8–10], the evacuation path risk depends on the combination between:

- hazard, mainly in terms of soil category, morphology and topography, local amplification phenomena also related to the position of the historical urban fabric (e.g.: on the top of a hill) [54];
- physical vulnerability as a function of: intrinsic vulnerability, which relates to the elements composing the street itself, the related infrastructural elements (i.e.: street pavements, foundations, embankment, and lifelines) [55] and the interfering

[2] Structural unit (SU): The Structural unit must have continuity from heaven to earth as regards the flow of vertical loads and, as a rule, it will be delimited either by open spaces, or by structural joints, or by structurally contiguous buildings but, at least typologically, different. (NTC2018 §.8.7.1)

[3] Buildings aggregate (Agg): «non-homogeneous set of buildings (structural elements), in contact or with a more or less effective connections, which can in general interact under a seismic or dynamic action. A structural aggregate can therefore be made up of a single building [...] or of several merged buildings, generally with different construction features» Italian Civil Protection Department definition: http://www.protezionecivile.gov.it/ (last access on 19/11/2020)

elements, such as underground structures) [52,56]; extrinsic vulnerability, which refers to the elements that do not directly belong to the path itself but can compromise or block it (i.e.: buildings that can collapse by blocking facing streets because of debris formation) due to the typical scenario of historic city centres (i.e.: narrow streets with high facing buildings; network complexity);

- exposure conditions (i.e.: high density of citizen, tourists' presence, mass-gathering events) [57,58].

Methods for estimating the influence of extrinsic vulnerability have been largely debated, by proposing different methodologies for building vulnerability assessment [59–61] as described above. Therefore, macroseismic methods seem to be more suitable for urban scale applications because their application is based on easy-to-detect building parameters [3]. A quick methodology for assessing the seismic vulnerability of paths network by considering interferences with building damages was also proposed [4].

On the contrary, few works inquired about intrinsic path vulnerability. Previous studies principally focused on paths' network capabilities evaluating earthquake-induced effects in terms of variations on possible traffic flows or social-economic consequences generated by one or more unusable paths [62]. Other approaches dealt with particular structural features (i.e.: technical provisions, structural project, soil compaction rather than liquefaction) of highway networks systems, by focusing their attention on typologies whose presence in urban fabrics (especially in historical ones) is limited (i.e.: trenches, embankments, bridges) [53,63]. Other researches proposed to analyse the paths network by separately considering intrinsic and extrinsic vulnerabilities for each composing element [55]. The application of this methodology needs a detailed description of each path link, by including specific local surveys and related data collection processes that could not be quickly employed in a wide-scale assessment. Similar methods adopt empirical and quick analysis criteria at the overall urban fabric scale, by trying to include hazard characterization in terms of soil features and response [2].

The intrinsic vulnerability features have been also associated with their seismic response through fragility curves [64,65]. These curves describe the possibility for buildings, streets and pipelines to reach a certain damage state in correspondence to specific earthquake severity values (e.g.: Peak Ground Acceleration - PGA). In this way, the extrinsic vulnerability could be combined with the analysis of intrinsic one by means of combinations of earthquake-induced effects. Since this approach associates its fragility curve for each studied street element, it seems to be quite onerous for application to a wide-scale urban area. Concerning such description of street damages due to earthquake effects, simplified methods based on discrete damage scale for paths elements (called "Road Damage Scale" - RDS) have been proposed [1]. Correlations between variables characterizing a seismic event (i.e.: magnitude, distance from the epicentre and hypocentre distance) and street damages were provided on real cases observations. Nevertheless, such approaches seem to overlook all the path risk-affecting factors.

Finally, the method for path risk assessment developed by Task-4 of SAVE project activities [58] tried to give a preliminary comprehensive overview of the risk-affecting factors concerning the aforementioned emergency path-related issues. In general terms, this method (called "Cherubini's method" in the following) is aimed at evaluating the seismic risk of the whole historical centre by defining the risk of each composing urban paths elements (i.e.:

streets; squares; crossroads). To this end, differently from previous studies, aspects involving paths structure and geometrical features are merged to the ones referring to paths conditions in terms of traffic and exposure (i.e.: establishing if the path is an interconnection route or an access route, if it is travelled in one-way, and evaluating its average traffic flow). Such aspects are then combined according to a weighted approach to defining the final path risk index. Cherubini's method offers wide capabilities on how to collect and merge the risk-affecting factors and innovatively includes path exposure issues, but it should be improved by including the local seismic hazard and the seismic effects on soil-related to the infrastructures. Currently, discussed improvements are recently reached only through the publication [39].

Other typologies of existing studies focusing on urban paths network after an earthquake are aimed at providing a quick methodology totally centred on emergency paths (that is the urban street) availability prediction in the immediate after the earthquake. The possible two status that could be occurred (depending on the interferences due to building debris) are:

1. "blocked", when debris from a considered building completely occupy the facing path section;
2. "clear", otherwise.

In this sense, the emergency plans should consider such conditions for each element of the path, to evidence which paths [66,67]: will have to be avoided because they could be blocked (unavailable) by debris; will maintain their usability allowing rescuers' access to stricken areas and possible inhabitants' evacuation in safe conditions.

In the last decades, rapid solutions to esteem the probability that debris falling from surrounding buildings could partially or totally occlude the urban streets, are widely debated in the literature. A recent publication has resumed the most valuable tools by comparing them in the same case study [68]. Methods based on geometrical aspects are the simplest and quick-to-be applied and they could be collected in the first group visible in Table 1. They generally consider that hazardous interferences (leading to possible paths blockage) are connected to streets local conditions where the ratio between buildings height (h) and streets width (W) is equal or higher than 1. This approach is codified in the analyses of the Limit Condition for the Emergency (LCE) of an urban settlement [48]. It is worth noticing that, in case of presence of a courtyard between the building and the street, the courtyard width has to be added to the overall street width. A more restrictive geometrical algorithm is proposed by Ferlito and Pizza since they propose that the path could result accessible only if the facing building height is lower than the half of street width itself so as to guarantee a free half side [2]. These methods are quick to be applied but they do not include buildings vulnerability or earthquake intensity/magnitude.

Other approaches try to jointly combine the geometrical aspects to the vulnerability of buildings assessed through rapid and low-cost methodologies. The method of [69] represents a first attempt to inquire street accessibility for evacuation in historical scenarios by jointly combining the importance of street itself (in case it belongs to a path with a strategic function) and its vulnerability (obtained starting to the worst macroseismic damage grade assessed among the buildings facing the street). However, this approach does not directly determine a condition for paths blockage that leads to predict their inaccessibility.

The second group of works involves two other alternative approaches that try to relate different factors (i.e.: geometrical features, earthquake intensity, and buildings vulnerability) proposing to assess the debris amount produced along the streets from facing buildings

through empirical relationships. For each building facing the street, these approaches calculate the debris percentage on the facing street QX [%] by jointly considering the effects of the moment magnitude associated with the seismic event and the building's vulnerability. In particular, macroseismic building vulnerability methods can be applied to ensure rapid implementation of the approach. For each building b, the multiplication between the calculated QX and the street width facing the considered building W_b [-] allows evaluating the effective debris depth d_{ruins} [m] according to the following Equation (1):

$$d_{ruins} = QX \cdot W_b \tag{1}$$

According to Equation (1) and the "blocked" path definition provided above, if the d_{ruins} is higher or equal than the street width, the street is considered as "blocked". Two different *debris estimation criteria* have been proposed by literature to calculate QX. The criterion suggested by [51], called *debris estimation criterion 1* in the following, adopts the rapid methods of [2] to define the building vulnerability. Then, the quantity of building produced external ruins (QX_1 *[%]*) is calculated through the experimentally based relationships reported in Equations (2) and (3):

$$V^*_1 = V_{FP} \cdot M_{ev}/M_{ev,max} \tag{2}$$

$$QX_1(\%) = \begin{cases} 0 & if\ V^*_1 \leq 0.17 \\ 295.28V^*_1 - 49.47 & if\ 0.17 < V^*_1 < 0.51 \\ 100 & if\ 0.51 \leq V^*_1 \end{cases} \tag{3}$$

where V_{FP} [-] is the normalized building vulnerability evaluated thanks to [2] and M_{ev} is the earthquake moment magnitude of the event normalized for the maximum moment magnitude expected $M_{ev,max}$.

The criterion suggested by [70], called *debris estimation criterion 2* in the following, takes advantages from the macroseismic building vulnerability method by [3], and additionally considers the building height/facing street width ratio to evaluate the debris percentage. It proposes to esteem the quantity of produced external ruins (QX_2 [%]) from buildings through the experimentally based relationships reported in Equations (4) and (5):

$$V^*_2 = V_{GL} \cdot M_{ev}/M_{ev,max} \cdot h/W \tag{4}$$

$$QX_2(\%) = \begin{cases} 115.55V^*_2 & if\ 0 \leq V^*_2 < 0.87 \\ 100 & if\ 0.87 \leq V^*_2 \end{cases} \tag{5}$$

where V_{GL} [-] is the normalized building vulnerability evaluated thanks to [3]. Although they can predict the debris depth, by allowing a punctual estimation of building-facing path interferences in a detailed way, these methods reliability is connected to their experimental database dimension.

The third group of works in Table 1 gives the possibility of introducing in the path blockage prediction algorithm the evaluation of the damage grade suffered by buildings. The method proposed by [71] for reinforced concrete buildings and extended to masonry buildings in the

conference paper by [72] elaborating a methodology to plan safe paths in case of emergency predicting possible occlusion for Civil Protection interventions. Thanks to a GIS tool the work proposes the definition of two different buffer zone (equal to 1/3 of buildings height that suffers by the 4th damage grade and 2/3 of the height for the 5th damage grade) establishing a maximum probable distance that the ejected material can reach, in this way it is possible to predict which part of the street will be cluttered with debris. The study provides a novel buildings damage grade estimation method (according to the vulnerability classes depending on the type of structure [7]). Then, damage grades are assigned by comparing the vulnerability index of a studied building with the established vulnerability thresholds (one for the 4th and another the 5th damage grade) for each macroseismic intensity level.
The macroseismic damages-based methodology proposed by [4] allows relating the building vulnerability to post-earthquake damage scenario prevision based on earthquake EMS-98 intensity obtaining the related damage grades [7], according to a probabilistic approach associating the 95^{th} percentile of its cumulative distribution function [3]. In such conditions, the critical debris level can block the facing path also according to geometrical ratios as reported by Equation (6).

$$B_{link} = \begin{cases} Blocked, \exists\ building \in path \mid h/W \geq 1 \wedge k95 \geq 4\ grade\ EMS98 \\ Clear, \quad elsewhere \end{cases} \tag{6}$$

This methodology requires the use of rapid detectable parameters (external inspection, by evaluating e.g. building typology, geometrical aspects, plano-altimetric irregularity) that can be obtained through "remote" inspections (e.g. by using photographic documentation and satellite sources) [46].
Finally, in literature is possible to find other methods that try to focus on out-of-plane walls failure modes combined to fragility curves [73] or probabilistic and fuzzy logic analyses of the potential interaction between building and roads [49]. Anyway, such models are complex since they require accurate on-site surveys (mainly: building geometry including data from internal inspections; building materials strength) to effectively produce a good estimation of a single failure model (out-of-plane). Hence, they are not applied to this study.

Table 1 Comparative table of considered methods to evaluate the urban path blockage where: h is the height of a building facing the street, W is the street wide and k95 is the damage grade according to [3].

Inquired methods	*Limit Condition for the Emergency (LCE)*	*Ferlito and Pizza*	*Debris estimation criterion 1*	*Debris estimation criterion 2*	*Artese Achilli*	*k95* macroseismic damages-based
Grouped by type:	(1) Geometric approaches		(2) Debris formation criteria		(3) Macroseismic damage-based approaches	
Ref. Blocked	[48] h/W ≥ 1	[2] h/(W/2) ≥ 1	[51] druins ≥ W	[70] druins ≥ W	[72] Damage=4; 1/3h ≥ W Damage=5; 2/3h ≥ W	[4] $h/W \geq 1 \wedge k95 \geq 4\ grade\ EMS98$

Clear	h/W < 1	h/(W/2) < 1	druins < W	druins < W	Otherwise	Otherwise
Influencing factors	Geometrical ratios	Geometrical ratios	Vulnerability, Magnitude, Geometrical ratios	Vulnerability, Moment Magnitude, Geometrical ratios	Damage grade as a function of Vulnerability, Intensity; Geometrical ratios	Damage grade as a function of Vulnerability, Intensity; Geometrical ratios
Advantages from other studies:			[2] for vulnerability estimation	[3] for vulnerability estimation	[7]	[3]

2.2 About buildings

2.2.1 How to speed up the buildings seismic vulnerability assessment through a low time and cost-consuming method

As previously said, a "remote" approach is aimed at applying vulnerability assessment methods without local survey and by only using remote data collection tools, so as to simplify and speed up the vulnerability evaluation process. The approach proposed by this work adopts desktop web mapping services, photographs and aerial maps to perform remote rapid visual screening on examined buildings. In particular, data from Google Street View and Google Maps[4] are here used. Anyway, this approach is not limited to employing only these tools. Indeed, other strategies to quickly collect information from buildings can be adopted by taking advantage of the application of different innovative technologies i.e., on-board cameras [74] or drone surveys [75,76].
Two well-known macroseismic vulnerability assessment methods (the Giovinazzi and Lagomarsino 2006 [3] and the Ferreira Vicente Varum 2014 [5]) are adopted in this thesis to verify the reliability of this approach and to quantify an eventual lack of information. To implement the second-mentioned method measure of façade geometry and area of wall openings for instance are required. In this sense, the remote approach tries to solve this data acquisition through images captured from Google Street View application. Then, such photographic material will be rectified and scaled. The rectification is conducted by using specific software (TriDmetriX[5]), while the scaling process is implemented through CAD elaborations starting from known measures assumed as benchmarks within the urban fabric. Needed geometrical information can now directly detected on such images with the CAD tool "Measure".
However, the application of chosen macroseismic vulnerability assessment methods (MVAMs) [3,5] through such a simplified approach, can affect the evaluation of some vulnerability influencing parameters by possible lack of information (i.e.: data connected to

[4] Google Maps direct link: https://www.google.it/maps/ last access: 19/11/2020.

[5] TriDmetriX rectification software website: http://www.tridmetrix.com/ last access: 19/11/2020.

indoor surveys and deep analyses). To overcome this issue, a conservative approach is proposed by "assigning" the worst related vulnerability-affecting factors condition as follow:

- in Lagomarsino and Giovinazzi 2006: "Structural System" parameter is assumed equal to 0.04 [3];
- in Ferreira Vicente Varum 2014: "Masonry quality" parameter is assumed equal to 37.50; "Connection to orthogonal walls" and "Connection to horizontal diaphragms" parameters equal to 25.00 [5].

The "remote" approach reliability can be verified by making comparisons between the detected damage grades from a real-world event and the predicted damage grades obtained through vulnerabilities indexes outcoming from methods application by following the proposed approach on the same sample of buildings[6]. The effects on buildings of a recent earthquake[7] are adopted thanks to both Satellite Grading maps of Copernicus European project[8] and photographs[9] (referring to the immediate aftermath). Both these damage grades are defined according to the European Macroseismic Scale EMS-98 [7] in discrete classes from 1 to 5 as reported in Figure 2.

[6] The considered sample suffered from the 2016 Central Italy earthquake, and in particular the Accumoli (RI) (42.70, 13.23) earthquake, 03:36:32 (UTC+2), 2016/08/24, Mw=6.06. It is composed by 118 structural units in masonry building typology, whereas a part of these is collected in 22 historic aggregates and the other one is referred to 15 isolated building. The whole sample is representative of European historical city centre.

[7] Seismic event information: http://cnt.rm.ingv.it/en/event/7073641 last access: 19/11/2020.

[8] Copernicus web portal: https://emergency.copernicus.eu/ last access: 19/11/2020.

[9] Images of buildings damages are collected from institutional web site: Corpo Nazionale dei Vigili del Fuoco http://www.vigilfuoco.tv/ last access 19/11/2020, Italian Civil Protection http://www.protezionecivile.gov.it/jcms/it/multimedia.wp last access 19/11/2020.

Classification of damage to masonry buildings	
	**Grade 1: Negligible to slight damage** **(no structural damage, slight non-structural damage)** Hair-line cracks in very few walls. Fall of small pieces of plaster only. Fall of loose stones from upper parts of buildings in very few cases.
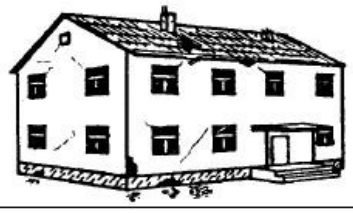	**Grade 2: Moderate damage** **(slight structural damage, moderate non-structural damage)** Cracks in many walls. Fall of fairly large pieces of plaster. Partial collapse of chimneys.
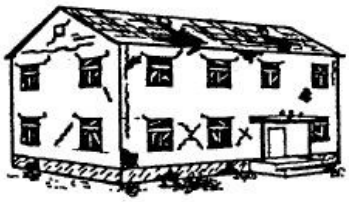	**Grade 3: Substantial to heavy damage** **(moderate structural damage, heavy non-structural damage)** Large and extensive cracks in most walls. Roof tiles detach. Chimneys fracture at the roof line; failure of individual non-structural elements (partitions, gable walls).
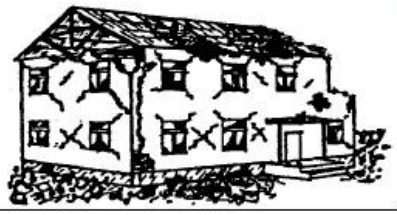	**Grade 4: Very heavy damage** **(heavy structural damage, very heavy non-structural damage)** Serious failure of walls; partial structural failure of roofs and floors.
	**Grade 5: Destruction** **(very heavy structural damage)** Total or near total collapse.

Figure 2 Damage grades scale for masonry typologies (source: EMS98 [7]).

Meanwhile, Equations 7 and 8 define how to calculate the predicted damage grade from methods application. The mean damage grade μ_D ($0 < \mu_D < 5$) for the Lagomarsino and Giovinazzi 2006 [3] and the Ferreira Vicente Varum 2014 [5] methods, respectively, are given as a function of earthquake intensity I, of the vulnerability (respectively, V_L for [3] and

V_F for [5]), and of the ductility index Q (in this study, respectively, Q_L equal to 2.3 [3] and Q_F equal to 2.0 [5]).

$$\mu_{D\,L} = 2.5\ \left[1 + tanh\left(\frac{I + 6.5V_L - 13.1}{Q_L}\right)\right] \quad (7)$$

$$\mu_{D\,F} = 2.51 + 2.5\ tanh\left(\frac{I + 5.25V_F - 11.6}{Q_F}\right) \quad (8)$$

Either, to make the damage grades comparison immediate, MVAMs offer a possible estimation of expected discrete damage k for a building of certain μ_D through the Probability Mass Function (PMF) defined in Equation 9. It shows the probability p_k that a building suffers from a damage k according to EMS-98 degrees (0 to 5) [3].

$$\text{PMF: } p_k = \frac{5!}{k!(5-k)!}\left(\frac{\mu_D}{5}\right)^k \left(1 - \frac{\mu_D}{5}\right)^{5-k}, k = 0,1,2,3,4,5 \quad (9)$$

For each building, predicted damage grades (calculated by applying each of the two MVAMs) considered in this study are: the *most probable*, according to a simplified approach [77]; the ones corresponding to the 95th (*k95*), 75th (*k75*) and the 50th (*k50*) percentile of its cumulative distribution function, according to a semi-probabilistic method [4].
Reached this point, each predicted damage grade is compared to the real-world damage grade and outcoming comparisons are organized to evidence the percentage of cases for which:

- predicted and real-world damages are equal;
- predicted ones are higher than the real-world ones (it means "the MVAM overestimates the building vulnerability");
- predicted ones are lower than the real-world ones (it means "the MVAM underestimates the building vulnerability").

Percentages about differences among damage grade classes are also calculated. According to a conservative approach in damage prediction [70], the "more reliable" method is the one that:

- does not underestimate the earthquake-induced damage;
- in case of overestimation, minimizes the difference between the experimental and predicted damage grade.

Finally, the best performing MVAM according to the remote approach is selected to be employed in the subsequent phase of this thesis.

Assuming that the "remote" approach can be adopted to speed up the data collection process to assess the seismic vulnerability of buildings an additional passage of scale should be implemented to take under control wide urban areas. Various attempts to individuate a formulation that rapidly permits to pass from available (because already evaluated according to the most reliable MVAM that will be outlined from previous consideration) vulnerability index of single structural units ($V_{L,SU}$ *or* $V_{F,SU}$) to a unique seismic vulnerability index for a building aggregate ($V_{L,Agg}$ *or* $V_{F,Agg}$). Moreover, it is necessary to specify that, for this evaluation phase each vulnerability index from the applied MVAMs has to be normalized by

considering the related absolute maximum values (according to their references are adopted 1.02 for [3] and 275 for [5]). To reduce the length of this section, equations in the following are reported only for the aggregate vulnerability assessed by the Lagomarsino and Giovinazzi 2006 method ($V_{L,SU}$ and $V_{L,Agg}$), but the same hold for Ferreira Vicente Varum 2014 method.
The first idea to consider to establish this formulation could be to propose the highest vulnerability value among the structural units composing the aggregate itself ($V_{L,Agg,Max}$) as the seismic vulnerability index of the whole aggregate. This significant simplification could lead to an important overestimation of the aggregate vulnerability, especially in case of great vulnerability values differences between the structural units composing the aggregate.
Considered this, an alternative idea can otherwise assume the average value of the vulnerability indexes of all the structural units within the aggregate ($V_{L,Agg,Ave}$). However, in this case, the influence of some structural units could be overestimated while others could be underestimated, leading to a sensible inaccuracy of the evaluated index for aggregates.
To overcome such estimation biases, the contribution of each structural unit on the whole aggregate vulnerability can be weighted as follows:

- by considering the covered area of every single structural unit ($Area_{SU}$) within the total covered area of the aggregate ($Area_{Agg}$), as shown in Equation 10. However, in the case of two structural units with equal covered area, the influence of differences in height or number of storeys is not considered, by limiting the effectiveness of vulnerability-induced effects in earthquake aftermath (e.g.: debris generation depending on building heights and consequent obstruction of facing escaping path within the historic centre [70]).

$$V_{L,Agg,Area} = \sum\nolimits_n \left[\left(Area_{SU}/Area_{Agg}\right)V_{L,SU}\right] \tag{10}$$

- by considering the ratio between the volume of every single structural unit (Vol_{SU}) and the one of the whole aggregate (Vol_{Agg}), as reported in Equation 11. In this way, a structural unit with high vulnerability index, but with smaller volume in respect to the total aggregate one does not influence the overall aggregate vulnerability like a structural unit with the same vulnerability level but with more extended dimensions.

$$V_{L,Agg,Vol} = \sum\nolimits_n \left[\left(Vol_{SU}/Vol_{Agg}\right)V_{L,SU}\right] \tag{11}$$

The proposed ratio on volumes in Equation 11 could generally produce differences in aggregate vulnerability assessment in respect to the ratio on areas in Equation 10. Anyway, in case of aggregates with compact and regular plan configuration (e.g. composed by multi-storeys structural units with similar height and similar covered area, as for the ones organized on urban narrow lots), such differences could be not influent. Hence, some basics statistics are proposed in the employed sample to understand how the results could be influenced by such aforementioned aggregates features. Statistical analysis is conducted on the per cent differences $\Delta_{A/V}(\%)$ obtained for each structural unit through Equation 12:

$$\Delta_{A/V}(\%) = \left|\left(Area_{SU}/Area_{Agg}\right) - \left(Vol_{SU}/Vol_{Agg}\right)\right|/\left(Area_{SU}/Area_{Agg}\right) \tag{12}$$

Finally, a further approach is based on Equation 11, but it tries to include further aggregates features connected to differences among the composing structural units (i.e.: main typology, number of composing units), as shown by Equation 13:

$$V_{L,Agg} = \left(\frac{\sum_n\left[\left(Vol_{SU}/Vol_{Agg}\right)V_{L,SU}\right]}{d}\right) * \frac{1}{q} \tag{13}$$

where vulnerability values of structural units belonging to the same aggregate are summed and weighted on volumes ratio. Coefficient d is introduced to increase vulnerability index depending on the presence of structural units having different masonry typologies (Equation 14). This parameter considers the main (more frequent) masonry typology within the aggregate and evidences the number of structural units having different ones. At the same time, $1/q$ can be seen as a corrective factor > 1, that takes into account the number of structural units within one aggregate: higher the number of composing structural units, higher the possible impact of interferences among them, and thus the final vulnerability value. In this way, for aggregates composed by only 1 structural unit, this parameter does not have to increase the vulnerability value, thus 1/q = 1 (Equation 15).

$$d = \begin{cases} 1 & if\ structural\ units\ have\ the\ same\ masonry\ typology \\ 1 - \dfrac{number\ of\ different\ structural\ units\ from\ principal\ typology}{total\ number\ of\ structural\ units\ composing\ the\ aggregate} \end{cases} \tag{14}$$

$$1/q = \begin{cases} 1 & if\ only\ one\ tructural\ unit\ is\ present \\ \dfrac{total\ number\ of\ structural\ units\ composing\ the\ aggregate}{total\ number\ of\ structural\ units\ composing\ the\ aggregate - 1} \end{cases} \tag{15}$$

As for Equation 10 and Equation 11, Equation 13 is additionally valid for both building aggregates and single buildings (since the final value is reduced to $V_{L,SU}$ *or* $V_{F,SU}$ itself, d=1 as well as the corrective factor $1/q$) by extending the capabilities of MVAM by proposing a unique theoretical definition.

Among the different approaches of the attempts proposed above, now the one that registers the capability to manage this scale passage without an excessive loss of accuracy in vulnerability estimation has to be determined. This preliminary validation can be solved by making comparisons between the novel aggregates vulnerability index obtained through the Equation above (i.e.: maximum index ($V_{L,Agg,Max}$), average index ($V_{L,Agg,Ave}$), (10), (11) and (13)) and the application results on the same sample of aggregates of another existing but less known vulnerability assessment method. The employed method to make the comparisons evaluates the seismic vulnerability directly of the whole building aggregate. It is named SISMA [24] and has been proposed by Mazzotti 2008. Here, the vulnerability index is obtained from an algorithm based on the evaluation of 10 independent parameters reported in Table 2. They underline the differences between the real aggregate and an ideal regular

condition, the more these differences are considered the more every single parameter assumes a higher value. Then, each parameter contribution (v_p) (maximum range from 0 to 1 according to the Mazzotti 2008 method) is weighted on its importance (w_s) to calculate the vulnerability index V_s [-], according to Equation 16.

$$V_s = \sum_{1}^{10} v_p * w_p \tag{16}$$

However, its application follows in this thesis the "remote" approach by applying the worst vulnerability conditions to the parameters below form a conservative point of view: "Construction age or last intervention date" and "Presence of buildings without box behaviour" that they cannot be remotely retrieved without local surveys. Finally, the aggregate vulnerability index is normalized on a scale from 0 to 100 by dividing it by a fixed value previously established by the method and equal to 5.4 (this value represents the maximum value of V_s from Equation 16).

Table 2 Vulnerability-influencing parameters are reported for assessment vulnerability method by Mazzotti 2008 (SISMA) specifying also their assignable range of variation (v_p) and their weights (w_s).

	Assessed parameters	Contribution range (v_p)	Weight (w_p)
1	Volumetric differences in elevation	0-0.6	1.0
2	Planar volumetric differences	0-0.6	1.0
3	Maximum differences between the number of building floors and the average number of floors	0-1	0.6
4	Differences in materials and constructive typologies	0-1	0.6
5	Construction age or last intervention date	0-1	0.6
6	Not aligned opening / staggered floor presence	0-1	0.6
7	Presence of buildings with non-box behaviour	0-1	0.4
8	Aggregate overall shape / planar symmetry	0-1	0.4
9	Conservation state / maintenance deficiency	0-1	0.6
10	Geomorphology of aggregate foundation	0-1	0.4

The effectiveness of possible correlations between aggregates vulnerability indexes obtained through proposed attempts and the others (outcoming from the SISMA method) is then traced on the same sample. Such comparisons are based on the possibility to define an increasing regression line, by verifying its double goodness through the Regression Coefficient analysis (R^2) and the Pearson Correlation Coefficient (ρ) [79]. Simple linear regression models, if they exist, are to be preferred in this study according to previous approaches [51] and to have coherently simple correlations to be used. In addition to the main regression line (MRL), other two trend lines are also highlighted: the monotonic increasing regression function on maximum values ($MIRF_{max}$) and the one on minimum values ($MIRF_{min}$). These last two functions are obtained interpolating only those $V_{L,Agg} - V_S$ pairs that are higher (for $MIRF_{max}$) or lower (for $MIRF_{min}$) than the previous ones proceeding from left to right of the

abscissa axis omitting the others. The introduced regressions could be considered as limit functions generating a reliability range within which vulnerability pairs should be placed.
An additional reliability test can be pursued on the best formulation declared in the previous comparisons. This time, the proposed formulation reliability can be gained by tracing a relation between the obtained V_{Agg} values and the detected damage grade according to EMS98 (as done before to demonstrate the reliability of the "remote" approach), underline if increasing V_{Agg} could represent the possibility to suffer from an increasing damage grade. However, this demonstration to be implemented requires an additional step: the damage levels definition for the whole aggregate. Firstly, through photographic material of each structural unit of the same sample collected after the earthquake by First Responders' associations is compared with the EMS-98 definitions to derive the detected damage levels (discrete values from 0 to 5) that from this point can be identified with *k*. Hence, a damage level index for the entire aggregate k_{Agg} in adherence with the formulations above is calculated as the mean damage level of the structural units weighted on related volumes, as shown by Equation 17:

$$k_{Agg} = \sum_n \left[\left(Vol_{SU}/Vol_{Agg}\right)k\right]/n \tag{17}$$

Where *n* is the number of SUs composing the aggregate. In conclusion, the experimental-based correlation between k_{Agg} and V_{Agg} can be now traced through a linear regression model where k_{Agg} is here considered as an independent variable since it refers to direct experimental data. In compliance with the previous tools to investigate the regression line, two additional trend lines for maximum and minimum increasing pairs will be adopted.

2.2.2 The "remote" approach and the rapid passage of scale for vulnerability visualization

The remote approach described in Section 2.2.1 and proposed to speed up the data collection process to assess the seismic vulnerability of masonry buildings is here tested. The reliability is proved by making comparisons among damage grades prediction obtained by MVAMs application (where vulnerability data on buildings are provided through the remote approach) and the detected damage grades from a real event observation. Table 3,Table 4, andTable 5 summarize the evidence of such results on a case study (as described in Section 2.2.1).
This simplified approach, in general terms, tends to not underestimate the predicted damages for both MVAMs [3,5], by supporting conservative evaluations on post-earthquake damage scenarios. However, a relevant presence of overestimated cases is noticed especially in relation to lower damage grades 2 and 3 as shown by Table 4. Hence, it is possible to affirm that lower damage grades correspond to a major uncertainty in the damage prediction process through the remote approach. On the contrary, the adoption of *k95* damage estimation can be conservatively adopted because it avoids damage underestimation cases as well as maximizing the occurrence of correspondence between predicted and real building damages. Apparently, from Table 3 no considerable difference between Lagomarsino and Giovinazzi 2006 and Ferreira Vicente Varum 2014 methods are noticed considering the 95th percentile. However, in detail, the first method limits the excessive overestimation case frequency in the 2nd damage grade, but the contrary is registered for the 3rd grade (Table 4). Anyway, an

overestimation of 3 damage grades is more probable by adopting the Ferreira Vicente Varum 2014 method (Table 5). These observations establish that the Lagomarsino and Giovinazzi 2006 method (related to the 95th percentile) seems to be the better choice in damage prediction if it is supported by the remote data collection approach. Therefore, for such reason, it will be used for carrying out the novel vulnerability index for building aggregates.

Table 3 Percentages results of correspondence/overestimation/underestimation cases according to the different approaches in Section 2.2.1 (*most probable; k95, k75, k50*) for each method are reported.

	Most probable		k95		k75		k50	
Method	[3]	[5]	[3]	[5]	[3]	[5]	[3]	[5]
Correspondence	28%	29%	32%	32%	30%	32%	26%	25%
Underestimation	17%	3%	0%	0%	7%	0%	26%	9%
Overestimation	54%	68%	68%	68%	63%	68%	48%	66%

Table 4 Percentage of overestimations related to each detected (from real event) damage grade (2nd, 3rd, and 4th); no effective damage grade equal to 1 are collected in the studied sample.

Overestimation cases for each damage grade according to EMS-98 definition	Most probable		k95		k75		k50	
Method	[3]	[5]	[3]	[5]	[3]	[5]	[3]	[5]
2nd damage grade	22%	28%	23%	28%	23%	28%	22%	28%
3rd damage grade	23%	21%	26%	21%	25%	21%	23%	21%
4th damage grade	9%	19%	18%	19%	15%	19%	2%	13%

Table 5 Percentage of overestimations with a difference of 1,2 or 3 damage levels between the detected (real event) and predicted ones.

Differences between the detected and predicted damage level (by considering overestimation cases)	Most probable		k95		k75		k50	
Method	[3]	[5]	[3]	[5]	[3]	[5]	[3]	[5]
1 damage grade	45%	30%	29%	28%	37%	28%	45%	32%
2 damage grades	39%	31%	39%	30%	35%	30%	53%	47%
3 damage grades	16%	38%	33%	41%	28%	41%	2%	28%

Formulations proposed in Section 2.2.1 to determine the seismic vulnerability index of whole aggregates by starting from the single structural unit values are evaluated in the following. The comparisons between results application on the same case study of such formulations and the existing one proposed by Mazzotti 2008 are revealed through the following graph.
In detail, part A of Figure 3 highlight how the first attempt (that considers the maximum vulnerability values $V_{L,Agg,Max}$) in spite of a considerable regression coefficient (R^2=0.59), it cannot be considered appropriate to the aggregate vulnerability evaluation because of its high probability in overestimate this index. On the contrary, the average ones ($V_{L,Agg,Ave}$) does not gain a suitable correlation (R^2=0.34) confirming the excessive divergence between the structural unit vulnerability values and the aggregate vulnerability index so estimated.
Part B of Figure 3 displays the almost correspondence of the regression lines obtained by weighting the influence of single structural units vulnerability on the areas ($V_{L,Agg,Area}$) and volumes ($V_{L,Agg,Vol}$) according to Equation 10 and 11 of Section 2.2.1. However, these results seem to be affected by collected sample features, in particular by the presence of many similar structural units within the aggregate in terms of plan and elevation (and so in terms of volume). For this reason, the statistical analysis made in Equation 12 is performed to confirm the goodness of the proposed approach. In fact, the average value evaluated on the $\Delta_{A/V}(\%)$ ratios, involving all the sample structural units is equal to 17%, the median value is equal to 13%, while 5% and 23% represent respectively the values for the first and third quartile. These statistical values nearly to zero as well as the mode demonstrates how casually the adopted sample of structural units is featured by very similar heights.

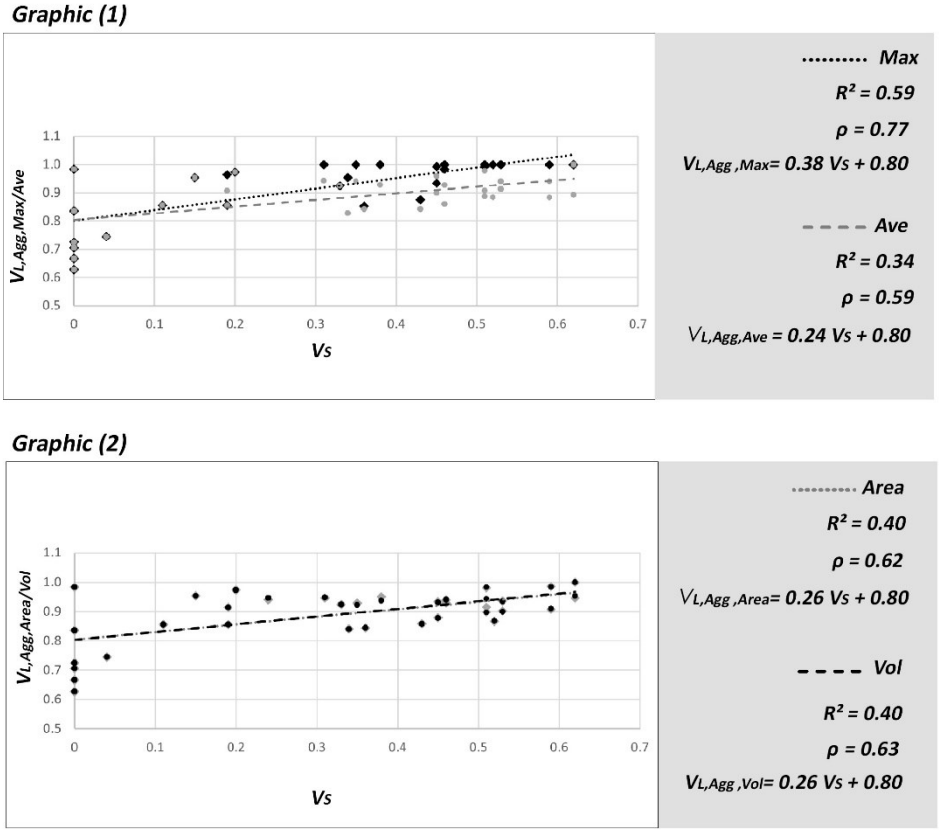

Figure 3 Lagomarsino and Giovinazzi 2006 based vulnerability indexes are paired with Mazzotti 2008 (SISMA) ones. Correlation trend lines with their equations, coefficient of regression, and their Pearson value are reported for $V_{L,Agg,Max}$ and $V_{L,Agg,Ave}$ (Graphic 1), and for $V_{L,Agg,Area}$ and $V_{L,Agg,Vol}$ (Graphic 2).

Finally, Figure 4 point out the main regression line (*MRL*) for $V_{L,Agg}$-V_S pairs adopting also the other increasing regressions defined in Section 2.2.1 ($MIRF_{max}$ and $MIRF_{min}$).
Results evidence how the *MRL* (black line) seems to be quite reliable according to its coefficient of determination (R^2) equal to 0.52 and to its consistent Pearson value (ρ) equal to 0.72 (fairly high correlation since ρ > 0.6 [80]). On the other hand, both the monotonic increasing regression function on maximum and minimum values embody a more conservative role, with a higher correlation coefficient due to the more restricted selection of sample elements less scattered. They constitute a conic domain in which all pairs can be retained satisfying. This last graph proved that a satisfying correlation between the existing SISMA by Mazzotti 2008 and the novel proposed approach from Equation 13 seems to exist.

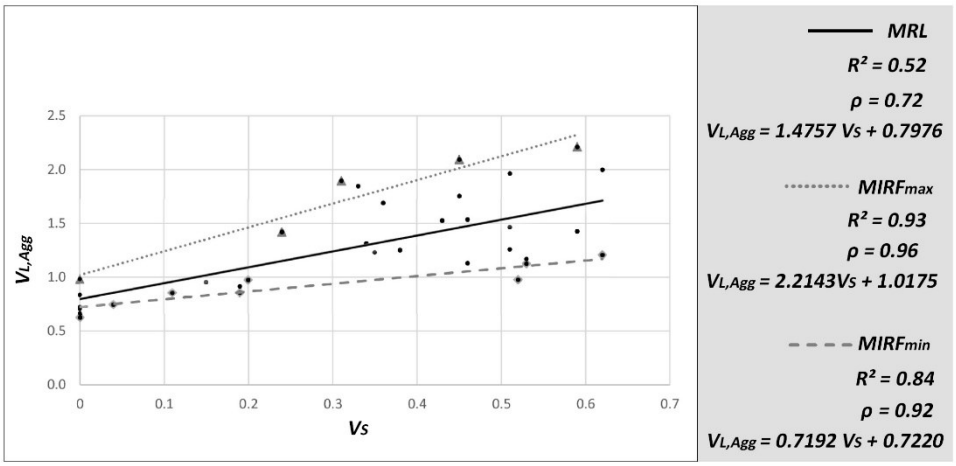

Figure 4 Vulnerability indexes pairs for aggregates evaluated through Equation 13 ($V_{L,Agg}$) of Section 2.2.1 and Mazzotti 2008 SISMA (V_S). The main regression line (MRL) with its equation, coefficient of regression and the Pearson value are offered. The graph evidences also the monotonically increasing regression function on maximum ($MIRF_{max}$) and minimum values ($MIRF_{min}$) of the sample with the related regression coefficients.

Even if vulnerability values of both methods cannot be directly compared to an expected damage grade the graphical results outlined in Figure 5 affirms that for a high aggregate vulnerability value a heavier damage grade of the whole aggregate is observed. The aggregate vulnerability V_{Agg} obtained through Equation 13 and the aggregate damage grade K_{Agg} (according to Equation 17) pairs confirm this trend: the main regression line (equation: *y=1.42x-1.13*) is delineated by a consistent R-squared value of 0.54 and a Person correlation coefficient (ρ) equal to 0.73. In adherence with the previous comparison tests the monotonic increasing regression function on maximum values (equation: *y=2.06x-1.80*) and the one on minimum values (equation: *y=0.86x-0.69*) show linear regression too, respectively with an R-squared of 0.78 and 0.87, and a Person coefficient (ρ) equal to 0.89 and 0.93.

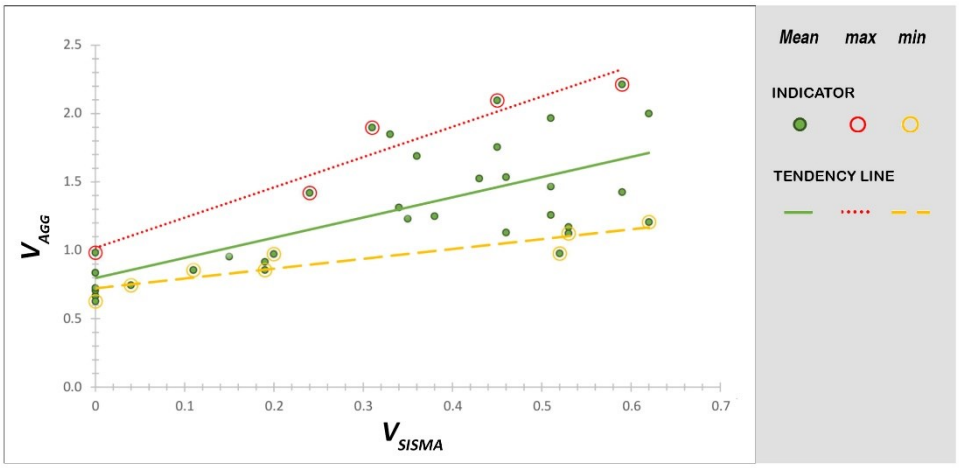

Figure 5 K_{Agg} - V_{Agg} pairs for aggregates and related regression lines.

Summarizing the obtained results, firstly a novel methodology to ensure in a quicker way the required data to enquire buildings vulnerability is proposed and tested (remote approach mainly oriented, but not limited to using desktop web mapping services) at the historic centre scale. In this way, is pursued an efforts reduction connected to often onerous and time-consuming vulnerability assessment methods requiring specific training level from the technicians. The further achieved contribution lead to extend expeditious Vulnerability assessment methodologies methods implementation on the entire urban centre passing from the single structural units to the scale of the aggregate, without losing in reliability. In this way, it is possible to link microscale rapidly (structural unit-related) to mesoscale (aggregate-related) vulnerability data. In addition, these quick investigations, allow the definition of vulnerability maps based on a relative vulnerability scale constituting a supporting tool to emergency management. In this way, vulnerability maps could allow taking easily under control wider risky areas of historical centres by giving a representation of which urban fabric parts could evidence critical safety situations, and so where interventions should be provided. A graphical example that supports these statements is given by comparing the vulnerability map in Figure 6 (microscale) from the one in Figure 7 (macroscale) on the implemented case study of Offida.

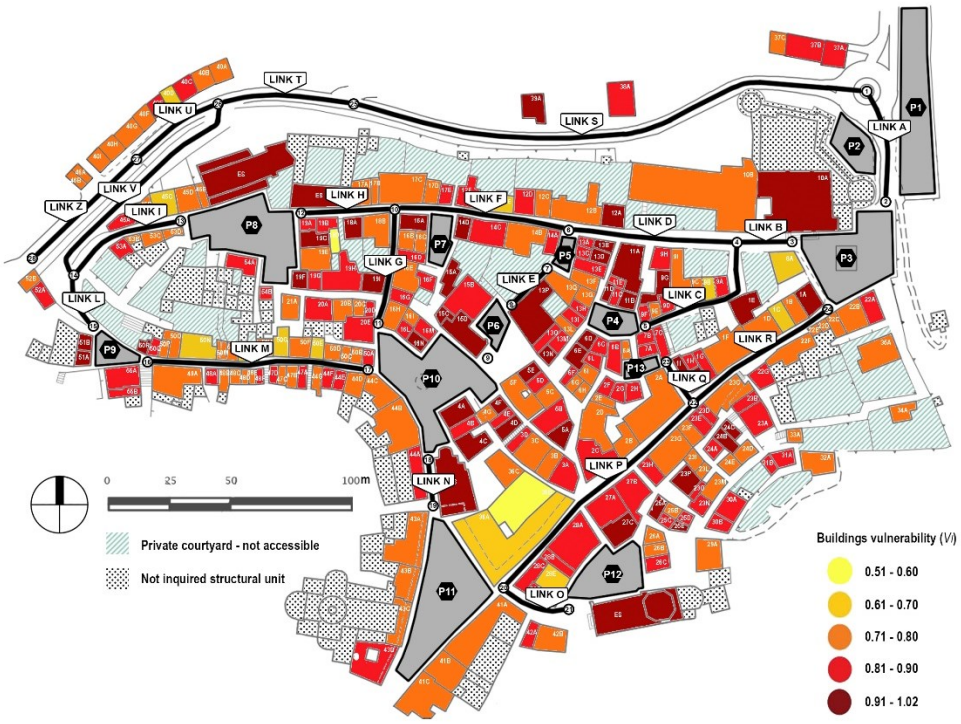

Figure 6 Vulnerability map of the Offida (Italy) case study, seismic vulnerability values are given on a chromatic scale for each structural unit according to the MAVM of Giovinazzi and Lagomarsino 2006

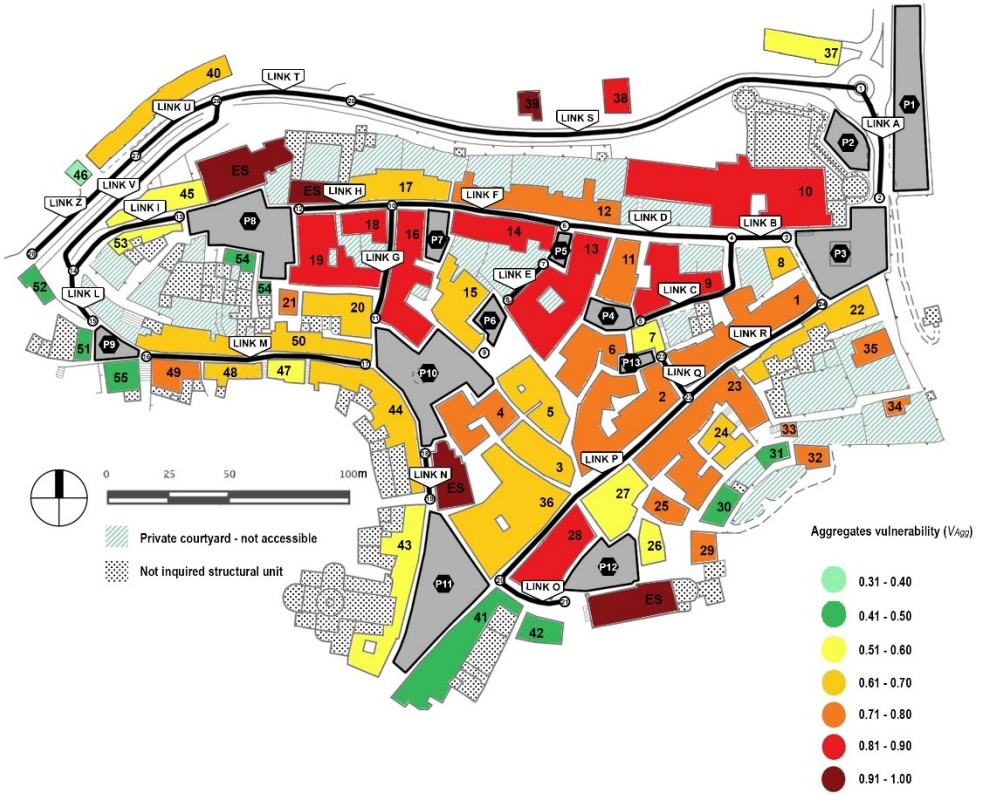

Figure 7 Vulnerability map of the Offida (Italy) case study, seismic vulnerability values are given on a chromatic scale for each aggregate according to Equation 13 proposed in this work

2.3 Paths network and open spaces

2.3.1 How to determine the risk factors connected to the emergency paths network

Starting to inquire about the other physical elements of the historic urban fabric, this thesis has to define univocally which those elements are. A path network is defined as a set of urban streets, faced by buildings, that put into communication the open spaces of a built-up area. Such streets becoming paths from an emergency point of view, indeed urban paths should be employed by evacuee to reach assembly areas and by rescue teams to provide first aid to trapped inhabitants. The urban path network is composed of *links* that connect *nodes* according to the definitions given in Table 6 [4,6]. A graphical example is offered in Figure 8.

Table 6 Street network schematization; Links definition, the subdivision between types of Nodes and related assessment tools.

Path elements	Definition	Identification code
Nodes	Crossroads, significant plano-altimetric and structural variations (i.e.: pavement features, the presence of structural elements such as retaining walls, protection measurements or bridges and tunnels) along the path network [4]	Numeric code
Square[10]	Nodes that can be considered assembly points or rescuers' first-aid areas (e.g. wide open spaces, where people spontaneously gather and can safely wait for rescuers' arrival) [6]	Alpha-numeric code
Links	The connection between two different nodes. A path composed of segments with different features can be schematized as an ensemble of consecutive links, divided by nodes.	Alphabetic code

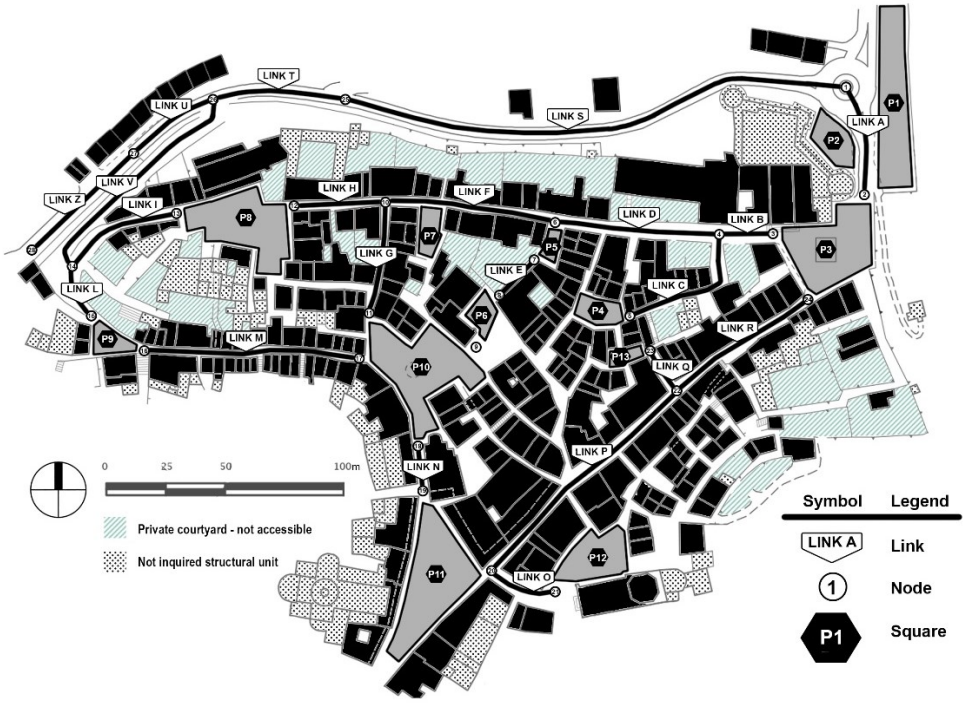

[10] A Square is a particular node where building facades projections do not entirely cover the square's area itself. Such condition allows Squares to hold people during an emergency. For this reason, Squares need an ad hoc earthquake evaluation.

Figure 8 Example of a graphical representation of the path network scheme in a historical city centre map: Links (black segments) are delimited by Nodes placed in each plano-altimetric or structural variations (Black circles). Squares defined according to Table 6, are highlighted by black polygons.

According to literature studies collected in Section 2.1 about which factors influence the seismic response of an urban path network, this thesis proposes to subdivide them into six categories. The collected risk factors are combined in topics and discussed in the following sub-sections. Following the approach of other literary works [58,81,82], each parameter can be associated with different conditions, named "alternatives" (generally between two and five), which are furtherly attributed to a numeric value. In such a way, this work tries to quantify numerically a risk index for each network element defined above. All the risk influencing factors are defined by considering both the path network itself (intrinsic vulnerability and exposure conditions) and the elements that could directly compromise its state (extrinsic vulnerability and seismic hazard).

Path analysis and Exposure. Link accessibility is firstly given to preventively investigate only usable paths in emergency conditions. Subsequently, within the exposure factor is necessary to assess the role of the path network element and the importance that it assumes among the others during the emergency through functional analysis. Hence, some links can constitute an access path to the urban centre of primary importance in emergency phases. Otherwise, they represent an interconnection among safe areas or strategic buildings [30]. Moreover, the link itself can be considered an effective evacuation path only in the case of the absence of barriers, traffic lane dividers, bollards, or further obstacles that could impede or make difficult the passage reducing the available width of lanes. Another aspect that influences exposure (according to its definition provided in Section 1.1) is the average flow referring to a semi-quantitative assessment of the traffic along the path. Speaking about squares the correspondent parameters involve their intended use: wide crossroad, characterized by the multi-directional movement of both vehicles and pedestrians; pedestrian zone; parking area, characterized by possible available areas limitations due to parked vehicles. In addition, other square-specific parameters refer to the presence of architectural elements like street furniture, fences, low walls, trees which could be widespread in the square area and could interfere with pedestrians' motion/rescuers' access or emergency operations.

Geometric features. The link length is not a futile parameter to consider, indeed it could affect the travel time required to reach a destination by an evacuee. At the same time, the link width can influence the evacuation flows especially in overcrowding conditions. Moreover, the presence of interfering obstacles (e.g.: urban furniture, parked vehicles, debris presence due to damaged buildings, etc) could also limit the effective width of the path. Longer and narrower links are considered more hazardous than others. The related dimensional parameters are the link width W and length L. The area extension can be considered as a geometrical parameter for squares evaluation.

Physical-structural features. Street surface conditions (asphalted, paved or rough) could influence the streets' accessibility also related to their conservation state. Indeed street

pavement typologies and their state of conservation could affect the evacuation process causing pedestrians accidents or injuries during the escape [83]. Potential slide down of soil and rocks on both sides of the path and the preventing measures (e.g.: retaining walls) are identified to include risks due to the blockage of the path to evacuees and rescuers' vehicles, causing problems and delays to the emergency mobility [54]. Furtherly, a specific parameter is innovatively added in this evaluation process to include the existence of caves, cisterns, and natural or artificial underground structures that are typical of the historical urban environment [56]. These subsoil vulnerable elements could provoke instability leading to local street collapses. Additionally, the presence of pipes placed at insufficient depths could be considered as weak points for the street integrity in case of an earthquake. Lifelines are distinguished between [84–86]: low-risk lifelines such as electrical power or water supply systems with restrained pipes dimension; high-risk lifelines like gas and oil distribution networks. In this way, the eventual cascade effects connected to pipelines of gas or water supply systems (i.e.: dangerous gas leaks, fires, local soil destabilization) are evaluated as well.

Extrinsic vulnerability. The here developed method following a holistic perspective is aimed at considering among the potential state of a paths network element also the extrinsic vulnerability aspects. Debris presence due to collapsed buildings indirectly influences the availability of passing through a link or the integrity of a square. The related rapid surveys are here performed by taking advantage of an existing street vulnerability method [4]. The method is referred to aspects concerning extrinsic vulnerability assessment by directly inquiring about the buildings facing paths or squares. Ad hoc vulnerability index for links (V_{link}) is provided. Thus, such index considers a building incidence I_b on the studied link defined as the ratio between building L_b and link L lengths, respectively ($I_b = L_b/L$). At the same time the building vulnerability V_b is expressed according to the macroseismic method of Lagomarsino and Giovinazzi 2006 [3] to ensure a quick application at historical city centre scale. For each link j, $V_{link,\,j}$ is calculated as shown in Equation 18 by considering all the buildings facing the link j:

$$\mathrm{V_{link,j}} = \sum_{b \in j} \mathrm{V_b} * I_b \tag{18}$$

In order to compare links belonging to the same urban centre, the obtained vulnerability index must be normalized by the maximum $V_{link,j}$ obtainable in the studied scenario. According to [2,4], $V_{N\ link,\,j}$ values are subdivided into four intervals (i.e.: four alternatives).

Seismic hazard. Seismic hazard factors are innovatively introduced by this work on path risk assessment. The observation of real cases highlights how both base and local features of soil can be relevant for the paths' damaging, because of cracks or damages occurring on the ground and directly affecting the link/square state [54]. Taking advantages of Eurocode 8 [87] this approach proposes to evaluate the seismic hazard basing on the design ground acceleration (a_g) [g] related to each seismic zones, the ground types and also, according to Italian building code, on the topographic amplification factors [88]. The adoption of the

Eurocode 8-based criterion ensures a quick application even if low-detailed resources and no geotechnical documentation or local surveys on soil (such as micro zoning studies) are available [89]. Here, the risk influencing factors discussed above are organized in two assessment tables one valid for the assessment of the link (Table 7) and the other where squares specific parameter are added/substituted to the ones specific for links (Table 8).

The proposed method arrangement and the assessment table construction are based on similar literature work presented by [58] already discussed in Section 2.1. Further consideration among differences between the literature reference and the proposed one will be provided below (Table 9). Furthermore, it is necessary to specify that nodes assume the maximum risk index of links converged in it. Additionally, parameters linked to specific street typologies (e.g.: bridges, viaducts, and tunnels) are omitted in the current work proposal because they are rarely present in historic city centres.

Table 7 Link assessment table: factors, parameters, and associated alternatives are reported to evaluate the risk-influencing aspects of links within the urban paths network. IDs for factors and parameters are assigned to connect this table with Table 10.

ID	Factors	ID	Parameters	Alternatives
A	Path analysis	A.1	Link code	-
			1° Node code	-
			2° Node code	-
		A.2	State	Clear
				Partially obstructed
				Obstructed
B	Exposure	B.1	Street type	Interconnection
				Access
		B.2	Direction of travel	Single
				Double
		B.3	Carriageway	Separated
				Unique
		B.4	Path type	Urban
				Suburban
		B.5	Average Flow	Low
				Medium
				High
C	Geometric features	C.1	Length (m)	$0 < L \leq 0.33\ L_{max}$
				$0.33\ L_{max} < L \leq 0.67\ L_{max}$
				$0.67\ L_{max} < L \leq L_{max}$
		C.2	Width (m)	$0.67\ W_{max} < W \leq W_{max}$
				$0.33\ W_{max} < W \leq 0.67\ W_{max}$
				$0 < W \leq 0.33\ W_{max}$
D	Physical-structural features	D.1	Finishing surface	Asphalted
				Paved
				Rough
		D.2	Potential landslides	No landslide, retaining walls on both sides
				Landslide, retaining walls in one side

				Landslide, no retaining walls
		D.3	Underground elements	Low-risk pipes
				High-risk pipes
				Caves, cisterns, or cavities
		D.4	Conservation state	High
				Medium
				Low
		D.5	Street Typology	Level link
				Hillside link, with retaining walls
				Hillside link, without retaining walls
				Tunnel
				Bridge and viaduct
E	Extrinsic vulnerability	E.1	V_{Nlink}	$0 < V_{Nlink} \leq 25\%$
				$25\% < V_{Nlink} \leq 50\%$
				$50\% < V_{Nlink} \leq 75\%$
				$75\% < V_{Nlink} \leq 100\%$
F	Seismic hazard	F.1	Design ground acceleration (a_g)	$a_g \leq 0.05$g
				$0.05\text{g} < a_g \leq 0.15$g
				$0.15\text{g} < a_g \leq 0.25$g
				$a_g > 0.25$g
		F.2	Ground-type	A
				B
				C
				D
				E
		F.3	Topographic amplification factor	T1
				T2
				T3
				T4

Table 8 Squares assessment table: parameters and associated alternatives are reported only for factors B, C, and D (and the related parameters) that are different from the links assessment table according to Table 6 definitions. The other factors (A, E, and F) are the same as reported in Table 7.

ID	Factors	ID	Parameters	Alternatives
B	Exposure	B.1	Usage	Wide crossroad
				Pedestrians' zone
				Parking area
		B.2	Presence of obstacles	Absence
				Presence
		B.3	Square type	Urban
				Suburban
		B.4	Average Flow	Low
				Medium
				High
C	Geometric features	C.1		$0.67\ A_{max} < \text{A} \leq A_{max}$
				$0.33\ A_{max} < \text{A} \leq 0.67\ A_{max}$
				$0 < \text{A} \leq 0.33\ A_{max}$

D	Physical-structural features	D.2	Potential landslides	No landslide, retaining walls in more than one sides Landslide, retaining walls in one side Landslide, no retaining walls
		D.5	Square Typology	Level Square Hillside Square with retaining walls Hillside Square without retaining walls

The final Risk Index $I_{R,j}$ for each link and square can be pursued according to three different calculation approaches. The risk-influencing factors proposed in Table 7 and Table 8 are here combined. Both approaches are operatively based on a Multi-Criteria Decision Making process [90] in which the above factors do not necessarily have the same relevance in the overall risk index. The main features of the three calculation approaches are resumed in Table 9 and the main differences between the literary work assumed as reference are highlighted as well.

Table 9 Features of the three calculation approaches are reported with the aim to compare the introduced modification in respect to [58].

	Task-4 SAVE project [58]	Modified Cherubini's approach	Expert judgment	Analytical Hierarchy Process
Modified parameters and factors	-	Added the parameter "Underground elements" in the Physical-structural features factor		
	-	Added the factor "Extrinsic vulnerability" with a single parameter (V_{link})		
	-	Added the factor "Seismic hazard" with the following parameters: "Design ground acceleration", "Ground-type" and "Topographic amplification factor"		
Values	Cherubini's approach	Values are given following Cherubini's approach	Values are given by the Expert judgment	Given through Analytical Hierarchy Process
Weights	Cherubini's approach	approach	Weights are given by the Expert judgment	Two sets of weights are given for each factor and parameters through the Analytical Hierarchy Process
$I_{R,j}$ calculation approach	The weighted sums are firstly normalized on factors maximum obtainable value and then on related weight for each factor	The weighted sum is firstly normalized on factors maximum obtainable value and then on related weight for each factor	The index is obtained through the sum of Sp_{iK} values weighted on related Wc_K for each factor	The calculation is given by a first weighted sum on Wi_K for each parameter and then on Wc_K for each factor
$I_{R,j}$ formulation	$\sum_{K=1}^{5}\left[\frac{(\sum_i Sp_{iK})}{(\sum_i Sp_{iK}^{MAX})} * Wc_K\right]$	$\sum_{K=1}^{5}\left[\frac{(\sum_i Sp_{iK})}{(\sum_i Sp_{iK}^{MAX})} * Wc_K\right]$	$\sum_{k=1}^{5}\left(\sum_i Sp_{iK} * Wc_K\right)$	$\sum_{k=1}^{5}((\sum_i Sp_{iK} * \mathrm{Wi_K}) * Wc_K)$

Modified Cherubini's approach. In detail, the first calculation approach based on Task-4 of the SAVE project [58], tries to fill its lacks through some changes including influencing factors and parameters defined in previous Table 7 and Table 8. Each factor containing influencing parameters is associated with a weight to establish a hierarchy of influence (values and weights are reported in Table 10). In this case, the final Risk Index $I_{R,j}$ is assessed through the Equation 19:

$$I_{R,j} = \sum_{K=1}^{5} \left[\frac{(\sum_i Sp_{iK})}{(\sum_i Sp_{iK}^{MAX})} * Wc_K \right] \quad (19)$$

where:

- Sp_{iK} is the value conferred to the *i*-th parameter of the *K*-th factor;
- Sp_{iK}^{MAX} is maximum attributable value to the *i*-th parameter of the *K*-th factor;
- Wc_K is the weight related to the *K*-th factor;

According to [58], Equation 20 permits to obtain the correspondent normalized index for each link ($I_{Rn,j}$):

$$I_{Rn,j} = \frac{I_R}{\sum_{k=1}^{5} Wc_K} \quad (20)$$

Expert Judgement. The second approach establishes an alternative hierarchy among factors based on expert judgment [91]. Different weights are associated with each factor and different values are linked to each alternative according to Table 10**,** while considering the Expert Judgement approach, thus another formulation for Risk Index $I_{R,j}$ assessment is defined in Equation 21:

$$I_{R,j} = \sum_{k=1}^{5} \left(\sum_i Sp_{iK} * Wc_K \right) \quad (21)$$

According to the previous definition of Sp_{iK}, Sp_{iK}^{MAX} and Wc_K, Equation 22 normalizes the obtained Risk Index:

$$I_{Rn,j} = \frac{I_{R,j}}{\sum_{k=1}^{5} (\sum_i Sp_{iK}^{MAX} * Wc_K)} \quad (22)$$

Analytical Hierarchy Process. The third proposed way to reach the Risk Index $I_{R,j}$ can be supported by the Analytical Hierarchy Process (AHP) developed by [82] and used with the same purpose in this field by [92]. This approach needs to introduce a second level of weights to each parameter (Wi_K) establishing an influence scale among them. The AHP considers that the sum of conferred weights must be equal to one both for factors and for each parameter. In this way, the generated Risk Index varies between zero and one and it does not require further normalization. The weight distributions (reported in Table 10 in AHP section)

are obtained through the open-source tool AHP Online System[11] and the calculated Ratio of Consistency (lower than 10%) confirms the acceptability of the proposed weights. Equation 23 shows the proposed calculation of the Risk Index, which is gained by defining $\mathrm{Wi_K}$ as the weight related to the *i*-th parameter:

$$I_{R,j} = \sum_{k=1}^{5}((\sum_{i} Sp_{iK} * \mathrm{Wi_K}) * Wc_K) \tag{23}$$

Regardless of the chosen approach, $I_{R,j}$ and $I_{Rn,j}$ can be collected in tables and graphically represented on urban centre maps to directly recognise where most dangerous paths (links) are collocated and how the safe areas (squares) are connected between them.

Table 10 Weights of factors (Wc_K), weights of parameters (Wi_K) and the related values (Sp_{iK}) are reported for the three different considered approaches: Modified Cherubini's approach, Expert judgment, and the Analytical Hierarchy Process.

		Modified Cherubini's approach		Expert judgment		Analytical Hierarchy Process (AHP)		
Factor ID	Parameter ID	Wc_K	Sp_{iK}	Wc_K	Sp_{iK}	Wc_K	Wi_K	Sp_{iK}
B	B.1	0.2	0.4	0.333	0.4	0.045	0.272	0.5
			0.6		0.6			1
	B.2		0.6		0.6		0.272	0.5
			0.1		0.1			1
	B.3		0.2		0.2		0.036	1
			0.1		0.1			0.5
	B.4		0.6		0.6		0.272	1
			0.3		0.3			0.5
	B.5		0.1		0.1		0.147	0.33
			0.3		0.3			0.67
			0.5		0.5			1
C	C.1	0.40	0.1	0.667	0.1	0.067	0.667	0.33
			0.5		0.5			0.67
			1		1			1
	C.2		0.2		0.2		0.333	0.33
			0.4		0.4			0.67
			0.6		0.6			1
D	D.1	0.80	0.3	1.000	0	0.381	0.143	0.33
			0.55		0.3			0.67
			0.8		0.5			1
	D.2		0.1		0		0.429	0.33
			0.8		0.8			0.67
			1		1			1

[11] AHP Online System available at: https://bpmsg.com/ahp/ last access: 23/11/2020.

	D.3		0.1		0.33		0.143	0.33
			0.6		0.67			0.67
			0.8		1			1
	D.4		0.3		0		0.143	0.33
			0.55		0.3			0.67
			0.8		0.5			1
	D.5		0.1		0		0.143	0
			0.4		0.4			0.25
			0.5		0.5			0.5
			0.6		0.6			0.75
			0.8		0.8			1
E	E.1	0.60	0.25	1.000	0.25	0.126	0.126	0.25
			0.5		0.5			0.5
			0.75		0.75			0.75
			1		1			1
F	F.1	1.00	0.25	1.000	0.25	0.381	0.400	0.25
			0.5		0.5			0.5
			0.75		0.75			0.75
			1		1			1
	F.2		0		0		0.400	0
			0.25		0.25			0.25
			0.625		0.625			0.5
			1		1			1
			0.75		0.75			0.75
	F.3		0		0		0.200	0
			0.25		0.25			0.5
			0.25		0.25			0.5
			0.5		0.5			1

Links and squares assessment tables are compiled for a real paths sample[12] concerning Italian historical city centres struck by the 2016 Central Italy seismic sequence, the 2012 Emilia Romagna region (Italy), and the 2009 Aquila (Italy) earthquake (Figure 9 reports some examples). $I_{R,j}$ and $I_{Rn,j}$ values are calculated following the three risk index calculation approaches (Modified Cherubini's approach, Expert Judgment, and the AHP approach) to evaluate their capabilities in describing possible critical conditions in post-earthquake scenarios and offer a preliminary validation of each one. To this aim, risk index – damage-state level correlations are traced, based on damage levels given by [1].

[12] The database is uploaded as supporting file and also available at: https://goo.gl/yzHNTQ last access: 23/11/2020

Figure 9 Urban scenario damages in the Central Italy seismic sequence in 2016: on the left side, street pavement cracking due to unstable slopes and landslides-induced effects (Intrinsic vulnerability); right side, a view of Amatrice's street (RI, Italy) blocked by ruins formation provoked by buildings collapse; debris impeded rescuers' interventions (Extrinsic vulnerability). Single video frames by "Corpo Nazionale dei Vigili del Fuoco" http://www.vigilfuoco.tv/ (last access 23/11/2020) re-elaborated by the author.

The damage level of each path is evaluated by comparing photographic documentation of links before and after the earthquake event, and by adopting the description of post-earthquake damages effects according to the Road Damage Scale (*RDS*) [1]. RDS can vary from 0 to 5 (integer scale). The adopted damage scale for paths considers damages due to landslides, unstable slopes and cracks to the street, debris presence along the street, and presence of failed external elements that could impede partially or completely the path accessibility (Figure 10 reports an example of damage state assignation to a case study link). Then, $I_{Rn,j} - RDS$ pairs are organized to evaluate if a higher risk index corresponds to a higher link damage grade. the risk index could demonstrate capability in describing possible critical conditions in post-earthquake scenarios. According to general tri-linear trends in earthquake safety and damage assessment, by including *fragility curves* and studies on seismic vulnerability [3,51,64,93], a linear interpolation between $I_{Rn,j} - RDS$ pairs is then performed according to previous studies' approaches [1]. Finally, a comparison of produced regression lines is provided through the evaluation of the coefficient of determination R^2 to define the more suitable calculation approach (based on data fitting effectiveness) among the considered ones. The best performing calculation approach to determine the risk index, (i.e.: the one having the highest coefficient of determination R^2) is chosen to be applied on a significant[13] case study referring to an Italian historical urban centre (Offida, Lat. 42.93, Long. 13.70), with the purpose to give a real application of the research. To conclude, a graphical representation of this risk index for urban paths network at the urban scale can be provided at two levels of detail: a Seismic Risk map aimed at supporting emergency management at a wide scale and the Priority Intervention map defined to assign resources for

[13]Seismic activity of Offida (Italy): https://emidius.mi.ingv.it/DBMI11/query_place/ last access on 23/11/2020.

risk-reduction strategies. The Priority Intervention Indices I_{IP} are obtained according to the Equation 24 below:

$$I_{IP} = I_{Rn,j}/I_{max,S} \tag{24}$$

According to literature studies [2,81], each map adopts four risk levels: Low risk (0%-25%), Medium-Low risk (25%-50%), Medium-High risk (50%-75%), High risk (75%-100%).

Figure 10 The left side of the figure reports the description of the third Road Damage Level according to the Road Damage Scale (RDS) [1], While the right-side displays a damaged urban street of Norcia (Central Italy Earthquake 2016) adopted as an example.

Alternative literature studies on emergency path availability (according to Section 2.1) allow to differently evaluate the obstruction of evacuation paths due to ruins formation by employing geometrical and damage-related criteria. In such cases, the preliminary evaluation of the risk index can be totally useless in case of a building collapse that impedes the rescuers' access point. Although the literature review (Section 2.1) provides different methods, only six (reported in Table 1) are deeply investigate and selected to be here applied mainly because the others do not fit with the research aim strictly limited to inquire critical condition in the emergency of historical urban fabrics with particular focus on masonry building typology. Other methods cited in Section 2.1 are excluded from the analysis because of their computational commitment and for the specific data required to be applied, also they could not be considered as methods of rapid implementation. For such reason, this thesis is aimed at individuating which one of such methodologies can be considered as the more affordable for this work scopes, by comparing and applying them on the same sample of urban street faced by vulnerable buildings. Such comparisons are made by combining the predicted result from a method application and the corresponding real-world effective observation registered after an earthquake. This last detention is possible to be realized another time thanks to the Satellite Grading maps visualization of Copernicus European project that is here used defining if the street-facing each building in the sample results blocked by debris accumulation. The involved sample composed of masonry buildings suffers from 1st to 5th damage grade according to EMS-98 scale and it is placed in a limited area comply the following urban centres: Accumoli, Amatrice, Arquata del Tronto, Capodacqua and Illica stricken by the Central Italy seismic sequence in 2016 (42.7,13.23), on 2016/08/24 03:36:32

(UTC+2), Mw=6.0[14]. According to previous works [46], vulnerability evaluation, structural units height (h) and facing streets width (W) are remotely evaluated thanks to the large availability of photographic documentation.
Comparisons could outline the following status:

1. correspondence between predicted and real path condition;
2. overestimation, in case the considered method predicts a "blocked" path, but the real-world observation refers to "clear" path conditions. In this case, the method prediction produces a conservative result;
3. underestimation, in cases the considered method predicts a "clear" path, but the real-world observation refers to "blocked" path conditions. In this case, method prediction produces an "unsafe" result.

For each method, the percentages of correspondence, overestimation, and underestimation cases are evaluated. The most reliable methods should minimize the underestimation cases to err on the side of caution while maximizing the correspondence cases.

2.3.2 A novel risk index for urban paths network and its availability in case of building collapses

The holistic paths network risk index proposed in Section 2.3.1 is here tested in its reliability. Among the three calculation approaches the individuation of the best performing is pointed out. Following the comparative approach of the previous methods tests outlined in Section 2.2.1 further correlations are here verified. The tri-linear regressions are offered in Figure 11 between noticed street damages (RDS values) and the assessed new indices. For both methods, a trilinear trend can be confirmed. Table 11 summarizes and compares the analytical results of such correlations demonstrating an R^2 values generally acceptable. While the modified Cherubini's approach has the lowest R^2, the Expert Judgement approach seems to expresse the more reliable regression model in respect to the other two approaches. However, the AHP-based approach is developed so as to follow an evaluating calculation approach previously applied in other studies (i.e.: [81,92]) that limits subjective interpretations about weights assignment. Anyway, comparing Appendices Table A 1 results among the three approaches they are slightly different (supported by an average percentage difference equal to the 5%) by confirming their similarities. For these reasons, could be preferable to adopt the most rigorous calculation format the one that follows the AHP.

[14] Seismic database: http://cnt.rm.ingv.it/en/event/7073641 last access 23/11/2020

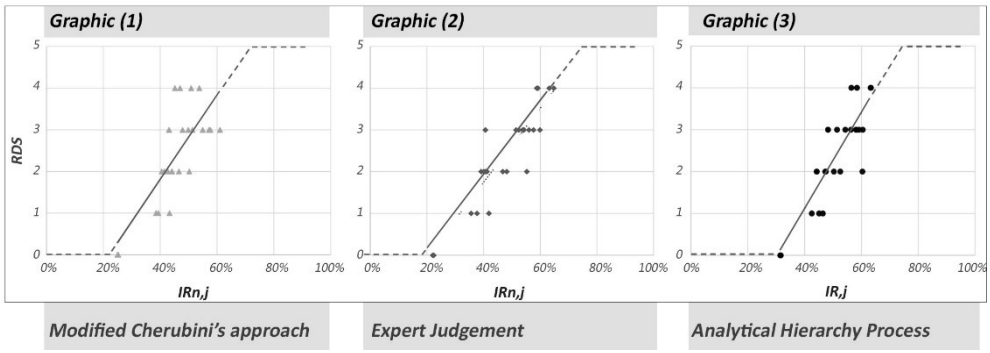

Figure 11 Tri-linear correlation between analysed path risk indices ($I_{Rn,j,}$ and $I_{R,j}$) and related street damages levels (*RDS*): Graphic (1) Modified Cherubini's approach; Graphic (2) expert judgment; Graphic (3) Analytical Hierarchy process. Dashed lines predict expected trends in domains where data samples are not currently present. Equations for the three regression trends are offered in Table 11.

Graphical representations are used also to note that both graphs present a lower risk index limit (about 20-30%) corresponding to the absence of damages. Indeed, the final risk index cannot be close to zero because of its construction that considers some risk-affecting parameters that are always present and different from zero (e.g.: the local seismic hazard). At the same time, from *RDS* 4 to *RDS* 5 the trend is only traced by forecasting it because of the lack of real-world data, due to the currently analysed sample characterization. The reliability of the proposed risk index is confirmed by observing that for higher the $I_{Rn,j}$ the *RDS* values increase. The novel holistic method leads to a satisfying sensitivity of the links assessment tables independently reached from the three involved approaches.

Table 11 Comparisons among proposed approaches in terms of trend lines equations. The table also shows data about the domain in terms of risk index and the obtained R-squares for $I_{Rn,j}$- RDS pairs correlations.

Compared approaches	Equations	Domains	R^2
Modified Cherubini's approach	$\begin{cases} RDS = 0 \\ \text{RDS} = 10.13\, I_{Rn,j} - 2.24 \\ RDS = 5 \end{cases}$	$I_{Rn,j} < 24\%$ $24\% \le I_{Rn,j} \le 73\%$ $I_{Rn,j} > 73\%$	0.57
Expert judgment	$\begin{cases} RDS = 0 \\ \text{RDS} = 8.86\, I_{Rn,j} - 1.79 \\ RDS = 5 \end{cases}$	$I_{Rn,j} < 20\%$ $20\% \le I_{Rn,j} \le 77\%$ $I_{Rn,j} > 77\%$	0.78
Analytical Hierarchy process	$\begin{cases} RDS = 0 \\ \text{RDS} = 11.46\, I_{R,j} - 3.47 \\ RDS = 5 \end{cases}$	$I_{R,j} < 30\%$ $30\% \le I_{R,j} \le 74\%$ $I_{R,j} > 74\%$	0.74

Graphically representing the results of novel risk index applied to the case study paths of Offida historic centre the risk maps permit to immediately have under control the overall

risky situation of the urban fabric. The Seismic risk maps allow us to compare maps of different city centres thanks to its risk index absolute scale representation. For this reason, from a general point of view, the paths that belonging to the sample seem to be all affected by the same Medium-Low level of risk. These results are also due to the involuntary homogeneity of the adopted urban fabric. However, some critical conditions can be determined especially for those links that show higher risk, for instance, the link "V" is located close to slope edges with possible landslides. In addition, the seismic risk map could be highly influenced by exposure factors. In fact, the same "V" link constitutes access to the urban centre, and it is used as a one-way street. For these reasons, it results in Medium-High risk. Otherwise, the intervention priority map because of its different formulation (see Equation 24) permits a deep detection of risk variation between links of the same urban paths network. Figure 12 highlights links "S" and "T" with a Medium-High priority level because they are placed near areas prone to landslides. Moreover, links "M" and "R" reach the same risk level due to the presence of facing buildings with relevant seismic vulnerability. Furtherly the critical conditions of link "V" previously described are here remarked as well confirming its strategic role for emergency planning. Additionally, Appendices Table A 2 gives the possibility to discuss partial results of the assessed risk index values. In fact, for each element of the network, due to its structure, the risk index permits to decompose itself in values referred to every single risk main section (i.e. accessibility, exposure, geometrical features, physical and structural features, extrinsic vulnerability, and hazard). Taking advantage of this subdivision the method is capable to justify and determine case by case the effective causes of a high-risk level rather than a low one, in this sense emergency planners can inquire punctually which factor leads inquired elements to a specific risky situation and they can promote ad hoc interventions.

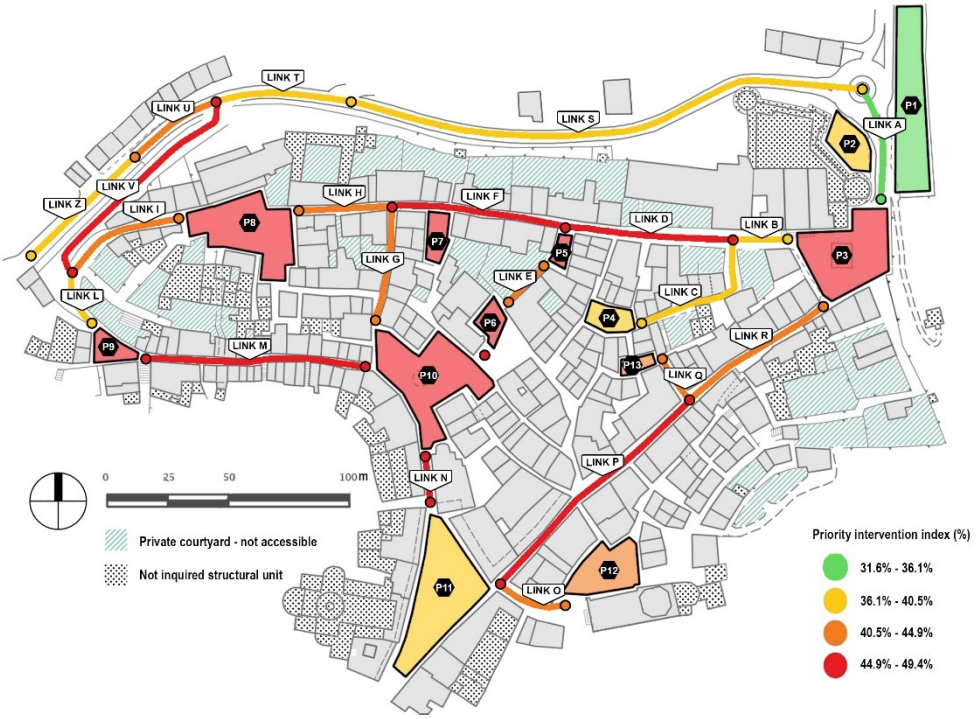

Figure 12 Intervention priority map of the emergency paths network of Offida (Italy) case study

To conclude on this presented method, all the risk-influencing factors are evaluated and merged from a holistic point of view. In fact, the overall evaluation does not involve a description for separate layers [2]. At the same time, the adoption of quick evaluation methods also guarantees to use it straightforwardly by detecting wide urban historical areas. In particular, differently from other previous studies, it tries to combine path intrinsic and extrinsic vulnerability. Special attention is here paid to eventual structural failures, landslides, or street pavement cracking. In respect to previous researches, the proposed methodology considers important factors that could represent vulnerable elements in historical urban areas such as caves, cisterns, or hypogeum hidden under street pavement or lifelines, pipes, and culverts according to the base reference method [58]. Moreover, it can also give significant basis for the integration of exposure factors in such evaluations.
Then, a preliminary methodology validation was performed, and a good agreement was found. Anyway, outlined risk maps allow to have under control the overall risk situation of emergency paths in historical centres and so to provide evaluation tools for scenario creation and emergency planning. Indeed, such results could suggest which links should be excluded from selected paths because of their high-risk level, and which could be considered safer toward an emergency plan definition. local authorities could take advantage of this method

to suggest where directing risk-reduction interventions and resources following the order of intervention priority.

As already explained in Section 2.3.1 from an emergency planning point of view, whatever effort aimed at evaluating the seismic risk (by considering streets intrinsic vulnerability issues discussed above) of an urban path could result inadequately and totally useless if the considered path is obstructed by ruins formation due to buildings collapse. Therefore, the most reliable rapid method has to be determined to perform this preliminary control. However, such obstructions could occur in relation to a certain seismic input. In other cases, the limited presence of debris along the lanes could not constitute an impediment to the passage of rescuers' vehicles but it could slow down the evacuation process. Hence, the path availability control should be associated in each case with a deeper paths network risk index evaluation.
Appendices Table A 3 reports the results of the tested sample (made by 50 structural units suffered by the Central Italy seismic sequence in 2016) in terms of "blocked" or "clear" paths. Each one of the existing rapid methods discussed in Table 1 of Section **Errore. L'origine riferimento non è stata trovata.** has been applied to every single building and the related street of the inquired sample.
Then, outcomings of such applications are compared firstly to the real-world conditions of the sample after the occurred seismic event (verifying their reliability) and secondly among them to determine which is the best performing (Table 12).

Table 12 Percentage results of comparisons between each considered method and real-world scenario conditions are reported indicating the total percentage of cases of correspondence (C), Overestimation (O), and their sum (C+O) on the overall sample made by 50 structural units associated to their underlying urban streets.

Method	*Limit Condition for the Emergency (LCE)*	*Ferlito and Pizza*	*Debris estimation criterion 1*	*Debris estimation criterion 2*
Ref.	[48]	[2]	[51]	[70]
C	64%	52%	50%	60%
O	36%	48%	2%	26%
C+O	100%	100%	52%	86%
Method	*Artese Achilli*	*Observed Artese Achilli*[15]	*k95 macroseismic damages-based*	*Observed macroseismic damages-based*[16]
Ref.	[72]	-	[4]	-
C	46%	76%	64%	96%
O	12%	2%	36%	4%
C+O	58%	78%	100%	100%

[15] This method is based on the *Artese Achilli* [72] and obtained by substituting of the damage prevision algorithm with the damage observed from a real-world event (a better description is provided in the followings)

[16] This method is based on the *k95 macroseismic damages-based* [4] and obtained by substituting of the damage prevision algorithm with the damage observed from a real-world event (a better description is provided in the followings)

Discussing percentages of comparisons between methods application and the effective conditions it emerges that the *LCE* one predicts correctly the street blockage in 64% of cases but_for the remaining 36% a considerable overestimation is noticed. *Ferlito and Pizza's* method shows a correspondence for the 52% of cases and the remaining 48%, the method predicts blocked some paths that in real conditions are not affected by such damages and they result available for rescuers passage. Nevertheless, both methods do not lead to underestimation errors. Thus, they could be used for the emergency plan definition according to a conservative approach. Anyway, they seem to be not the most appropriate ones to suggest available paths to rescuers. In fact, too many streets could be wrongly predicted as unavailable, slowing down the emergency team's arrival.
Similar considerations are then traced for the *debris estimation criterion 1* proposed by [51] Avoiding its implementation in urban emergency planning because of its scarce capability in predicting correctly the blockage of the path (in 48% of cases the method suffers from underestimation by declaring as clear the blocked paths in real conditions). On the contrary, in the other approach *debris estimation criterion 2* by [70] in 60% of cases the algorithm predicts correctly the path conditions. While in 26% of cases, the method declares as blocked the paths differently from the reality of the Satellite images. In the remaining 14%, the algorithm errs because of the employed vulnerability assessment method that underestimates the vulnerability of buildings suffered by very heavy structural damages. The *debris estimation criterion 2* confirms better reliability rather than the *debris estimation criterion 1* since it limits the underestimation occurrences due to a better method to esteem the buildings' vulnerability and to its capability to influence results by also considering the buildings height and streets width ratio.
Passing through the analysis of the macroseismic damage-based approaches the one named by *Artese Achilli* evidences a relevant percentage of cases 46% where the blockage of the path is correctly predicted. Although this method considers not only geometrical features but also the macroseismic damage grades as a function of buildings vulnerability and seismic intensity, it considerably errs underestimating the blockage in 42% of cases. A further reliability test can be performed on such *macroseismic damages-based* approaches by substituting the damage grade prevision assumed by the method with the effective damage grade observation on a real post-earthquake scenario according to the EMS98 scale (made possible thanks to the large availability of seismic damages photos). Thus, the *Observed Artese Achilli* reveals a notable increase in reliability until 76% of correspondences. However, an underestimation of 22% is also noticed confirming previous observations of the original method application. Finally, the *k95 macroseismic damages-based approach* shows the punctual correspondence between the predicted availability of paths in emergency and the real-world conditions in 64% of analysed sample cases. The residual 36% of the algorithm tends to overestimate the path blockage. Hence, this method provides the best conservative results for 100% of inquired cases. Considering the same further reliability test done for the *Artese Achilli* approach involving the substitution of the damage prevision method with the observed one from the real-world the new "*Observed macroseismic damages-based*" is established. This investigation is additionally performed by subdividing the whole tested sample in the suffered five damage grades analysing separately the reliability in relation to the different damage grades. Its application results register an optimization of the percentage of correspondence between the prediction capabilities of this method. From real-world

images analysis emerges that the $h/W \geq 1$ constitutes the main driver in facing path blockage especially for buildings that suffered from high damages. In addition, low damage grades equal to 1st, 2nd, and 3rd does not interfere with rescuers' access, confirming the goodness of the literature limit fixed for the *macroseismic damages-based* method at the 4th grade. At the same time, buildings that suffered from the 4th damage grade are related to paths blocked in 71% of cases and to the 88% when buildings are affected by the 5th damage grade. The hypothesis that the higher the building damage grade suffered higher the probability that paths can be blocked by debris formation is confirmed. Figure 13 shows a typical result obtained from this method applied to a case study pair (i.e.: building and related path) reported as an example.

Figure 13 Comparison between the *Observed macroseismic damages-based approach* prevision and real conditions of path blockage for a building of the sample (Element ID code: 4.a_IL in Appendices Table A 3): the path is effectively blocked because the observed damage is higher than the 4th grade and the ratio between building height and street width is higher than 1.

To conclude on this theme, it can be affirmed that the current methodologies (often adopted by Local Authorities and Civil Protection Bodies) based only on geometrical aspects (i.e. building height and street width) seem to be affected by many scenario prediction limitations. Unfortunately, such approaches neglect the evaluation of other fundamental factors that alters the urban path network especially in historical contexts (i.e.: the vulnerability of the buildings). In this way, they ideally consider as "blocked" the majority of possible access/evacuation paths. Moreover, they do not take into account the possibility to predict different scenarios in terms of earthquake severity. For these reasons, macroseismic approaches are preferred, including the vulnerability and the earthquake severity as input data, which seem to be the most appreciable. At the same time, such methods can be preventively employed by safety planners (e.g.: Local Authorities and Civil Protection Bodies) to investigate different emergency scenarios. Figure 14 reports as an example of the application of the macroseismic damages-based method to predict path blockage on the general Offida case study. This map as the ones previously presented for the other developed inquiring methods constitutes a rapid visual screening of the whole urban centre conditions.

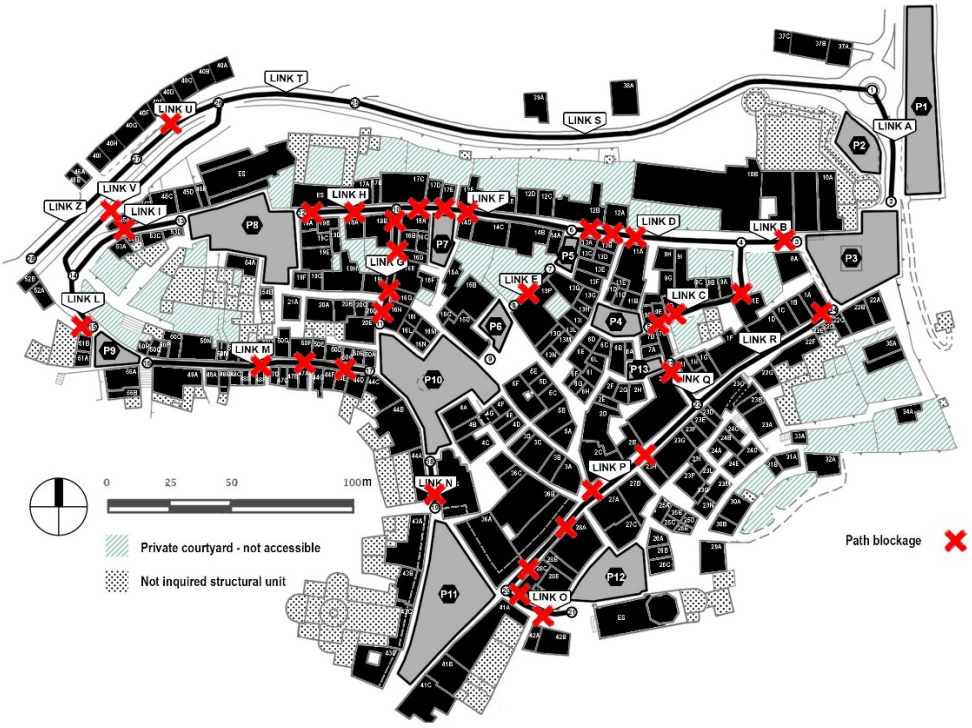

Figure 14 Graphical outputs of the application of the *macroseismic damages-based* criterion for paths blockage according to [70] on the Offida (Italy) case study

Chapter 3

3 The Behavioural-based approach

3.1 The human being in an emergency: an investigation on behavioural aspects

According to the definitions provided in Section 1.1 the exposure, intended as one of the risk components, is mainly oriented towards the human presence detection in the scenarios (e.g. to determine the impact in terms of potential human losses) [94,95]. However, the exposure should be also put into relation to social vulnerability issues. Both risk components are focused on human beings. But while exposure determines the people quantities in the BE, the social vulnerability, on the contrary, codifies typical or specific behavioural aspects performed by evacuees connected to the emergency (collective vulnerability, e.g. population risk awareness and response) and by individuating users' categories (individual vulnerability, e.g.: based on people ages and familiarity with places) [6,37,38]. On such basis, several types of research are developed in the last decades to improve the inhabitants' resilience through the study of human response to emergencies [96,97]. However, this kind of work can be retained relevant only if dealing with all the situations in which the disaster conditions can appear unpredictably or rapidly (SUODs) [98]. In these cases, the individuals' response to BE disaster-induced modifications is mainly critical during the first emergency phases, i.e. the evacuation process [99]. Indeed, occupants decide how to quickly behave and move while interacting with the surroundings and the other individuals, by performing or not, safe behaviors.

Literature underlines the existence of significant differences in disaster reaction between spontaneous behaviors and Civil Defence Bodies recommended rules [97]. Hence, understanding evacuees' spontaneous behaviors are essential to find proper strategies (e.g. emergency management, BE layout configurations, interventions on most vulnerable BE elements interfering with evacuees, interactive solutions based on rescuers-damaged population cooperation, individuals' training) to reduce the possibility of risky choices adoption, thus limiting the number of injuries and deaths resulting from heavy earthquakes [97]. Recent works (one among all [100]) on the analysis of earthquake evacuation were performed by underlining the importance of sustainable tools aimed at collecting data about spontaneous human behaviors during such events [99], which are generally characterized by particular disaster features that are difficult to be replicated in evacuation drills, such as the presence of debris and dust, the building damages, the ground shaking [96,97].

Although several methods and tools exist [96], a critical literature analysis underlines how the most significant and sustainable ones in the earthquake context seem to be mainly two [101–106]. Firstly, the analysis of real-world videotapes, e.g. by CCTV (Closed Circuit Television), whose approach was consolidated over time and allows to evaluate effective emergency situations without additional biases. Secondly, the novel immersive technologies like the Virtual Reality (VR)-based ones, which can ideally reproduce the earthquake-prone

BEs with a high level of realism [106] and by considering complexity issues (e.g. BE features, earthquake-induced damages).
Besides what it concerns the immersive virtual reality not influent for this study purpose, the material from surveillance cameras can be handled with the support of dedicated software for video analysis to extract specific actions and physical measures that can be easily employed for evacuation process modelling purposes. From a qualitative point of view, the emergencies videos are employed to directly individuate and categorize the human behaviors in reference to typical actions of responders, that could recur in each emergency situation or be specific for the earthquake case, as well as for an evaluated particular event or BE [23,107]. Additionally, detected behaviors are organized by associating them to a specific evacuation phase chronologically divided into [23]: pre-movement time, motion towards the evacuation target, safe area reaching. From a quantitative standpoint, output data can be obtained by tracking systems for pedestrians' trajectories, which allow evaluating, for every single individual, his/her instantaneous position, speed, and acceleration, to additionally derive fundamental diagrams of pedestrians dynamics (e.g.: speed-density and flow-density) [23]. Similarly, the individuals' time spent to reach a safe area from the starting point can be calculated to establish the diagram of people arrivals during the time and evaluate the overall BE evacuation capacity [99].
Further quantities involve [6]: (a) pre-movement times, in relation to the ground shaking and to the related self-protection activities; (b) distances among evacuees to avoid collisions, so as to additionally evaluate the possible density of crowds or the presence of social aggregation behaviors (e.g. shared motion decisions); (c) distances between evacuees and BE elements during motion towards a safe area, due to repulsion phenomena towards obstacles which can hinder or slow down the process (i.e. earthquake-damaged BE elements, debris). Existing literature works [28] take advantage of such data directly for developing evacuation simulation models. In microscopic modelling approaches (especially, Agent-based models and Social Force models) videotapes data can be essential to determine the factors that could influence every single agent's choice made in the evacuating environment depending on [13, 15, 17, 18]: the agents' surrounding conditions of the BE (i.e.: damages generated by the earthquake, presence of obstacles along pathways or debris formation along outdoor streets); interactions among other agents (e.g.: the attraction towards other evacuees and the necessity to establish group bounds; gathering into groups guided by an evacuation leader; repulsive mechanisms to avoid physical contact during the escape). Additionally, each simulated agent owns particular individual characteristics that influence his/her response to the surrounding stimuli. A decision tree creation made by actions that exposed people could perform in the aftermath of an earthquake can be obtained by videotapes data [101], depending on: seismic severity; social context/social shared identity, initial location of the individual (during the seismic event); activities performed when the earthquake occurred; age and gender of the individual. At the same time, individual motion quantities can be retrieved according to the videotapes data, mainly depending on age, gender, motion abilities.
Such existing simulation models to be employed requires specific input parameters not only, as previously debated, to create seismic-induced modifications to the scenario but also concerning the human figure and its main involved typologies. To this aim, in the following subsections, a unique methodological framework for exposure and social vulnerability detection is outlined. The novel proposed framework adopts specific literature-based methods in a combined, cooperative, and structured way. According to adaptability criteria

in line with previously proposed methodologies, the employed tools are not exclusive, but they could be replaced by other existing and validated ones. Quick methods collecting data from easily available data sources are preferred to: 1) avoid costly in situ surveys; and 2) permit to replicate the workflow by non-expert technicians. According to individual vulnerability issues, different BE users' typologies (e.g. for different ages and different familiarity with places) will be defined also considering time-dependent variations. The proposed framework provides also the possibility to rapidly detect possible exposure peak scenarios (in terms of people presence) by overlapping ordinary conditions to eventual mass gathering events from a multi-hazard point of view.

3.2 Methodology

3.2.1 BE users' typologies and their distribution the urban centre: time and space issues

According to individual vulnerability aspects, among the individuals that populate an urban centre, some users' typologies have to be determined in relation to specific features that could influence the evacuation process[94,95]. In fact, when an individual is used to frequent a specific place (that is an urban context) is also aware of its general layout by having an idea of possible escape paths, risky areas, or available spaces where to refuge. Otherwise, people that do not have familiarity with places can be easily stressed in case of emergency losing time to understand the right direction to follow in the evacuation. Additionally, the first typology could also have knowledge of predisposed evacuation and emergency plans. For such reasons, this work is focused on distinguishing these main possible different typologies: inhabitants, where local workers are also included, versus tourists or daily visitors, totally unaware of emergency dispositions.

Another factor to evaluate that constitutes a possible evacuation impediment regards the presence of people with eventual disabilities in motion during the escape. These aspects can be mainly related to the presence of disabled people, especially if within the urban fabric are located public facilities connected with homecare activities or hospitals. At the same time, a reliable indicator easy to detect of such motion impairments can be the ages of hosted inhabitants. In fact, elderly people record a lower motion speed during the evacuation than an adult. A similar consideration can be valid for children as well. Hence, knowing a specific condition that interests the studied urban centre constitutes a key aspect that cannot be omitted.

At this point the attention is moved to the exposure issue, hosted population quantities have to be esteemed. A critical peak of exposure could be defined in terms of the maximum human presence in the BE, so as to consider the maximum impact on direct (e.g. casualties due to buildings damage/collapse [94,110]) and indirect (e.g. evacuation related ones [38]) losses. The most rapid exposure evaluation could just consider the density of people (pp/km^2 where *pp* stands for the number of people) according to [9] and census databases referred to the considered urban centre (e.g.: national on-line census, local municipalities or tourist office) [95]. In rare fortune cases, census databases could be linked to the detailed position of the population (e.g. street survey-based; integrated with GIS tools), by mainly focusing on standard occupancy levels, e.g. residents [95]. However, the number and position of exposed

people can additionally vary over time and space essentially depending on uncertain factors collected and discussed in Table 13 below.

Table 13 Time and space issue influencing the human presence variation in the BE.

Human presence typologies and their combinations	Visitors	Inhabitants + neighboring of the local municipality area	Inhabitants + visitors	Visitors presence in mass gatherings events
People familiarity with places and emergency plans	Scarce familiarity with the urban spaces and with the emergency plans	Satisfying level of familiarity with spaces depending on their (frequent) BE attendance	Different familiarity levels	Generally scarce familiarity with the urban spaces and with the emergency plans
Time issue	By considering visitors' flows during the year: critical conditions in exposed individuals' presence (e.g. monthly) correspond to the periods with the higher number of tourists' presence (considering both daily visitors and holidaymakers).	By considering inhabitants and neighbors during the week: estimating critical conditions in exposed individuals' presence (e.g. weekly)	By considering inhabitants and visitors during the day: these analyses allow considering the variations during the working time and between night and day (e.g. sleep time, working time, working, and resting time).	Critical conditions characterized by a high crowd density can occur in the urban tissue (e.g. concert venue, festivals).
Space issue	Visitors can be mainly placed in accommodations (e.g. hotels, tourist homes, such as for night-time periods) depending on their effective capacity, or even according to a homogenous dispersion (including public buildings, as for day-time periods).	Local markets, recurring fairs, or festivities hosted by the BE bring in town habitual visitors from near towns or peripheral areas that populating open spaces.	For some municipalities (e.g.: tourist cities/areas), further evaluations should consider the daily presence of individuals spending their time in some urban attraction.	Specific risk-increasing BE features (e.g. in historical scenarios, the crowd in narrow spaces) have to be considered. Such an event in the BE can be overlaid to the critical conditions for resident people obtaining overcrowding conditions among narrow urban environments.
References	[111]	[112]	[95]	[112]

Census databases and municipal tourism promotion companies, regional tourism management bodies, trade organizations[17] can be jointly inquired to esteem the capacity [pp] and the related people positioning in the BE layout. To do this, Table 14 reports specific references for the Italian case-study application. Hence, the capacity estimation can take advantages of standard data from occupant load [pp/m^2] assessment as described in the following bullet points:

- buildings open to the public, and their use have to be identified, especially if they can be affected by potential high occupants' density/overcrowding conditions. For such public building's occupants' capacity [pp] is rapidly provided by the occupant load factors ([pp/m^2] or [m^2/pp]) also employed in the code of practice for Fire Safety Design. This factor is multiplied for the building area extension depending on the hosted functions (see Table 14). Further similar sources for different countries can be used to this end[18];
- residential buildings capacity can be determined by evaluating the number of hosted inhabitants [pp]. A detailed map of residents can be generally provided by the General Land Office[19] surveys, such maps could report additional useful data as previously said (e.g. age, disabilities) for each housing unit identified by the own civic number. However, data about disabled people can be collected according to the Privacy Act by local healthcare agencies or civil protection bodies [113]. Finally, time-dependent assumptions of Table 13 has to be considered to adequately evaluate the inhabitants' presence in their house and other buildings intended use according to Table 14 [95];
- Public spaces occupant capacity [pp] evaluation can be susceptible to overcrowding phenomena in case of temporary mass gatherings. According to a conservative approach, the maximum crowding-related occupant load range[20] of assembly areas could be reasonably considered from 2 to 4 pp/m^2. Moreover, to simplify this process the occupant load of outdoor local markets can be considered equal to commercial buildings data (compare to Table 14). Precautionarily the occupant capacity is esteemed in reference to gross (including parking, events stages, stands, and other urban furniture) or net area of the public spaces. Speaking about possible exposure peak situation, hypothetically occupants could leave their dwellings and occupy public spaces by overlapping to the people presence bring in town by organized mass gathering events. Thus, such conditions constitute a multi-hazard scenario due to the merging of inhabitant and visitor's presence in the same open spaces. Hence, in such cases, the overall overcrowding can be esteemed through the evaluation of its density [pp/m^2] in reference to the whole public spaces. From a

[17] E.g.: for Italy, the National Institute of Statistic https://www.istat.it/; for USA, United States Census Bureau https://www.census.gov/data.html last access 30/11/2020

[18] E.*g.: in England* https://bit.ly/2JcT6Vi, in the United States https://bit.ly/2UweLwX, *and in Canada* https://bit.ly/3dmj6v8 last access 30/11/2020.

[19] (e.g. http://www.protezionecivile.gov.it/resources/cms/documents/Manuale.pdf, last access 30/11/2020

[20] e.g. from Italian regulations such as Ministerial Decree (DM) 19/08/1996; Ministerial circular letter (Ministry of interior) 18-07-2018, n. 11001/1/110/(10)

simulation perspective, this data can be also expressed in terms of capacity [pp] as well, so as to outline the effective maximum exposure scenario that can constitute input data for simulation-based methodologies [29,94,95].

Table 14 Evaluation of the crowding density in buildings opens to the public in relation to the Italian fire safety codes due to their connection with the case-study application. In the case of historical buildings hosting the intended use, regulations could be integrated, from a general point of view, according to the rules provided by Ministerial Decree (DM): DM 3/8/2015, DM 8/6/2016, DM 9/8/2016, Circular letter n° 3181 del 15/3/2016

Intended use	Methodology	Quick occupant load factor	References to Italian regulations
Residential buildings	The crowding density for private dwellings is related to their surface	0.05 pp/m2 (imposed by regulations)	For residential buildings: DM 3/8/2015
Institutional buildings including architectural and historic ones used as offices, museum, and art gallery	Infield survey to trace information about the number of the occupant (personnel) with a precautional increase of 25% rounded to the upper bound-. The number of possible visitors has to be added by considering the area extension of public office In the absence of further information, use the quick occupant load factor.	Office close to the public: 0.1 pp/m2 Office open to the public: 0.4 pp/m2 Areas gathering public: 0.7 pp/m2	Generally, assimilable to the crowding of working place: DM 10/3/1998, DM 3/8/2015; for other public exhibition places, i.e. hosted by historical buildings: DM 20/5/1992, DPR 30/6/1995; for areas hosting cultural events with the public: DM 19/8/1996, DM 6/3/2001, DM 3/8/2015;
Religious buildings	For each building, the number of seats has to be counted adding the number of standing places	0.7 pp/m2 applied to the available area extension	For this intended use, assimilable to entertainment and public exhibition places: DM 19/08/1996, DM 6/3/2001, DM 18/12/2012;
Hospital and healthcare buildings	Infield survey to trace the information regarding the number of available beds. The number of in-service personnel is added and the variation due to visitors esteemed through the average data of at least three typical days	Ambulatory and similar: 0.1 pp/m2 Spaces for visitors: 0.4 pp/m2	For this intended use, assimilable to the crowding for working places: DM 10/3/1998

School buildings	The number of seats for each classroom and eventual annexes (e.g.: refectory, gym) has to be collected in relation to the number of students, teachers, and personnel, according to the headteacher declaration	Refectory and gymnasium: 0.4 pp/m2 A maximum of 26 individuals can be considered for each classroom	DM 26/8/1992, DM 12/5/2016, DM 3/8/2015
Cultural and entertainment buildings (public exhibition and sports facilities)	Evaluation of the main activities and the presence of seats for the public (number of seats)	In a precautional way: ballroom - 0.7 or 1.2 pp/m2; theaters parterre -3 pp/m2, standing places - 3.5 pp/m2 Sports facilities: 2 pp/m2	DM 18/3/1996, DM 6/6/2005, DM 19/8/1996, DM 18/12/2012
Commercial buildings	The crowding index is related to the surface of the overall floor	0.4 pp/m2	DM 27/7/2010, DM 3/8/2015
Accommodation facilities	Data about a general scale could be provided by tourism organizations subdivided for periods or seasons (e.g.: the municipal tourism promotion companies, regional tourism management bodies, trade organizations). Infield surveys are necessary to obtain the single structures maximum capacity, the number of beds and personnel (increased by 20%)	0.4 pp/m2 (i.e. common spaces)	DM 27/7/2010, DM 3/8/2015
Public shops such as restaurants bars and cafes	The crowding values can be reasonable esteemed in relation to the extension of the area, for bars and cafes infield surveys are desirable to esteem the number of customers during each time slot	0.7 pp/m2 (precautionary evaluations)	For this intended use, assimilable to public exhibition places: DM 19/8/1996, DM 6/3/2001, DM 18/12/2012; from a general point of view: DM 3/8/2015

A second part to discuss in an emergency planning process [29] concerning the collective vulnerability-related factors regard the individuation of urban outdoor areas where the population (inhabitants and visitors) can gather and wait for the rescuers' arrival [48,49,57]. The definition of assembly areas should encompass some criteria. Such area for instance should be easily reached by pedestrians at whatever moment by guaranteeing a free entrance to the area (e.g. no access gates closure) over time, as well as the absence of obstacles related to particular space uses (e.g. spaces used to host fairs and exhibitions; parking areas). At the same time, spaces should host evacuees in safe conditions controlling the overall overcrowding situation by avoiding the possibility of physical contact among individuals (i.e., maximum Level of Service D according to [114]). To guarantee that, related occupant

load values can essentially range from about 2 pp/m^2 to about 3.5 pp/m^2 [115]. Finally, the counting of assembly areas extension A_a [m^2] should be reduced of potential unavailable parts, i.e.: (1) potentially affected by buildings debris; (2) small prefabricated structures (including temporary ones) and fixed urban furniture; (3) parking lots (precautionarily considered as occupied); (4) carriageway reserved to emergency vehicles access (3.5 m, considering the width of the heavy rescue vehicle).
Another time, the proposed data collection activities are performed on the case study of Offida (Italy) which is representative of a typical European settlement. Besides the fact that Offida is highly affected by earthquake risk, exposure-related factors are furtherly exacerbated by many hosted tourist attractions in the BE from the cultural and architectural points of view and several numbers of mass gathering events are organized during the year bringing in town a considerable number of tourists.

3.3 Results

3.3.1 A quick methodology to point out the individuals' distribution in the BE

The data collection methodology established in Section 3.2.1 provides rapid tools to delineate the social vulnerability scenarios and to precautionary consider possible exposure peaks from a multi-hazard point of view. Related databases and provided sources are investigated adopting Offida's case study to provide evidence of the method's capabilities. On such basis, the maximum daily presences [pp] is esteemed. To do this, the visitors flow during the year is firstly assessed by using monthly data from the Regional Observatory of Tourism[21]. Results can be resumed in Figure 15-A. At the same time, Figure 15-B displays the daily visitors' presence directly retrieved according to databases from museums and tourist attractions[22]. From both these graphs, a considerable increase in population is registered in the city during the summertime especially in August (holiday season in Italy) when the urban centre is crowded by sightseers.

[21] http://statistica.turismo.marche.it/DatiTurismo, last access:30/11/2020

[22] http://www.fabbricacultura.com/socio/oikos, last access: 30/11/20

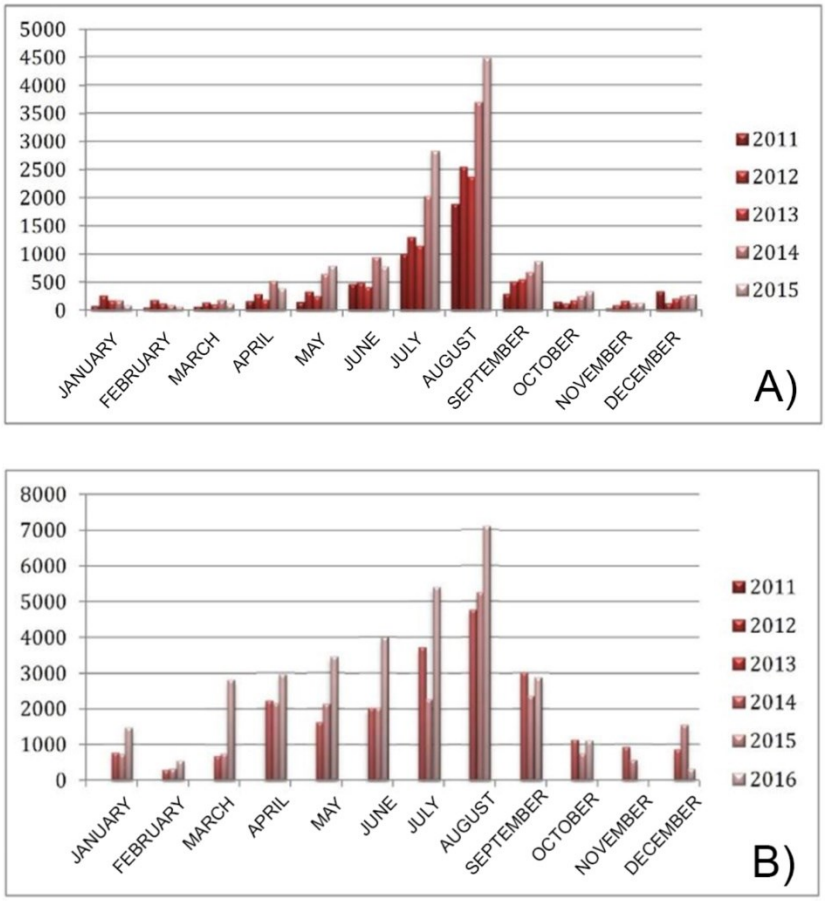

Figure 15 Monthly presences related to: A) visitors (tourist flows; years 2011-2015) of the whole historic centre (source: http://statistica.turismo.marche.it/DatiTurismo; last access:30/11/2020); B) daily visitors (years 2014-2016) to museums and tourist attractions (source: http://www.fabbricacultura.com/socio/oikos; last access 30/11/2020); image source: [116] re-elaborated by the author

In order to precisely distribute the inhabitant within the urban fabric, the municipal database is investigated by jointly considers every single residential unit and the resulting value for each building aggregate, in terms of the total number of inhabitants. Moreover, additional information related to hosted communities can be retrieved including the citizens' age. Users' typologies by age are obtained by subdividing the population into different age-related ranges [117] (i.e.: 0-14 years, parent-assisted children; 15-19 years, autonomous young people; 20-65 years, adults; >65 years, elderlies including those with potentially reduced motion abilities that affect the evacuation times). Figure 16 below summarizes results for the overall historic

centre of Offida. However, specific information about age-related users' typologies is provided only for the study area (black contour) of previous methods described in chapter 2. Therefore, the total number of inhabitants to consider in exposure scenario creation amount to 750 residents for the entire tissue of Offida which 319 of them within the study area.

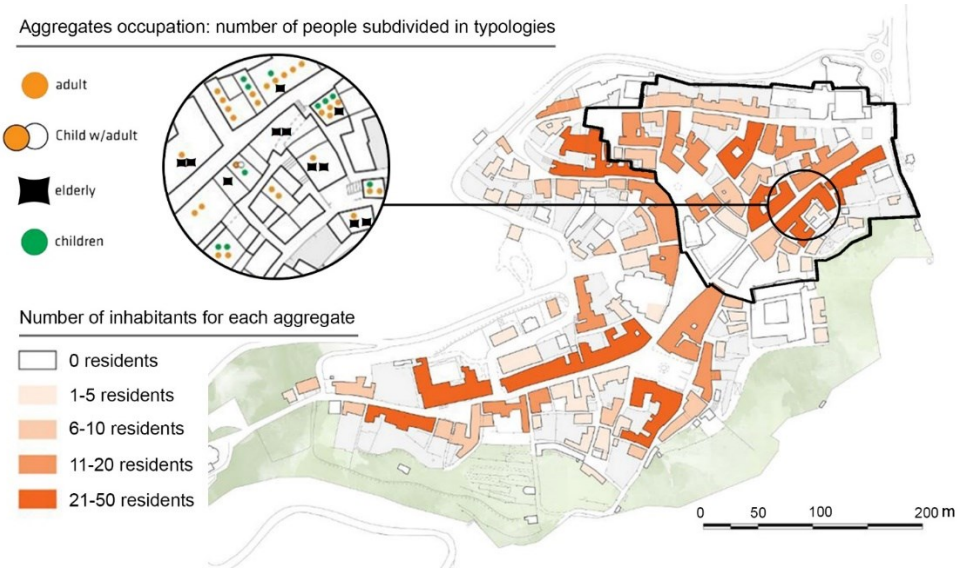

Figure 16 Characterization of inhabitants for the historic city centre by outlining the number of inhabitants for each aggregate (the black contour highlights the case-study area). The detailed planimetry excerpt (inside the circle) focuses on aggregates occupation in terms of the number of people by distinguishing them into four typologies according to [6]: parent-assisted child, young people, adult, and elderly; image source: [116] re-elaborated by the author

Focusing the attention on the occupant capacity of public buildings and facilities, results can be pursued according to the indication provided in Table 14 of Section 3.2.1 implemented through the use of a quick evaluation of the occupant load [pp/m^2]. The needed passage before consists of the preliminary determination of the building's intended use, separating common dwellings by public structures. These data are merged in the map reported in Figure 17 where numerical results are shown for private buildings as well in order to quantify the scenario in a complete vision. Then, indoor occupancy should be furtherly combined with the occupant load esteemed for outdoor public spaces. The total crowding density (pp/m^2) in open spaces and urban streets is graphically provided in Figure 18. This map also highlights the main urban spaces (both squares and links) susceptible to overcrowding conditions due to mass gathering events (multi-hazard). Potential risky areas for the inquired case study could be the main street "Corso Serpente Aureo" due to the local market presence on Thursday morning and of the main square "Piazza del Popolo" that frequently hosts festivals, popular and cultural celebrations. In particular, the above mentioned central urban square during Saturday night could be host additional visitors due to open activities (e.g. restaurants

and pubs) also considering that in the same square stand on the foyer of the local theatre. Additionally, tourists' presence during the summer can be added to the overall capacity. In such conditions, the square is able to host a maximum level of crowding equal to 3200 people on a limited gross area of 1600 m^2 (by considering a density of 2 pp/m^2, according to Table 14 of Section 3.2.1).

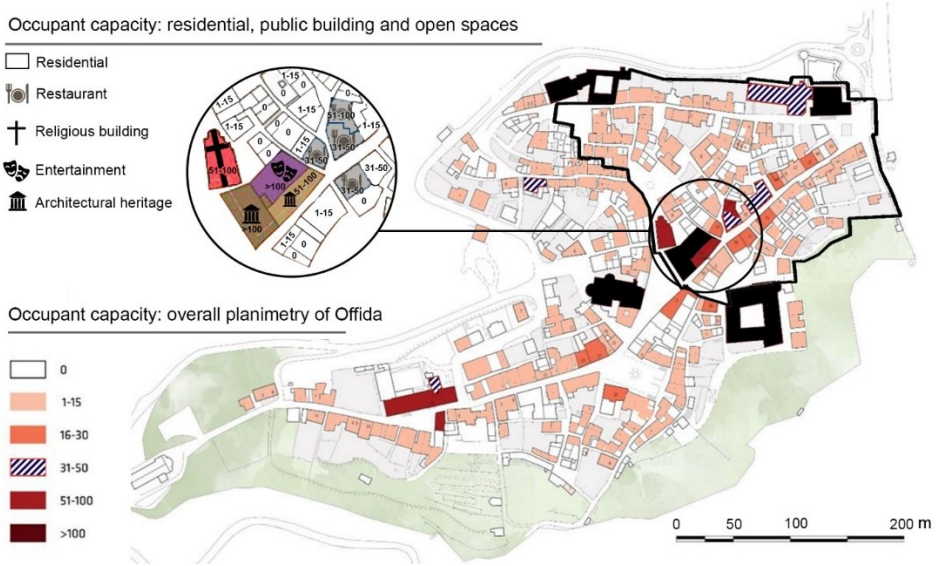

Figure 17 Overall planimetry of Offida with the individuation of the total occupant capacity of buildings, expressed in terms of the number of hosted people (the black contour highlights the case-study area). The upper circle shows an excerpt from the analysis in terms of the buildings' intended use; image source: [116] re-elaborated by the author

To conclude, it possible to comprehend the urban fabric's main criticalities from an exposure point of view by overlapping through the maps the obtained data. Occupants' presence in the case-study area allows delineating critical scenarios. Additionally, such results can be analytically quantified in

Table 15 below contributes to delineate a complete framework assumed as representative of recurring maximum achievable crowding conditions all over the year.

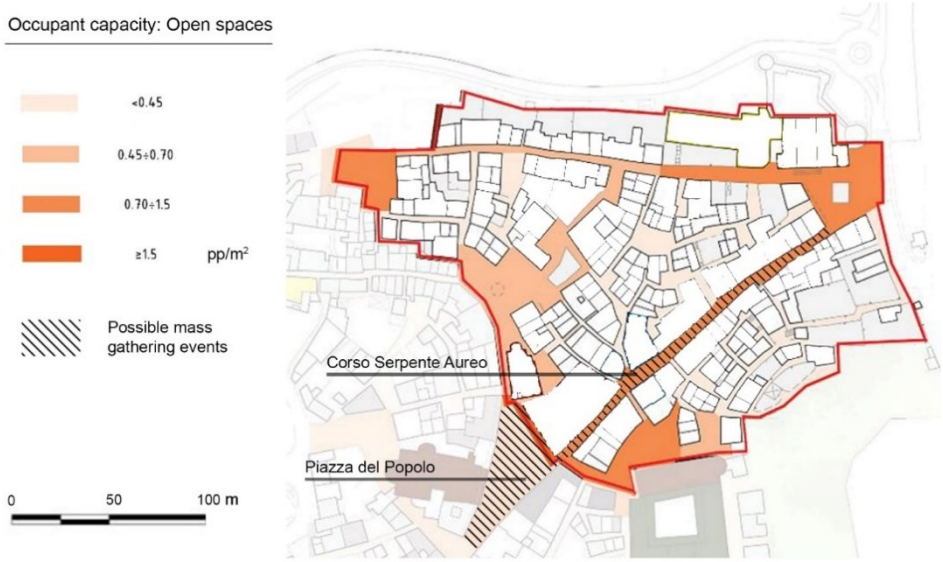

Figure 18 Planimetry of the case-study area in Offida with the evaluation of the crowding density (pp/m2) in public spaces, by evidencing the selected area border. The areas that can host mass gathering events are also evidenced by the hatching texture; image source: [116] re-elaborated by the author

Table 15 Case-study maximum crowding scenarios

Building intended use:	Thursday (9-12 a.m.)	[pp]	Saturday (8-11 p.m.)	[pp]
Building heritage (museums, churches)	considering offices in the municipal buildings	121	considered as closed	-
Hospital and healthcare buildings	both personnel and patients	110	long term care	40
Cultural buildings (i.e. theatres)	cultural activities normally held during evenings and weekends	-	cultural activities held imply maximum crowding conditions	300
Commercial buildings	holding maximum occupant loads	176	are closed	-
Tourists accommodation	closed due to day-time activities	-	empty due to evening-time activities	-
Restaurants	are closed because of out of the lunchtime	-	maximum crowding conditions	189
Bars and café	holding maximum occupant loads	47	maximum crowding conditions	47
Inhabitants	people between 20 and 65 years old are supposed out of the historic centre, at work	143	dwellings are occupied by residents at the dining time	319
Open spaces:				
Pedestrians	crowding conditions in open spaces of the BE hosting the weekly market along the main street "Corso Serpente Aureo" considering 0.4 pp/m^2	560	BE could host additional events (e.g. other local markets), assuming an occupant load equal to 0.4 pp/m^2	560
Total:		1157		1455

Chapter 4

4 Risk reduction solutions based on evacuation simulation outputs

4.1 Combining scenarios modifications and human-centred aspects to test the effectiveness of proposed risk mitigating strategies

Resuming what presented since this point, it is possible to affirm that the complexity of the Built Environment entails considering a challenging relations system between its physical (i.e.: buildings, path network and spaces layout), human (i.e.: hosted occupants) and organizational (i.e.: emergency planning and management) factors to move towards better design and operation in both normal and emergency conditions [32–34,118].
On the basis of previous discussions related to human and BE interactions, in this last chapter a proposal to evaluate the effectiveness of whatever safety-increasing solutions of natural hazard-prone areas will be advanced [27,119–122]. The present work follows the methodological approach validated before in [29]. Especially, sudden-onset disasters such as earthquakes have the potential to trigger critical situations, mainly in the first disaster aftermath phases, impeding the evacuation and rescuers' access to damaged areas [4,30,67,123].
Special attention has to be paid to inhabitant safety, especially during the evacuation process along urban paths network. In many cases, human losses are related to people that are not put in condition to reach an assembly area because of blockade paths. At the same time, modification to the scenarios could limit the operativity of the emergency management plan by first responders [4,67,124,125]. To avoid such impediments, Local authorities and Civil Defense Bodies foresee interventions on buildings to reduce their vulnerability and damage possibility through retrofitting actions [126–128] or they prevent critical situations by promoting emergency management strategies to improve citizens' safety levels [30,48,125,129]. At this point, the question is: how to perform an effective solution? and how can be this last retained valid and affordable for a specific case study?
Hence, first of all, the analysis of disaster scenario conditions should be preliminarily adopted to plan appropriate risk-mitigation strategies. For such purpose, a performance-based standpoint able to jointly combine human behaviour-related aspects and seismic effect on the BE should be preferred [28,34,118,125,130]. To this end, the rapid seismic vulnerability assessment of buildings (mainly historical one and in masonry typology) have to be performed [67,131]. The one that necessitates expeditious data (e.g. typology, state of preservation, geometry, presence of aseismic devices) [3,132] that can be also analysed through external or remote surveys [5,70,77], are preferred, as already indicated in Section 2.2.1. The prediction of post-earthquake damages scenarios for instance able to understand eventual ruins presence along the urban paths is then employed. Empirical-based methods

that adopt a quick correlation between earthquake severity and vulnerability values can speed up the scenario creation process [3,70]. In this way, a macroseismic earthquake characterization and real-world data can be used to validate these approaches [77] as proved in Section 2.3.2. Indeed, the statistical significance of the out-of-plane response of the façade walls, which can block the urban paths increases the importance of ruins formation prediction algorithms.
Additionally, pedestrians' evacuation process has to be adopted to understand which and where critical conditions can occur and where to direct rescuers' access procedure by including the abovementioned post-earthquake scenario conditions [8,28,124,133]. For such purposes, microscopic models [134] have to be preferred since they take into account behavioural aspects associated with each simulated individual. Moreover, specific interactions among evacuees and between them and the modified BE are adopted to perform the evacuation simulation [6,28,135,136].
Finally, to analyse evacuation simulation outputs necessitate objective tools. For such scopes, the definition of Key Performance Indicators (KPI) can be considered a rapid way to directly evaluate the effective impact of proposed risk-reduction strategies [126]. Such tools provide numerical quantities to compare obtained results among different scenarios conditions [137]. These indices allow to analyse the overall populations' safety levels [31,32] and also possible related hazards that can affect them while reaching rescuers [28,125,129]. KPIs giving the possibility to focus on the safety level of specific BE elements as well (e.g.: assembly areas and paths).
In view of the above, this last chapter pursued the aim to close the methodological framework (i.e.: the PDCA cycle) declared in Figure 1 of Section 1.3. All the above issues are here addressed proposing an innovative simulation-based methodology aimed at the identification of the best path choice for evacuees and rescuers' access, the evaluation of safety levels for each path and assembly area, and finally at comparing the impact among implemented emergency strategies. To corroborate the overall methodological framework its implementation will be performed on the Historic Centre of Coimbra (Portugal) adopted as a case study.

4.2 Methodology

4.2.1 PLAN the actions by creating scenarios for safety assessment analysis

The first step necessary to propose resilient solutions against seismic disasters should involve a detailed characterization of the whole physical scenario. Thus, to speed up the process in a way that can be implemented at the urban scale rapid data collection methodologies are chosen to perform different scenario conditions as well [30]. This step (i.e.: PLAN) and its tools to be actuated are widely debated in the previous chapters of this thesis. Essentially the first data to collect should concern the urban layout. The related key role elements are the paths' width in relation to the facing buildings' height and the overall configuration of the urban path network including its composing elements. Links, nodes, and squares assessment are crucial in emergency planning. Wide-open spaces could embody the role of assembly areas. Additionally, the possible access point for rescuers to this network constitutes another fundamental element to depict [4,6,48]. Moreover, exposure issues are often related to the

building intend use, the presence in the BE of strategic buildings (e.g. hospitals, hotels, public administration structures) characterize the position and the number of inhabitants involved in the evacuation, especially for those who require special cares. Finally, man-made constructions (both buildings and path network elements) should be inquired from a vulnerability point of view employing simplified assessment techniques. Differently from the works proposed above, for this last goal, the methods of Tiago M. Ferreira, Vicente, and Varum (2014) for masonry buildings and the one proposed by Santarelli et al. (2017) for urban paths are chosen. In this way, the replicability of the general operational framework is pursued because the employed methods are not exclusive, but they could be replaced with similar others, improved in the future, guaranteeing general adaptability. Although the seismic input intended as the hazard component of the risk is not deeply analysed in this thesis, different emergency scenarios (related to the severity of the seismic event) can be determined in relation to its variation. Hence, in this study, the prediction of debris quantities due to damaged buildings on urban streets is represented in terms of ruins depth (linear dimension) by adopting a validated experimentally-based method that proposes correlations between seismic magnitude, geometrical building/facing street characterization, and building vulnerability [70]. Finally, eventual current predisposed emergency plans in each case should be considered by verifying their adequacy. In the cases where there is no evacuation plan, national or international evacuation guidelines can be used.

4.2.2 DO by performing evacuation simulation

Validated evacuation simulation models have to be involved to assess the safety levels of BE elements and hosted inhabitants in case of an earthquake [6,31,32]. Related software tools are able to jointly analyse both the earthquake-induced scenario modifications and the evacuation process.
On the first matter, how previously said this operational framework adopts the Santarelli et al. (2018)'s method that is focused on the estimation of debris depth formed in the immediate aftermath of an event. The eventual availability of post-event evacuation paths are so esteemed by taking into account the earthquake magnitude, the analysed building vulnerability, and the analysed building/facing street geometry.
Meanwhile, regarding the evacuation process, it should be evaluated from the analysis of the individuals' actions performed during and in the aftermath of the earthquake. For this purpose, advanced simulation tools have already collected all the typical and specific human behaviour through the techniques discussed in Section 3.1. In this way, such microscopic tools are able to describe the recurring individual-individual and individual-environmental elements interactions, while preserving the general adopted holistic approach [138–141]. Additionally, an Agent-Based Model (ABM)-oriented approach [142] can enrich the overall advanced simulation model by deeply focusing on specific evacuees' behavioural rules in motion simulation and by modelling environmental modification as separate agents [6,142].
In this thesis, the Earthquake Pedestrians' Evacuation Simulator (EPES) [6] is adopted also because it is developed a few years ago in the same research department of the author. This validated software is based on a combination of the ABM and Social Force Model (SFM) techniques [141]. Additional specification of the involved simulator, that do not constitute an object of this thesis but is limited to be employed as a tool, is provided in Appendices 6.2.

Describing deeply the purposes of the evacuation process simulated by the model, the final objective of each agent is to reach an assembly area (AA) where to wait for rescuers' arrival. Such assembly areas are previously determined also according to the current local emergency plan. According to Section 2.3.1, the evacuation path followed by evacuees is made by the union of consecutive links and nodes, the final node that can be generally embodied by a square correspond to the assembly area. However, like in the real-world unfortunately not all the simulated people are able to reach the predisposed AA often because of the surrounding environmental modification (e.g. blocked paths by ruins) or because of behavioural issues related to path choices criteria (e.g. influenced by other evacuees). Through the employed techniques discussed in the introduction of chapter 3, it is demonstrated how in these cases trapped evacuees tend to gather around the same point remaining together. Such additional assembly areas can be defined as "spontaneous" (SAA). So as described at the end of Section 3.3.1 for AA such places are often characterised by the following points. Those areas should offer the best safety and comfort conditions to evacuees such as the limited presence of debris, higher distance from tall and damaged buildings, enough space to gather and accommodate people preferably not in overcrowding conditions.
In view of the above, the simulations are performed according to the following necessary assumptions [6,28,124,136,143]. The individual's path choice could be influenced by links' geometry, damage levels, and social attachment phenomena [6], as furtherly described in Appendices 6.2. The evacuation starts to be performed by the agents after the earthquake shake (do not move during the earthquake shake, according to Civil Defence Bodie's dispositions [97] by avoiding riskiest conditions due to human body instability and possible falling of objects [144]). All the produced debris are considered already generated at the starting of pedestrians' motion. Simulated agents can be generated directly outside of the buildings where they are hosted or randomly scattered in the scenario's opens spaces according to what is discussed in Section 3.2.1. They start their evacuation from such points and ends it in three possible ways: reaching an AA, gathering with others into a SAA, stopping along an emergency path at the end of the simulation time, or remaining in the place where they are trapped (e.g.: enclosed by debris presence). According to previous EPES tools validations, the individual's motion preferred speed $v_{pref,i}(t)$ in the SFM is equal to 2.1±0.5m/s (Gaussian distribution). The maximum simulation time could be fixed by considering the time needed to reach a AA by the farthest individual that moves at 1 m/s. Five simulations are carried out for each scenario and mean output values (and related standard deviations) are considered to highlight possible variations of simulated pedestrians' behaviour due to introduced stochastic errors [6,141]. According to [6,139], 10% is the maximum allowed difference in the simulation outputs. An HP ProDesk 400 G1 MT workstation (Intel® CoreT2M i-4570 CPU @ 3.20Ghz, RAM: 8GB; OS: Windows 7 Professional 64-bit) is used for simulation running.

4.2.3 CHECK the safety levels by analysing simulation results

Evacuation simulation outputs have to be quantitatively analysed through the employment of ad hoc Key Performance Indicators (KPIs). Hence, KPIs, based on human-centric metrics [33,34], have to be defined aimed at combining the main factors that are able to characterise urban scenario criticalities. Such factors involve vulnerability and damages issues, trapped population, and the state of rescuers' access paths, implemented risk-reduction strategies, and

community safety levels. Results, according to previous work developed in chapter 2, should permit the rapid evaluation of the entire urban fabric. Therefore, such determined indexes could be synthetically reported on risk-maps to quickly localize specific risks for each urban component (e.g. buildings, paths, assembly areas). According to the employed software for simulation, each of the KPI should be referred to all the different simulation outputs giving their punctual interpretations. For such reason, each urban tissue element has a related KPI, a complete description of all the involved KPIs is offered in Appendices 6.3.
The safety level of each link of the urban paths network (Table B 1 Appendices 6.3) is obtained by considering both its usage by evacuees and the possible interaction among them (evacuee-evacuee due to the overcrowding condition) and to debris presence along the path. Additionally, every single link if combined with the contiguous ones can be assessed by KPIs in the view of constituting rescuers' access paths to reach the assembly areas.
The assembly areas (AA) are evaluated in (Table B 2 Appendices 6.3). Firstly, AA safety is connected to the minimization of directional variations and coming-and-going behaviors. Then, according to its definition given in Section 3.3.1, each AA has to host evacuees in safe conditions (adequate levels of crowding and satisfying surface without debris and away from unstable buildings). Moreover, AAs should be directly reached by rescuers after the event. For such purpose, the path conditions toward the analysed AA necessitate a specific KPI that evaluates the possibility to find streets devoid of debris minimizes interferences between rescuers and seismic-induced scenario alterations [4,48,49,124,136]. An ideal access path towards an AA should be the shortest and safest one. Additionally, in this thesis rescuers are considered equipped with emergency vehicles (e.g.: ambulances or fire trucks) thus a street width of at least 3.5 m should be guaranteed for main street accessibility [67]. Anyway, in the historic urban fabric, this could be not possible for many alleys, so first responders could move only on foot.
At the same time, safety levels of spontaneous assembly area (SAA) can be equally evaluated by KPIs (Table B 3 Appendices 6.3). In these areas, evacuees decide to spontaneously stop their motion induced by visible low-risk conditions. However, such areas could not be easily reached by rescuers. Hence, alternative paths should be established and singularly evaluated through KPIs. Related results will be compared to define which is the best path.
Focusing on further technical aspects of KPIs definition, it is worth noting that some indexes are normalized within the area data to define a priority list for interventions, by characterizing risk levels into 4 classes: low (0-0.25), medium-low (0.25-0.50), medium-high (0.50-0.75) and high (0.75-1).

4.2.4 ACT by proposing risk reduction solutions

According to different authors [121,126,127,145,146], risk-mitigation strategies are generally based on building retrofitting interventions, evacuation planning (i.e. the position of assembly areas, rescuers' access paths, evacuation path definition), preparedness and population awareness (by providing to citizen the right actions to perform), and emergency management, including support to population (i.e. wayfinding signage implementation, positioning of rescuers within the urban layout, etc.). Although, all of these strategies could be retained valid and useful some of them can be more effective than others if implemented in a specific case study. Hence, the proposal of a risk-mitigation strategy has to be based on

the more critical aspects outcoming from the evacuation simulation of a specific case study by taking advantage of KPIs description and resulting risk maps as well [28,32,125,147].
Risk-mitigation strategies proposed in this thesis are based on results outcoming from the simulation of an "initial scenario". Then, the "post-intervention scenario" (i.e.: the one that includes the proposed strategies is simulated) so as to close the PDCA cycle by going back to the very first stage of the process (according to Figure 1 of Section 1.3). Therefore, the PDCA cycle can be reiterated to evaluate again the safety levels and to test the effectiveness of different adopted risk-mitigation strategies. Specifically, each risk-mitigating strategy should intervene on certain KPIs. Comparing the initial scenario results with the subsequent reiterations a strategy can be assumed as valid if: the $A_{eff,AA}$ is maximized, the J_{SAA} is maximized as well, by minimizing the number of AA, avoiding the formation of many SAA and by limiting the evacuation time, so as to focus rescuers' access (and by considering that $LOS_{AA} \geq 0.3 m^2/pp$). On the contrary, V_{link}, T, $S_{link,AA}$, $S_{AA,}$ should be minimized by guiding people towards the AA. Comparisons among such results of different scenarios (with risk-strategies differently implemented) have to be determined by evaluating their mutual differences dx [%] defined in Equation 25:

$$dx(\%) = \frac{x_{pi} - x_0}{x_0} \cdot 100 \tag{25}$$

where x is a general KPI, and the subscripts refer to simulation in the original (subscript *0*) and post-intervention (subscript *pi*) conditions. In conclusion, each KPI variation to improve the safety levels should be minimized or maximized depending on the considered KPI definition.

The entire PDCA cycle is here performed on the Coimbra (Portugal) case study to better evidence the effectiveness of the proposed operational framework. The city of Coimbra is one of the oldest and most important Portuguese cities, especially for its historical and cultural significance [148]. A complex and irregular urban fabric characterise the historic centre of Coimbra with its historical unreinforced masonry buildings that face narrow streets and windings alleys. This centre could be representative of many European historical city centres such as the one of Offida for the Italian case study. Indeed, the majority of buildings does not actually present any seismic design or detailing and therefore are extremely vulnerable to an eventual seismic event, even of a low to moderate intensity [149].

4.3 Risk reduction solutions based on evacuation simulation outputs: a case study results

According to Section 4.2.4, two different scenarios are simulated in this work. The first, "initial scenario" is discussed in the following Section 4.3.1 and represents the current conditions of the case study area. The second one ("post-intervention scenario"), addressed in Section 4.3.2, considers the adoption of a series of risk reduction strategies specifically designed to mitigate the criticalities pointed out by the first scenario.

4.3.1 PDCA to assess the initial scenario

Starting from the PLAN, the case study area is the one marked in Figure 19 within the historic urban fabric of Coimbra. How previously said this area is mainly constituted by masonry buildings and their vulnerability values (assessed with the method proposed by Tiago M. Ferreira, Vicente, and Varum (2014)) are directly retrieved taking advantages from the previous study of [67]. In such contribution, the main classes of buildings vulnerability distribution are provided for the case study area. Additionally, Figure 19 identifies those buildings that are excluded from the evaluation because the adopted vulnerability assessment method could lead to not significant values (i.e. monuments, churches, and other different typologies from masonry buildings).

Figure 19 Vulnerability maps: (a) global vulnerability distribution over the Historic Centre of Coimbra; (b) study area and identification of the building facade walls with vulnerability index values higher than 45; image source: [29] re-elaborated by the author

Figure 20 highlights the urban paths network of the case study and subdivides the network elements according to Section 2.3.1. A total amount of 32 links delimited by nodes are determined. Since no data about the current emergency plan have been retrieved, within the same area are preventively determined nine possible assembly area (AA). Individuated areas, according to their definition (Section 3.2.1), are preferably the one that is placed in the widest open spaces (i.e. squares, wide avenues) and the ones placed out of the narrowest paths area because their peripheral location allow rescuers to reach them more easily (e.g. the ones

placed along the main roads). Finally, 3 main access points for rescuers' vehicles are highlighted by arrows. Figure 20 reports through a chromatic scale the outcomes of the paths network elements (i.e.: only link in this case) vulnerability values assessed through the V_{link} values according to Santarelli et al. (2018)'s method. As can be seen in this figure, the most vulnerable links are the numbers 7, 9, 10, 13, and inner parts of links 2 and 6 (characterized by most vulnerable buildings, by comparing with Figure 19).

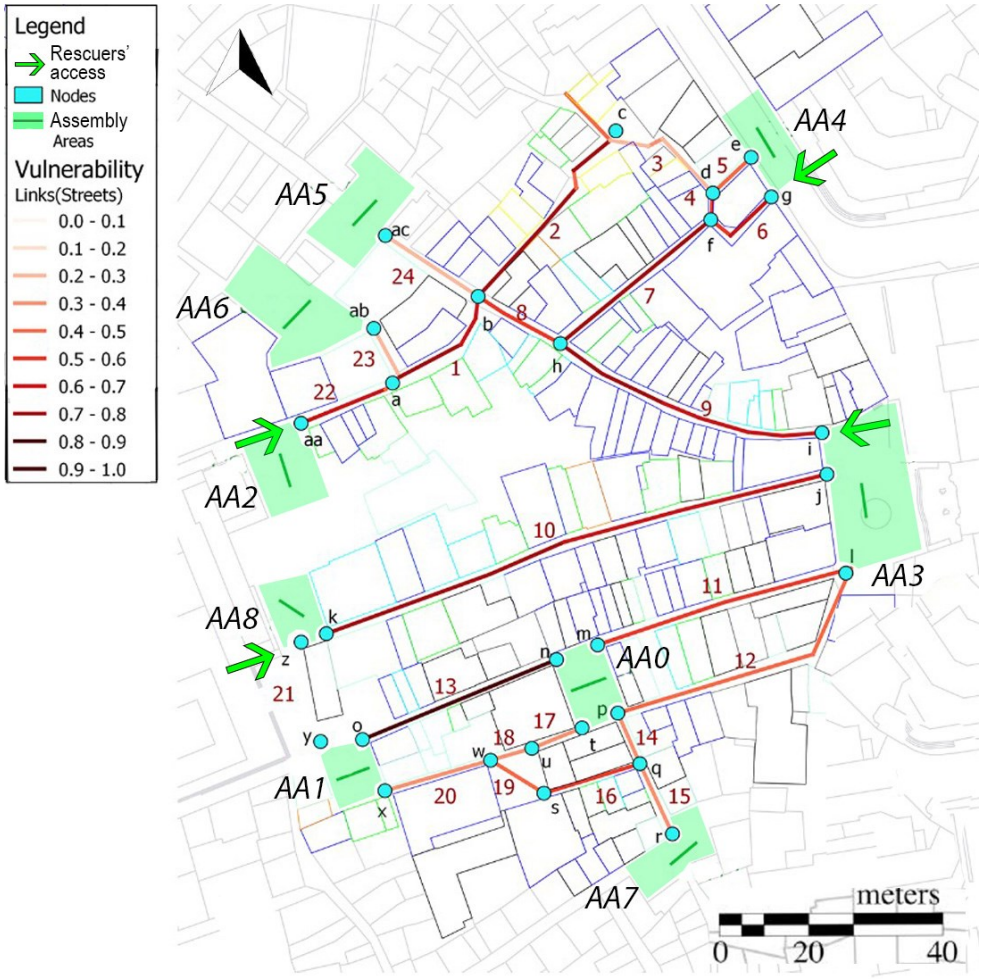

Figure 20 Urban paths network schematization and V_{link} values for the case study area. Rescuers' vehicle access and possible designated assembly areas (AA) from the number 0 to the 8 are also evinced; image source: [29] re-elaborated by the author

The seismic input considered for the simulated scenario (that will be the same in all post-intervention scenarios to make them comparable) is here expressed in terms of magnitude and assumed equal to 5.6 M_w that is the maximum historical local magnitude [150]. According to chapter 3, the hosted individuals are determined with the aim of the exposure scenarios creation. 1200 agents are simulated, but to simplify the simulations (also in terms of computational time) they are assumed only as inhabitants. Hence, residents are distributed in the environment according to the buildings where they live. Is also necessary to underline how for the only inhabitant category (compare to Section 3.2.1) it is supposed that all the evacuees know very well the surrounding environment and the position of the designated AAs. Rapid visualization of the exposure scenario is provided in Figure 21.

According to Section 4.2.2, the maximum evacuation time is fixed equal to 350s, since the evacuation paths are much shorter than 350m and earthquake evacuation speeds are generally higher. For these reasons, the same time is adopted as the total duration of each simulation. Thus the 5 simulations are performed (DO) according to the scenario creation task just now discussed.

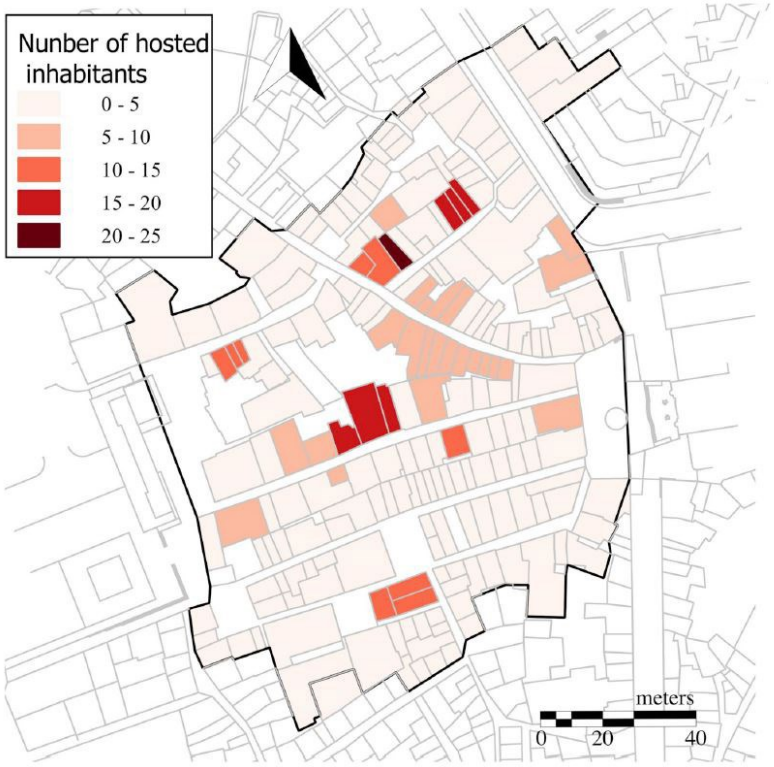

Figure 21 Exposure scenario: hosted inhabitants within the area buildings; image source [29]

The performed evacuation simulations of the initial scenario give their first results (CHECK), indeed Figure 22-A reports the average evacuation curve in terms of arrived evacuees to the designated assembly area (AA) in the simulation time. Because of the 5 simulations, the same graph shows the maximum and the minimum evacuation curve as well. The maximum differences among these curves according to Equation 25 is equal to 5%. According to [6] it is possible to assume that the analysis converged to an accurate solution (<10%). Figure 22-A highlight the presence of 766 evacuees that corresponds to the 64% of the simulated agents that are able to reach an AA within the adopted simulation time equal to 350 s. Going deeper to analyse each assembly area, Figure 22-B displays the average evacuation curves for each single assembly area individuated by their codes. In addition, Table 16 summarizes for each assembly area its main KPIs giving an idea of the evacuees' number and their occupancy in safe conditions while they are waiting for rescuers' arrival. In this way, some first considerations could emerge.

Discussing obtained results related to the number of evacuees that are able to reach the AAs they are heavily influenced by the effect of debris formation on considered paths. Figure 23 reports the percentage of ruins along paths. These links conditions, especially for the narrowest ones (e.g. links 5 and 6), could slow down the evacuation motion towards the AAs and in many times impede evacuees to reach the nearest assembly area. Possible paths occupied by ruins in the initial scenario could be links 1, 22, and 23 where evacuees try to reach AA2 and AA6, links 5 and 6 towards AA4, and finally, links 14 and 15 towards AA7. Such AAs are reached only by those agents that are placed in proximity of the assembly area at the start of the evacuation process. Moreover, KPIs for AA2 (Table 16) evidence how this assembly area is underused in comparison to its wide dimension. This condition could be due to the huge amount of debris presence along link 22. In this case, pedestrians coming from links 1, 2, 8, and 24 prefer to reach the AA5 and the AA6 instead of the AA2. Suggestions for risk-reduction strategies could emerge by guiding the evacuees that actually move towards AA5 and AA6 toward the available AA2, while reducing the building's vulnerability through retrofitting intervention along link 22.

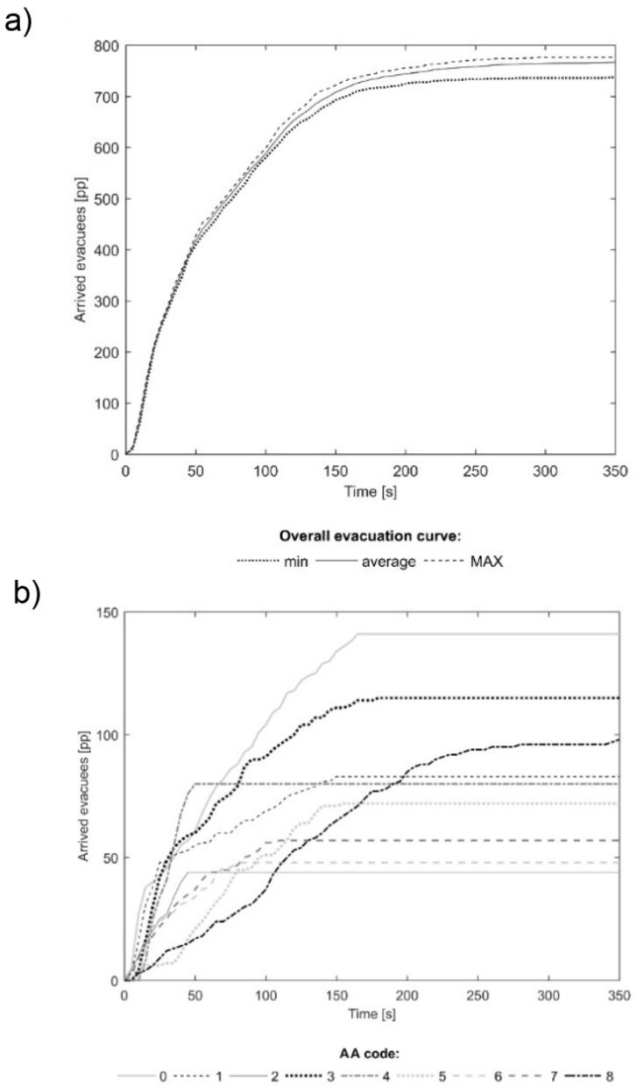

Figure 22 Original scenario evacuation curve results: (a) average, minimum and maximum curves for the whole area; (b) Evacuation curves obtained for each assembly area (AA); image source [29]

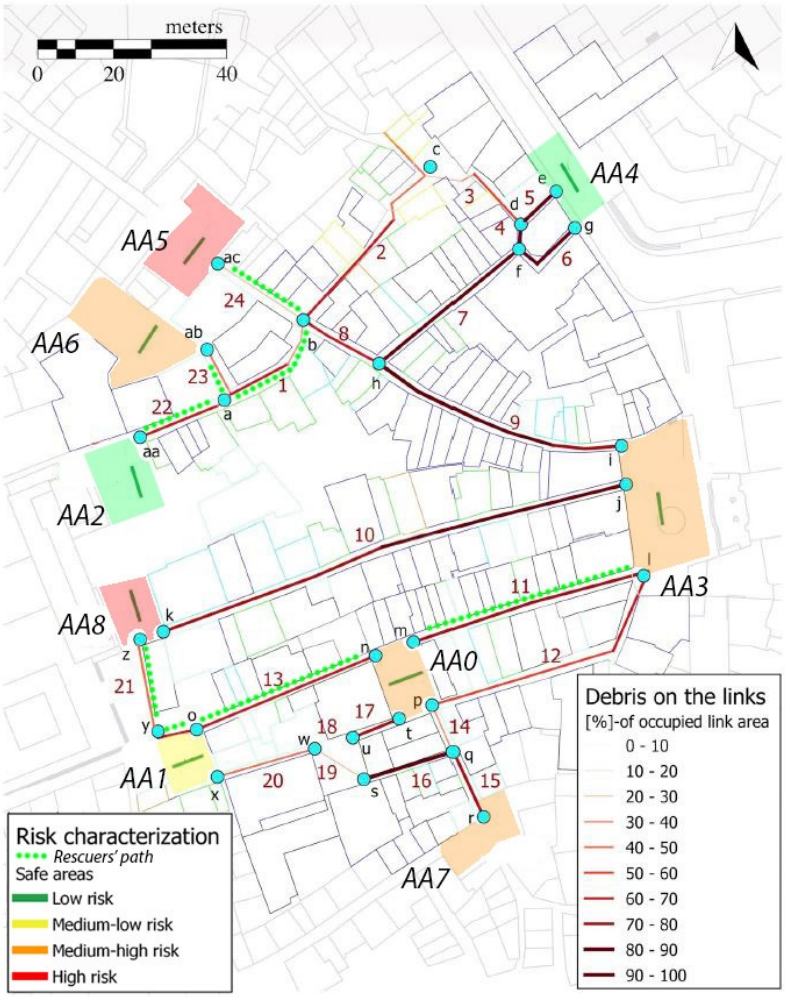

Figure 23 Case study debris percentage on links for the initial scenario according to the Santarelli et al. (2018)'s method. The map reports also the assembly area (AA) risk characterization according to KPIs and the possible rescuers' access paths for the internal AA0, AA5, and AA6; image source: [29] re-elaborated by the author

The highest J_{AA} and LOS_{AA} values in Table 16 for the AA0 demonstrate how many people reach this AA. Indeed, AA0 is placed in a central part of the Coimbra BE also exacerbated by the high values of inhabitants' density due to the urban fabric configuration. Additionally, the links that connect this AA to the others are affected by debris presence (compare to Figure 23) that impede the evacuation towards the nearest AA3 and AA7.

Table 16 Key Performance Indicator related to overcrowding conditions in each assembly area (AA). The "*" refers to evacuees who, although have not reached the AA, have stopped close to it and therefore are not included in the J_{AA} calculation.

AA	0	1	2	3	4	5	6	7	8
$A_{eff,AA}$ [m^2]	303	237	550	545	265	250	250	300	380
Np [pp]	141+20*	83	44	115+12*	80	72	48	57	98
J_{AA} [%]	18%	11%	6%	15%	10%	9%	6%	7%	13%
LOS_{AA}	2.2	2.9	12.5	4.3	3.3	3.5	5.2	5.3	3.9

Table 17 Key Performance Indicators related to the level of safety in each assembly area (AA).

AA	0	1	2	3	4	5	6	7	8
T [-]	1.254	1.157	1.059	1.265	1.034	1.437	1.323	1.227	1.402
$\Sigma S_{link,AA}$	0.036	0.012	0.000	0.000	0.000	0.265	0.317	0.000	0.000
S_{AA} [-]	0.369	0.219	0.083	0.314	0.110	0.630	0.649	0.261	0.408
$S_{AA\ (Norm)}$	57%	34%	13%	48%	17%	97%	100%	40%	63%

Slowing down effects of the evacuation are shown for links 9,10, 11, and 12 converging to the AA3 such link are the longest ones in the area. In some situations, the evacuation time increases because of debris-related slowing down effects. The same conditions are registered along link 10 which is characterised by no crossroads. Table 17 summarises the KPI values of $S_{link,AA}$, S_{AA} and $S_{AA,norm}$. Figure 23 displays the $S_{AA,norm}$ values directly on the urban centre map and by highlighting the possible access paths for rescuers towards the inner assembly areas that could not be reached by the main peripheral streets of the study area. While, for the remaining AAs the $S_{link,AA}$ is evaluated. The $S_{link,AA}$ for the AA2, AA3, AA4, AA7, and AA8 is equal to 0 since they are placed at the boundary of the area, and so are considered as directly reached by rescuers coming from the external parts of the studied area. Finally, it is possible to conclude from Figure 23 how the highest risk level is registered for the AA5 and AA6 mainly due to the highest number of hosted evacuees and due to the highest debris presence that affects both the path tortuosity (T) and the overall safety link values.

On the contrary, the average number of simulated agents that gatherings together out of an assembly area is about 316, generating different spontaneous safe areas. Individuals out of assembly area (AA) and the spontaneous assembly area (SAA), about 10% of the total number of inhabitants, stop their evacuation along links because of blocked by debris, slowed down by their disabilities in motion, or by the tortuosity of the path. Figure 24 offers the SAAs risk map by only evidencing the ones with J_{SAA}>5%: such spontaneous assembly areas contains the 62% of pedestrians gathering in SAA. The same figure also evidences two main alternative rescuers' access routes towards such SAA placed in the inner part of the urban fabric. To determine which is the best path for rescuers the related KPI is involved by each comparing the $S_{route,SAA}$ values. The $S_{route,SAA}$ reported in Table 18 is referred to the better alternative. The same Table resumes the remaining evaluated KPIs providing S_{SAA} and $S_{SAA,norm}$ values as well.

Table 18 Key Performance Indicator for spontaneous assembly areas (SAAs).

SAA	0	1	2	3	7	8
$A_{eff,SAA}$ [m^2]	18	39	33	23	63	63
$S_{area,SAA}$ [-]	0.345	0.075	0.118	0.193	0.056	0.046
$S_{route,SAA}$ [-]	0.091	0.044	0.044	0.083	0.042	0.042
$J_{p,s}$ [%]	19%	10%	10%	8%	7%	6%
S_{SAA} [-]	0.406	0.137	0.159	0.225	0.103	0.088
$S_{SAA\ (Norm)}$	100%	34%	39%	56%	25%	22%

According to previous works on real-world scenarios analysis [28], people collect in such SAAs because paths to a near AA is blocked by debris or surrounding conditions along the urban fabric are better in terms of damage levels and available space. In narrow and very damaged areas, i.e. SAA0 and SAA6, evacuees seem to spontaneously gather in intermediate nodes. In particular, SAA0 is characterized by the worst conditions within the whole area because of the most significant presence of debris that reduces the effective area where people can stop their evacuation in safe conditions (compare with $A_{eff,SAA}$ and $A_{debris,SAA}$ in Table 18). The same hazardous conditions characterize both the links converging to the SAA0 and the possible access routes (see $S_{route,SAA}$ value). Similar conditions are fundamental along the most vulnerable and long links, i.e. for SAA1 and SAA2 (along link 2), SAA3 (along link 7), SAA7 and SAA8 (along link 10). According to Table 18, SAA2 is less safe than next SAA1, mainly because of a significant risk in the SAA surface (i.e., due to debris presence, see $S_{area,SAA}$ and smaller $A_{eff,SAA}$). On the contrary, SAA3 is more "dangerous" than the other nearby ones because the better choice for access route is sensibly influenced of debris and evacuees' density conditions along it (i.e., people moving towards AA3), as shown by related $S_{route,SAA}$. About SAA7 and SAA8, they can be affected by a minor facing buildings vulnerability and by related lower debris presence, as suggested by $A_{eff,SAA}$ and $S_{route,SAA}$. Anyway, similar $S_{route,SA}$ characterize the two alternative access routes, so the shortest path is assumed to be the best one (rescuers access from AA8).
To conclude on the determined spontaneous assembly areas simulations evidence that some agents also can gathers in areas very close to an AA, as for SAA9 and SAA10, mainly because of slowing down phenomena in groups moving together (such areas not furtherly analysed collect only the 4% of not arrived evacuees) [28,129].

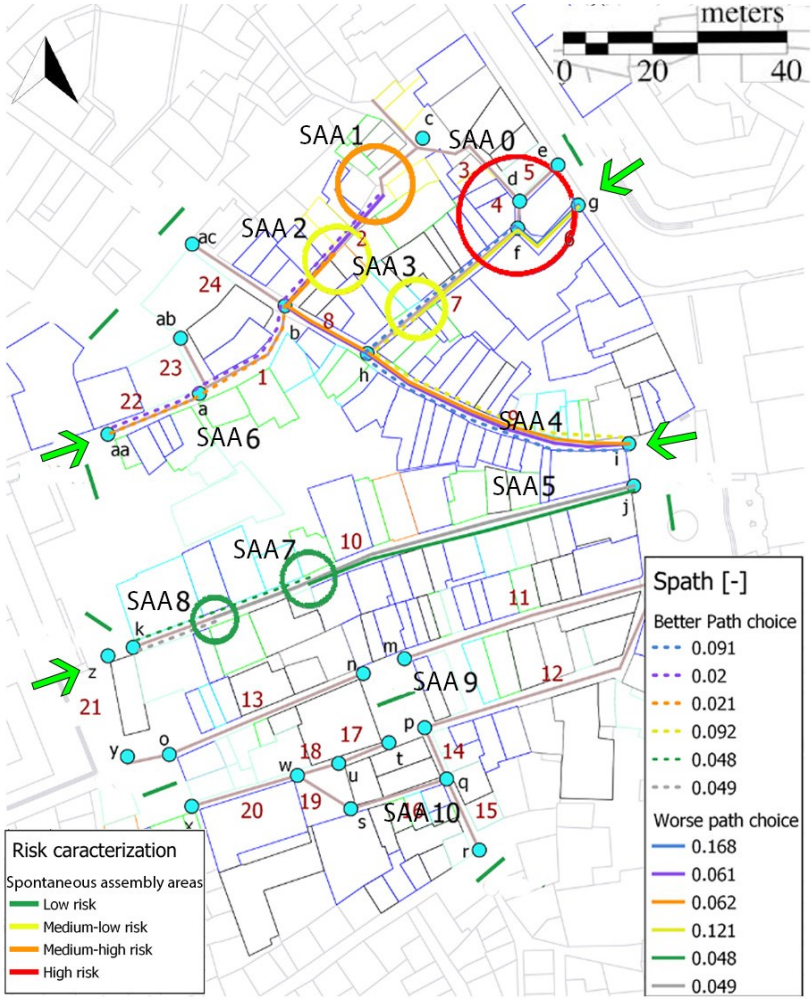

Figure 24 The spontaneous assembly area (SAA) risk maps in original scenario conditions: SAAs identification form 0 to 10 (SAAs where the J_{SAA}>5% are marked by a coloured circle), risk characterization (circle radius roughly define a priority in the $S_{SAA,norm}$ values). Paths to reach SAA: dashed lines represent the better alternative paths to reach each SAA (related KPIs results are reported for the worse case as well, continuous lines); image source: [29] re-elaborated by the author

At the end of the evaluation of collected and assessed simulation outputs, thanks to KPIs involvements, the main risk-reduction strategies adopted in this thesis are resumed into two main points (according to Section 4.2.4, the ACT phase is now started).

- Retrofitting interventions on buildings are proposed starting from the most vulnerable located along the longer paths so as to reduce their vulnerability. This solution could affect the total amount of generated ruins due to buildings collapse. Decreasing this impediment for the evacuation and rescuers' actions should be visible in the next "post-intervention scenario" for what it concerns the related KPIs (T, $S_{path,AA}$ and $S_{route,SAA}$ values). Figure 25 display on the Coimbra urban centre maps the 21 buildings located along critical links 4, 6, 7, 9, 10 where a reduction of vulnerability values is introduced by simulating the following improvements. According to [126], the introduced retrofitting interventions regard: the wall-to-wall connections by means of effectively tying walls together with steel tie-rods; the wall-to-floor connections by means of the introduction of steel angle brackets adequately anchored to walls through steel connectors and anchor plates; the structural performance of the roofing system by introducing steel tie-rods underneath the ceiling joists.
- The second level of possible solutions involves the evacuation management by providing a new plan (Figure 25) to optimize the AA number and location from the criticalities previously discussed and emerged by KPIs analysis. In this way, rescuers' actions will be focused and directed to fewer points where collects a major concentration of agents in difficulties. In detail, the AA7 is removed in the emergency plan because of its excessive proximity to the AA0 and for its low J_{AA} level by also supporting people to move towards it through plan dissemination actions or installing wayfinding signs; at the same time, the AA2 and the AA8 can be together merged in a unique AA because of KPIs highlight how such areas appear affected by low crowding conditions; finally, a new AA, named AA5 in Figure 25, is adopted instead of both the previous AA5 and AA6. The new AA5 is placed in correspondence with a crossroad of two main rescuers' paths (see Figure 24) and it could be aimed at collecting evacuees from nearby links.

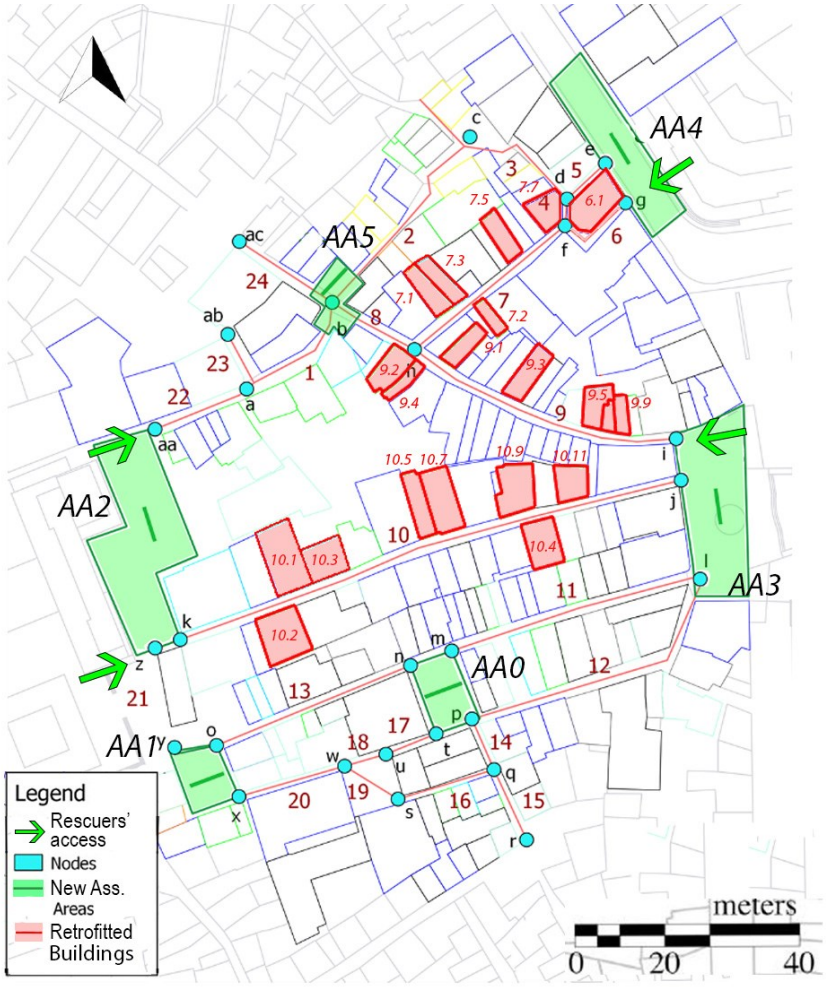

Figure 25 Proposal of risk-mitigation strategies: a) buildings with retrofitting interventions are marked in red b) the new assembly areas (AAs) position from an emergency planning perspective by including related identification codes; image source: [29] re-elaborated by the author

4.3.2 Verifying the effectiveness of proposed resilient solutions: post-intervention scenario

The possible solution discussed above (Section 4.3.1) are then both implemented to perform another time the entire PDCA cycle on the post-intervention scenario. Table 19 introduces the effectiveness of the first risk-reduction strategy that is aimed at reducing the amount of

produced debris along the paths by intervening in the seismic behaviour of buildings. Here, vulnerability values (I_{vf}) are compared to directly underline the introduced difference between the initial scenario (PLAN). The involved buildings are highlighted in Figure 25 as well, the identification code is also provided to compare their position with the values of Table 19.

Table 19 Selected buildings vulnerability index for seismic retrofit, before and after the retrofitting interventions.

Link	Building code	Original I_{vf}	Post-intervention condition I_{vf}	I_{vf} Reduction [%]
Link 4	6.1	35.78	26.13	26.97
	7.7	32.61	23.04	29.35
Link 6	6.1	35.78	26.13	26.97
Link 7	7.1	50.00	42.17	15.66
	7.2	48.48	41.30	14.81
	7.3	59.57	52.61	11.68
	7.5	34.5	24.50	28.99
	7.7	32.61	23.04	29.35
Link 9	9.1	42.17	23.91	43.30
	9.2	45.00	33.48	25.60
	9.3	33.61	26.02	22.58
	9.4	56.52	49.13	13.08
	9.5	50.07	38.65	22.81
	9.7	59.13	41.74	29.41
	9.9	50.07	38.65	22.81
Link 10	10.1	56.96	34.35	39.69
	10.2	46.37	38.65	16.65
	10.3	59.20	37.44	36.76
	10.4	54.13	32.17	40.57
	10.5	45.72	23.09	49.50
	10.7	74.78	53.04	29.07
	10.9	43.26	23.91	44.73
	10.11	49.13	26.52	46.02

The vulnerability reduction affects not only the depth of produced debris on the links where the buildings rest but also on the values of urban path network vulnerability [70] (i.e.: the links 4, 6, 7, 9, and 10). Figure 27 shows the graphical outputs to compare with the previous Figure 23). Such strategy demonstrates how is possible to reach a visible safety increase by intervening on a limited and well-determined number of buildings. Evacuation improvements are translated into the availability for pedestrians' motion of the effective area especially within a typical historical scenario characterized by many narrow streets. Hence although the difference between the absolute values of both scenarios can seem not so impressive, it can be crucial in ensuring safe paths for evacuees and safe access routes to rescuers. To confirm such statements, Table 20 offers a comparative framework of the obtained KPIs from both

the inquired scenarios (pre and post). The effects of the second implemented risk-reduction strategy will be observable only after performing the simulations (DO).

Table 20 Links vulnerability index, debris amount, effective areas before and after retrofit interventions the considered earthquake magnitude.

		Original condition			Post-intervention conditions		
Link	Total Area [m^2]	V_{link}	A_{debris} [m^2]	Free Area [%]	V_{link}	A_{debris} [m^2]	Free Area [%]
Link 4	14.75	0.53	11.87	20	0.38	10.78	27
Link 6	55.06	0.57	45.21	18	0.49	43.25	21
Link 7	150.76	0.71	128.10	15	0.65	122.90	18
Link 9	240.72	0.66	210.93	12	0.60	202.73	16
Link 10	441.33	0.69	342.04	22	0.59	325.27	26

The KPIs evaluation phase for the post-intervention scenario (CHECK) openings with the graphical outputs given in Figure 26 where the evacuation curves are considered for both the whole simulated scenario (average, maximum, and minimum evacuation curves) and for each AA. Comparing such results with the ones obtained for the initial scenario, the difference between the maximum and minimum evacuation curves is acceptable since it is equal to 4% (<10%). Average results show that 746 evacuees (62% of the hosted population) seem to be able to reach a AA within the considered simulation time (350s), which is almost the same conditions for the original scenario. Table 21 summarizes the occupancy conditions of each AA and in Table 22, S_{AA} and $S_{AA,norm}$ are evaluated by also reporting the comparisons with the initial scenario data.

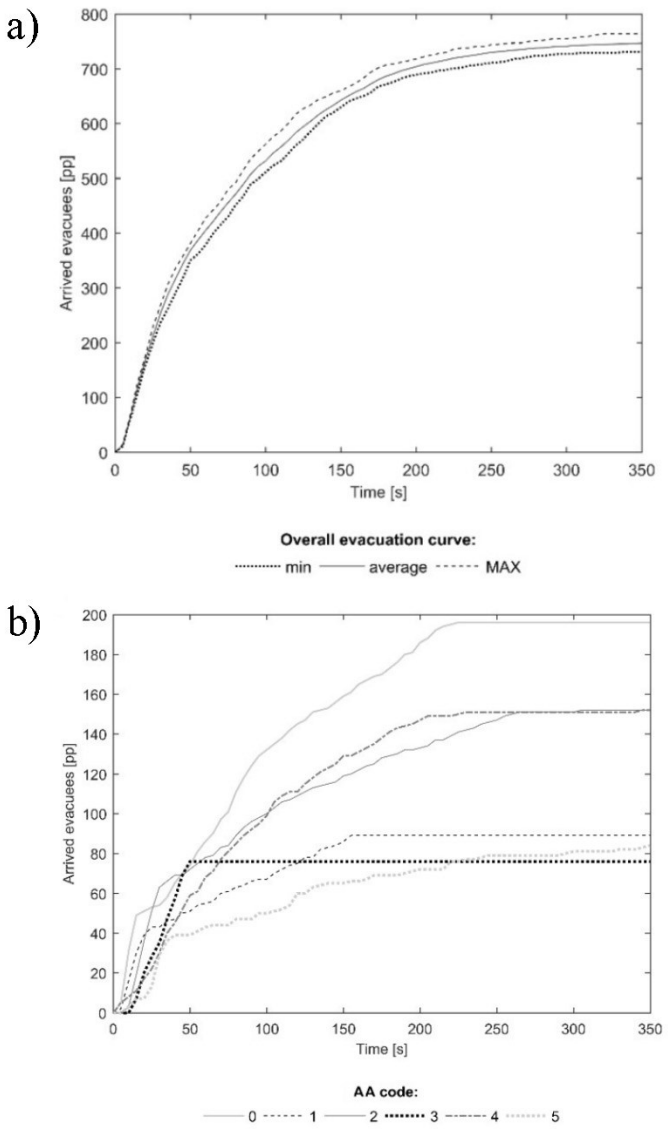

Figure 26 Post-intervention scenario evacuation curve results: A) Average, minimum and maximum curves for the whole area; B) Evacuation curves obtained for each of the new considered AA according to Figure 25; image source [29]

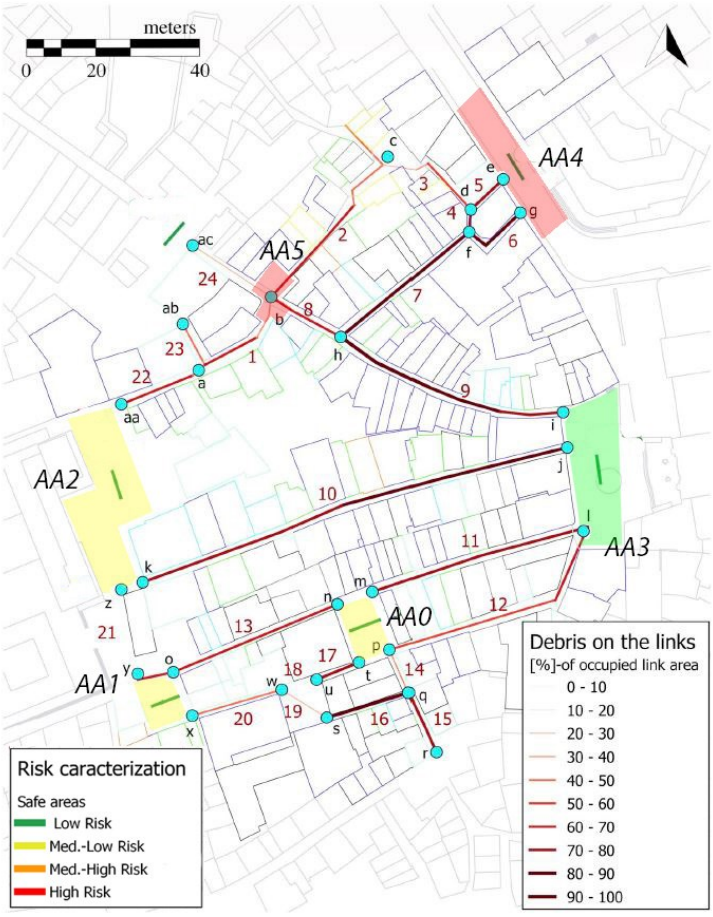

Figure 27 Post-intervention building debris estimation scenario; image source: [29] re-elaborated by the author

The previous graphs and the evaluated KPIs confirm that a number of agents very similar to one of the initial scenario conditions can gather in a reduced number of AA (see dJ_{AA} data in Table 22), without significant LOS_{AA} levels increase, with not increasing risk conditions along the access routes (see $\Sigma S_{link,AA}$ data in Table 22). Moreover, AA safety levels are quite similar. Although some extreme conditions related to the debris production effects can be reduced due to introduced retrofitting interventions on buildings (compare to Figure 27), the evacuees' motion conditions get worsen. In particular, the risk for the AA4 is more evident than the initial scenario. Although the retrofit actions on the two most vulnerable buildings along link 4 allow preventing the path blockage, the J_{AA} can so increase by boosting negative interactions between evacuees and debris, as mainly shown by T (and so S_{AA}) higher values. For this reason, AA4 has now $S_{AA,Norm}$=100%. Figure 27 graphically summarizes with four different colours such as $S_{AA,norm}$ values on the urban risk map.

Table 21 KPIs for overcrowding conditions for each assembly area (AA) in post-intervention conditions and comparison with the original scenario. (*) refers to people not arrived in the AA but stopped really close to it and that are not included in the J_{AA} calculation. The subscript *Pi* stands for "post-intervention" and the subscript *0* stands for initial scenario conditions.

AA	0	1	2	3	4	5
$A_{eff,AA}$ [m^2]	303	237	930	545	265	167
N_p [pp]	196	89	152+5*	76+11*	152	84+17 *
LOS_{AA}	1.546	2.663	5.931	6.279	1.743	1.653
$J_{AA,pi}$ [%]	26%	12%	20%	10%	20%	11%
Compare to initial scenario	0-7	1	2-8	3	4	5-6
$J_{AA,0}$ [%]	18%+7%	11%	6%+13 %	15%	10%	9%+6 %
dJ_{AA} [%]	5%	8%	7%	-32%	104%	-25%

Table 22 KPIs for assembly area (AA) in post-intervention conditions and comparison with the initial scenario. The subscript *Pi* stands for "post-intervention" and the subscript *0* stands for initial scenario conditions.

AA	0	1	2	3	4	5
Jp,s [%]	26%	12%	20%	10%	20%	11%
T [-]	1.329	1.181	1.273	1.023	1.578	1.248
$\Sigma S_{link,AA,pi}$	0.001	0	0	0	0	0.170
S_{AA} [-]	0.421	0.216	0.341	0.104	0.613	0.494
$S_{AA,Norm}$	49%	35%	50%	17%	100%	81%
Original AA to compare	0	1	8	3	4	5
T_o [-]	1.254	1.157	1.402	1.265	1.034	1.437
dT [%]	6%	2%	-9%	-19%	53%	-13%
$\Sigma S_{link,AA,o}$	0.020	0.000	0.000	0.000	0.000	0.288
$S_{AA,o}$ [-]	0.369	0.219	0.408	0.314	0.110	0.630
dS_{AA} [%]	14%	-1%	-16%	-67%	457%	-22%

In this new performed scenario, the average number of evacuees who decide to gather in a spontaneous assembly area is about 320. The value is similar to the one of the original scenario, but the majority of evacuees gather in a reduced number of SA, as shown by Figure 28 that offer the SAAs risk map by mainly evidencing the ones with J_{SAA}>5%: such SAA contains the 62% of pedestrians gathering in a SAA. Figure 28 also evidences the two main alternative rescuers' access routes to reach each SAA. Table 23 resumes the related KPIs for them by finally providing S_{SAA} and $S_{SAA,norm}$ values. $S_{route,SAA}$ is referred to the better alternative route within the ones of Figure 28. In Table 23, SAA0 and SAA1 can be respectively

compared to SAA0 and SAA2 of the original scenarios because they are placed in the same areas.

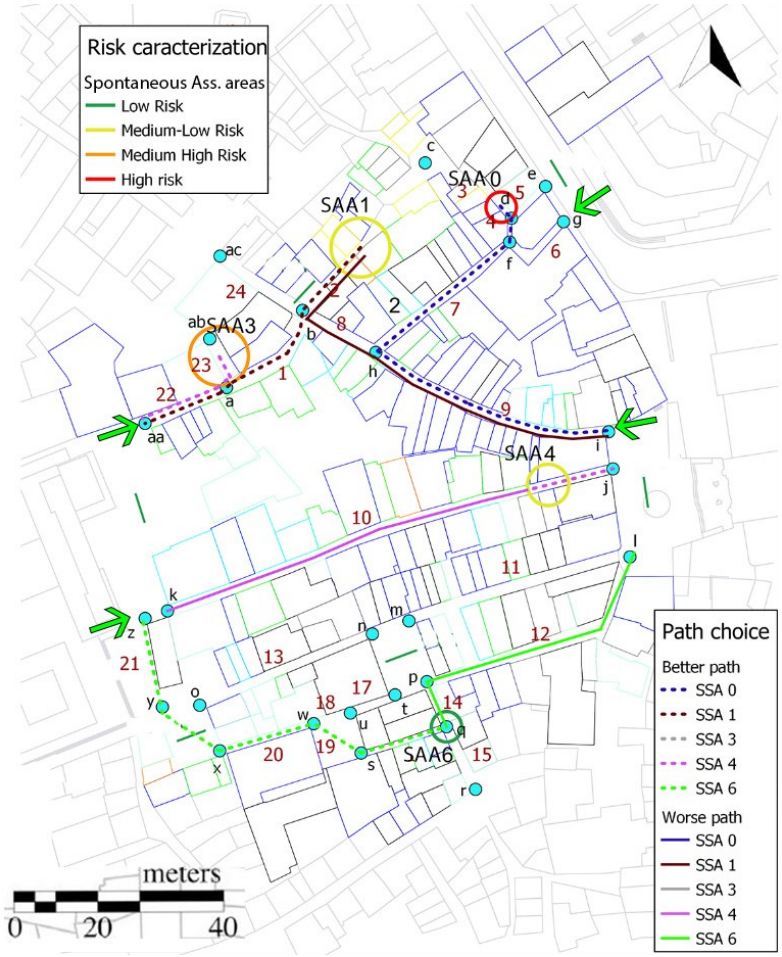

Figure 28 Analysis of the improved urban scenario: spontaneous assembly areas (SAAs) risk characterization and identification of the best paths to reach each SAA, rescuers' access points to the area are also reported on the urban layout map; image source: [29] re-elaborated by the author

In detail, SAA0 hazardous conditions are reduced in terms of the number of gathered individuals and in terms of debris influence, while $S_{route,SAA}$ increases because of the higher number of evacuees moving along the access route. SAA1 in post-intervention conditions owns a higher risk in respect to SAA2 of the initial scenario, but this is mainly due to the significant increase in the number of gathering individuals and its effect on $S_{area,SAA}$. For this reason, SAA1 is the most risk area in post-intervention conditions.

Risk reduction interventions along link 10 allow limiting the formation of SAA. Now people seem to spontaneously gather in SAA4 since they were slowed down by debris interference, but not blocked by them. The variation of AA position influences the evacuation process for the nearest area. The deletion of AA7 provokes a higher crowding in the AA0 while evacuees from areas near links 15, 16, and 20 prefer to collect in SAA6, which is placed in a wider square. SAA6 can host them without significant interactions with debris (see related $A_{eff,SAA}$). Anyway, the S_{SAA} for the SAA6 is affected by the significant evacuees' usage conditions.
To conclude, SAA1, SAA4 and SAA6 can be easily reached by rescuers, as pointed out by $S_{route,SAA}$ values in Table 23. Furthermore, they are also located very close to AAs: gathering evacuees could be invited to continue their evacuation towards AAs through, for instance, the punctual installation of wayfinding systems.
Such results underline how absolute S_{SAA} values are generally lower than the ones for the original conditions, by demonstrating the effectiveness of both the implemented risk reduction strategies.

Table 23 KPIs for spontaneous assembly areas (SAAs) in the post-intervention scenario and comparison with the initial one.

SAA	0	1	3	4	6
$A_{eff,SAA}$ [m^2]	21	33	54	45	122
$S_{area,SAA}$ [-]	0.077	0.157	0.013	0.150	0.021
$S_{route,SAA}$ [-]	0.110	0.042	0.024	0.020	0.003
J_{SAA} [%]	5%	15%	9%	13%	20%
S_{SAA} [-]	0.144	0.221	0.094	0.203	0.197
$S_{SAA,norm}$ [-]	65%	100%	43%	90%	89%
Original SAA to compare	0	2	-	-	-
$A_{eff,SAA,o}$ [m^2]	18	33	-	-	-
$d\ A_{eff,SAA}$ [%]	33%	0%	-	-	-
$S_{area,SAA,o}$ [-]	0.345	0.118	-	-	-
$dS_{area,SAA}$ [-]	-78%	33%	-	-	-
$S_{route,SAA,o}$ [-]	0.091	0.043			
$dS_{route,SAA}$ [%]	20%	-2%			
$J_{SAA,o}$ [%]	19%	10%	-	-	-
dJ_{SAA} [%]	-73%	-55%	-	-	-
$S_{SAA,o}$ [-]	0.345	0.118	-	-	-
dS_{SAA} [%]	-61%	41%	-	-	-

Discussing about adopted risk-reduction solutions, the reduction of AAs combined to retrofit interventions on specific buildings, lead to evacuation improvements. Although the same number of evacuees arrives at a similar time to the AAs, differences in evacuation curves slope are evinced. Such discrepancy is essentially due to the individuals' traveled distance to an AA. From the rescuers' standpoint, evacuees are collected in a few AAs, so first aid actions can be better focused on them. At the same time, access paths have a lower risk (see Table 22). On the other side, evacuees-debris interactions are reduced, especially for the narrowest,

most complex, and longest links in the historical urban path network, and for the urban network areas hosting the most used SAAs, by improving motion and gathering conditions. Effects on links are mainly noticed for links 7, 8, and 9 towards the AA3 and SSA5 (reduction in difference-in-path-ratio index T and related reduction of S_{AA}) and for link 10 in relation to the SAA4 (i.e., access paths conditions). Effects on areas hosting SAA are also evidenced by an increase of the effective area (i.e., not occupied by debris), especially in SAA1 (see related $S_{area,SAA}$ in Table 23).
Finally, the analysis of post-intervention conditions allows to point out how some additional strategies should be implemented (ACT). Figure 29 offers an additional plan for the historic part of Coimbra based on the following notes.

- Although their new position and optimization, the AAs are not totally exploited in terms of hosted people capacity. A further selection of AAs could be promoted (e.g.: merging the AA1 with the AA5 also trying to collect evacuees from the SAA6). Anyway, many SAAs are now very close to previous AAs (i.e.: SAA1 and AA5; SAA4 and AA3): this result suggests that wayfinding strategies could be adopted to guide people towards the nearest AA [28]. In particular, evacuation signs could be installed along the paths or small first responders' groups should be immediately sent to such SAAs (i.e. see the green arrows in a row in Figure 29).
- Additional retrofit interventions could involve other buildings along critical links, especially along links 9 and 10 since they connect the two AAs, and link 7 since this remains the most vulnerable one within the case study area. Economic analyses for supporting public-private partnerships in such operations could be evaluated to define the sustainability optimization of such solutions.
- Analyses on the selected area of the Historic Centre of Coimbra should be combined with other ones in surrounding parts of the overall historical urban fabric. The division within sectors (for simulation and emergency management purposes) could be more effective to plan focused and agile solutions also by involving different input scenario configurations (i.e. a different earthquake magnitude, considering visitors and tourists among the hosted population). Boundaries between sectors (and related AA on the boundary), nevertheless, should be jointly analysed as far as possible.

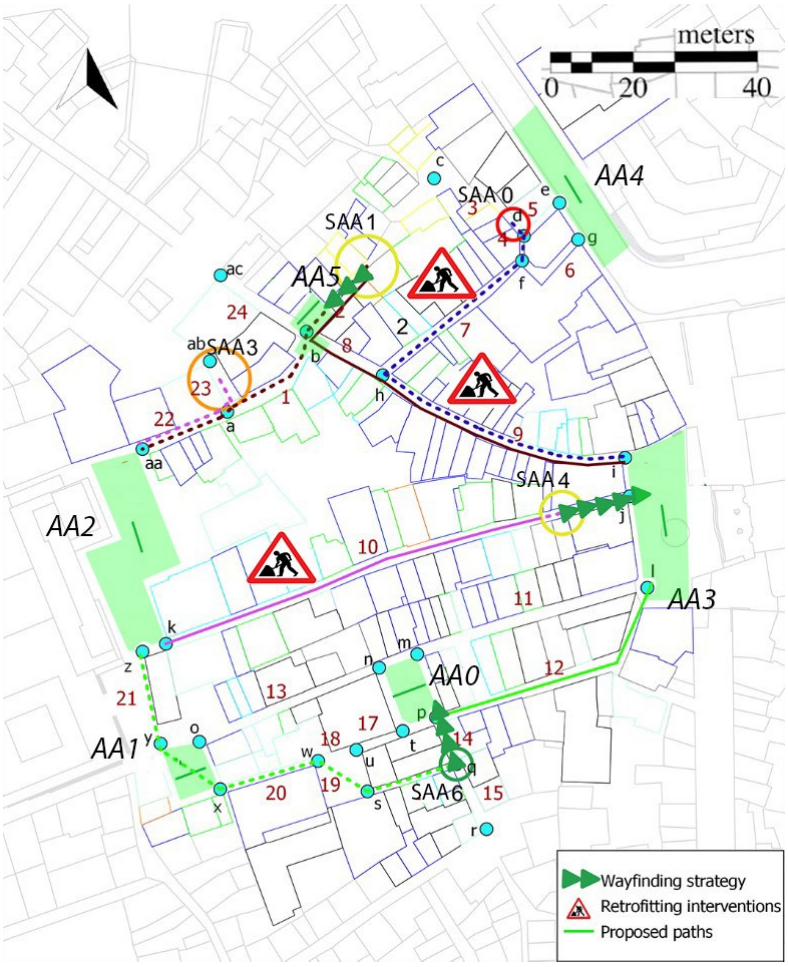

Figure 29 Proposal of additional risk-mitigation strategies on the post-intervention scenario, by defining possible wayfinding solutions, additional retrofit interventions, and proposed access routes to assembly area and spontaneous assembly area; image source: [29] re-elaborated by the author

Chapter 5

5 Conclusions and future works

Currently, local administrations and Civil Protection Bodies generally underestimate the influence of emergency management based on the innovations introduced by recent research achievements. They plan evacuation strategies (e.g.: earthquakes in this thesis) without jointly considering both a comprehensive prediction of the disaster-induced modification on the Built Environment and their possible interactions with the hosted populations. From this point of view, earthquakes are one of the most important disasters to face off that modify the daily scenarios and frightened hosted communities.

The present thesis is aimed at developing a general operational framework that could guide safety planners through the proposal of calibrated, effectiveness and resilient solutions towards different scenarios where the combined effects of multi inputs are dynamically implemented. Firstly, this work tries to define immediate criteria for urban scenario characterization in case of a seismic event through rapid data collection approaches. Indeed, literature is populated by many works on the same issues that deeply focus on specific aspects and require detailed and dispendious analysis to derive a risk quantification on single BE elements (e.g.: public buildings, private dwellings, but also infrastructures, bridges, etc). Otherwise, the main aim of this kind of work is to rapidly provide an overall risk characterization on wide urban areas.

Hence, the adoption of speditive and holistic methodologies to investigate such aspects can be adopted to have a quick and interdisciplinary knowledge of the scenario and disaster conditions and hence to manage the risk-reduction operations. A large part of this thesis is aimed at proposing methodologies to answer this necessity for emergency planning. Developed and tested tools are centred on the quantification of buildings aggregates vulnerability by speed up the evaluation process by taking advantage of existing methods. Moreover, the innovative employed tools are based on available and easy to detect parameters without the necessity to conduct costly in-situ surveys on materials quality and constructive techniques by trained personnel. Vulnerability issues are deeply investigated because of their connection to building damage levels. Indeed, debris presence due to buildings collapse has heavily consequence on the availability of evacuation paths, which play a key role in immediate earthquake aftermath conditions for both rescuers and hosted population. Thus, the risk levels of the urban path network including both direct and indirect damages to the infrastructure system are here determined by developing an innovative and holistic tool. Differently from similar previous studies, here the involvement of a reliable and “remote” approach allows to rapidly create scenarios by non-expert technicians as well. Although the thesis developed ad hoc methods such evaluations can be also performed by replacing suggested but not exclusive methods with others that giving the same inquired parameters (also in the view of future methodological improvements). This adaptability criterion enriches the operative framework innovation.

The other side of the emergency management medal is the employment of a behavioural based perspective pursued to evaluate the impact of exposed individuals' behaviours in an

emergency. Understanding which evacuation threats could influence people while moving in the earthquake-affected urban fabric, and where people stop their evacuation because of behavioural, psychological, and surrounding environmental conditions (i.e. group phenomena, familiarity with the urban spaces, debris presence in post-earthquake environment), becomes essential to identify which are the emergency process requirements. Innovatively, this work takes into account and widely debates the exposure issue introducing several users' typologies that populate the BE at different times and for different purposes (e.g.: age-related inhabitants typologies, presence of tourists, and daily visitors). Furthermore, the crowd density of outdoor spaces and public buildings are detected and considered to determine eventual overcrowding conditions that could exacerbate the emergency from a multi-hazard perspective. Buildings with specific intended uses (e.g.: hotels, hospitals, theatres, restaurants) are recognised to this end. All these kinds of data will be considered to create more detailed scenarios on hosted populations in simulation-based risk assessment.

In view of the above, a validated urban earthquake pedestrians' evacuation simulation software allows to retrieve and compare probable behaviours and motion evacuation decisions in relation to different environmental conditions, including damages and different emergency management decisions. In this way, the different risk-influencing factors are jointly combined, and man-man and man-environment interactions are simulated to determine their effect on citizens' safety levels. Then, simulation-based raw data have to be interpreted. To this purpose, ad hoc Key Performance Indicators (KPIs) are defined to provide inquired safety levels on risk maps and related suggestions for risk-reduction strategies to be implemented in the urban paths network (management and retrofit action). The method can be applied in an iterative way, so as to compare different scenarios based on the proposed risk-reduction strategies. This way, the operational framework appears able to offer a more comprehensive community resilience assessment in a given scenario. Results reached in this thesis, constitute the starting point to plan the emergency from a sustainable and incisive perspective.

The capabilities of the proposed work are evidenced by significant case study applications which demonstrate how the proposed framework is: holistic since it handles input data on seismic hazard, vulnerability, exposure, and emergency response; structured, because it combines data to define emergency scenarios to move towards advanced simulation-based methodologies; sustainable, since it is mainly based on available and quick-to-access databases and tools; reliable, due to its experimental-based approach; and finally oriented towards a human-centred perspective that constitutes the main significant novelty of the proposed work in view of risk assessment and emergency management actions.

Future efforts should firstly apply the general operative framework to other case studies, to possibly derive some general rules and trends in the evacuation management and safety levels. Furthermore, the investigation of different solutions impact should actively involve additional factors, by also including deeper characterization of population, i.e. in terms of age/gender classes, differences due to population densities and localization of individuals (e.g. creating scenarios at a different time of the day/week/year), emergency procedure and plan awareness, interaction with wayfinding and rescuers' motion (including vehicles access). Defined KPIs can provide quantitative support to safety designers, urban planners, not only by assessing the impact of different risk mitigation strategies but also by defining the effective use of assembly areas by evacuees. In this way, the number of people arriving

in assembly areas can be improved and rescuers' priority actions are guided. Anyway, future works could combine such KPIs to additional elements (e.g. economic aspects also in relation to cost assessment issues; social vulnerability aspects) to move towards a more comprehensive community resilience assessment in the given scenario. From a general point of view, the outputs of this novel proposed framework could be integrated with the GIS tool as fundamental improvements for a quick urban scale application, thus being useful for its management and analysis. The possibility of spatial presentation of results, associating the whole probabilistic algorithm, makes GIS a very effective tool in the dissemination of such data and for supporting the definition of seismic risk mitigation and management strategies for both urban safety planners and policymakers and Civil Protection Bodies. Finally, this novel proposed framework can be employed with other disaster typologies (e.g. further multi-hazard conditions and climate change-related disasters). To do this, some adjustments will be required on the definitions of risk-related factors connected to different disaster sources to face off.

6 Appendices

6.1 Supplementary material

Table A 1. Method validation sample data. The assessed link is identified through to the relative ID by showing related: location and reference earthquake; evaluated risk index ($I_{R,j}$) and normalised index ($I_{Rn,j}$) according to the three approaches (in the AHP approach, such values are equal); Road Damage Levels (RDS).

code	Location	Earthquake	Modified Cherubini's approach		Expert judgment		AHP	RDS
			$I_{R,j}$	$I_{Rn,j}$	$I_{R,j}$	$I_{Rn,j}$	$I_{R,j}$	
A	Arquata del Tronto (AP)	Central Italy 2016	1.22	41%	3.57	40%	44%	2
B	Pescara del Tronto (AP)	Central Italy 2016	1.65	55%	5.13	58%	58%	3
C	Norcia (PG)	Central Italy 2016	1.18	39%	3.36	38%	43%	1
D	Norcia (PG)	Central Italy 2016	1.30	43%	3.73	42%	46%	1
E	Norcia (PG)	Central Italy 2016	1.50	50%	4.79	54%	56%	3
F	Castelluccio di Norcia (PG)	Central Italy 2016	1.51	50%	4.92	55%	60%	2
G	Castelluccio di Norcia (PG)	Central Italy 2016	1.54	51%	4.99	56%	60%	3
H	Tra Valli Umbre (PG)	Central Italy 2016	1.53	51%	5.18	63%	63%	4
I	Forca Canapine (PG)	Central Italy 2016	1.61	54%	3.17	65%	63%	4
J	Amatrice (RI)	Central Italy 2016	1.16	39%	1.96	36%	45%	1
K	Offida (AP)	Central Italy 2016	0.75	25%	2.00	22%	32%	0
L	Tolentino (MC)	Central Italy 2016	0.76	25%	5.33	22%	31%	0
M	Accumoli (RI)	Central Italy 2016	1.72	57%	4.58	60%	59%	3
N	Amatrice (RI)	Central Italy 2016	1.73	58%	4.83	51%	54%	3
O	Amatrice (RI)	Central Italy 2016	1.83	61%	4.82	54%	58%	3
P	Onna (AQ)	Aquila (Italy) 2009	1.36	45%	4.29	59%	56%	4
Q	Onna (AQ)	Aquila (Italy) 2009	1.32	44%	4.29	48%	53%	2

R	Fossa (AQ)	Aquila (Italy) 2009	1.41	47%	4.86	59%	58%	4
S	Arischia (AQ)	Aquila (Italy) 2009	1.44	48%	4.66	52%	51%	3
T	San Felice sul Panaro (MO)	Emilia (Italy) 2012	1.28	43%	3.84	47%	44%	2
U	San Carlo (FE)	Emilia (Italy) 2012	1.24	41%	3.49	39%	47%	2
V	San Carlo (FE)	Emilia (Italy) 2012	1.29	43%	3.62	41%	48%	3
W	Mirabello (FE)	Emilia (Italy) 2012	1.33	44%	3.62	41%	47%	2
X	Sant'Agostino (FE)	Emilia (Italy) 2012	1.40	47%	3.66	41%	50%	2
Y	San Carlo (FE)	Emilia (Italy) 2012	1.29	43%	3.62	41%	48%	3

Table A 2. Case study application results from the historical centre of Offida (Italy), by collecting obtained values from AHP approach subdivided into topics for each link and squares. For both paths network elements, the evaluated risk indices ($I_{R,j}$) and the normalised ones ($I_{Rn,j}$) are shown.

ID case	A	B	C	D	E	F	$I_{R,j}$	$I_{Rn,j}$
Links								
A	Clear	0.47	0.20	0.73	0	1.25	2.65	29%
B	Clear	0.50	0.33	0.97	0.25	1.00	3.05	33%
C	Clear	0.43	0.33	0.97	0.50	1.00	3.24	35%
D	Clear	0.50	0.60	0.97	0.50	1.00	3.57	39%
E	Clear	0.60	0.47	1.27	0.50	1.00	3.84	42%
F	Clear	0.50	0.60	0.97	0.75	1.00	3.82	42%
G	Clear	0.60	0.33	1.27	0.50	1.00	3.70	40%
H	Clear	0.50	0.33	0.97	0.75	1.00	3.55	39%
I	Clear	0.50	0.33	1.57	0.50	1.00	3.90	42%
L	Clear	0.50	0.33	1.57	0.25	1.00	3.65	40%
M	Clear	0.50	0.73	1.47	0.50	1.00	4.20	46%
N	Clear	0.50	0.33	1.27	0.75	1.00	3.85	42%
O	Clear	0.60	0.20	1.27	0.50	1.00	3.57	39%
P	Clear	0.67	0.60	1.27	0.75	1.00	4.29	47%
Q	Clear	0.60	0.33	1.27	0.75	1.00	3.95	43%
R	Clear	0.67	0.33	1.27	0.75	1.00	4.02	44%
S	Clear	0.53	0.93	1.63	0.25	1.25	4.60	50%
T	Clear	0.53	0.33	1.93	0.25	1.25	4.30	47%
U	Clear	0.53	0.33	0.63	0.50	1.25	3.25	35%
V	Clear	0.73	0.60	2.47	0.25	1.25	5.30	58%
Z	Clear	0.53	0.33	0.33	0.25	1.25	2.70	29%
Squares								

P1	Clear	0.43	0.07	1.73	0	1.25	2.45	30%
P2	Clear	0.47	0.67	0.33	0.25	1.25	2.96	35%
P3	Clear	0.53	0.07	1.67	0.50	1.00	3.77	45%
P8	Clear	0.67	0.07	1.27	0.50	1.00	3.50	42%
P10	Clear	0.67	0.07	1.27	0.50	1.00	3.50	42%
P11	Clear	0.50	0.07	0.97	0.50	1.00	3.04	36%

Table A 3. Results of the case study buildings application (50 structural units with their streets). For each of them, the table shows their geometrical measures and ratios, the buildings damage grades (μ_D) according to EMS-98 and results from the application of: civil protection method, Ferlito and Pizza's 2011, both debris estimation criteria, the original Artese Achilli method and the Observed one, the *k95* macroseismic damages-based method and the Observed macroseismic damages-based one and finally, the conditions of the real scenario (C stands for "clear" and B for "blocked"). Each element ID is related to a structural unit, according to the following criterion: the numbers identify the aggregate; the letter identifies the related structural unit; the capital letters stand for the urban centre of origin (IL for Illica, AS for Amatrice south part, AN for Amatrice north part, CD for Capodacqua, AC for Accumoli, AT for Arquata del Tronto).

Element ID	*h* [m]	*W* [m]	*h/W*	μ_D	*Limit Condition for the Emergency (LCE)*	*Ferlito and Pizza*	*Debris estimation criterion 1*	*Debris estimation criterion 2*	*Artese Achilli*	*Observed Artese Achilli*	*k95 macro-seismic damages-based*	*Observed macro-seismic damages-based*	*Real scenario*
4.b_IL	7.1	3.5	2.03	1	B	B	C	B	C	C	B	C	C
4.c_IL	6.5	4	1.63	1	B	B	C	B	C	C	B	C	C
21.a_AS	7.1	5.5	1.29	2	B	B	C	C	C	C	B	C	C
21.e_AS	5.7	3.1	1.84	2	B	B	C	B	B	C	B	C	C
21.f_AS	5.5	3.1	1.77	2	B	B	C	C	C	C	B	C	C
21.g_AS	2.9	3.1	0.94	2	C	B	C	C	C	C	C	C	C
2.g_AN	3.0	3.8	0.79	2	C	B	C	C	C	C	C	C	C
1.a_CD	6.4	8.5	0.75	2	C	B	C	C	C	C	C	C	C
8.e_AC	10.2	3.5	2.91	2	B	B	C	B	C	C	B	C	C
1.b_IL	7.3	5.6	1.30	2	B	B	C	C	C	C	B	C	C
4.h_IL	6.8	1.5	4.53	2	B	B	C	B	B	C	B	C	C
9.a_IL	6.7	3.1	2.16	2	B	B	C	B	C	C	B	C	C
9.b_IL	9.2	1.9	4.84	2	B	B	C	B	B	C	B	C	C
2.c_AN	10.7	9.7	1.10	2	B	B	C	C	C	C	B	C	C
9.c_AS	7.0	2.1	3.33	3	B	B	C	B	B	C	B	C	C
9.c_IL	4.8	3.1	1.55	3	B	B	C	B	B	C	B	C	C
1.f_AS	7.5	5.7	1.32	3	B	B	C	C	C	C	B	C	C
1.b_AT	12.5	6	2.08	3	B	B	B	B	C	C	B	C	C
6.f_AN	8.7	3.7	2.35	3	B	B	C	B	C	C	B	C	C
19.a_IL	7.5	2.5	3.00	4	B	B	C	B	B	B	B	B	C
20.a_IL	7.3	3.8	1.91	4	B	B	C	C	C	C	B	B	B
9.d_AS	6.6	2.1	3.14	4	B	B	C	B	C	B	B	B	B
21.c_AS	7.1	5.5	1.29	4	B	B	C	C	C	C	B	B	B
22.a_AC	9.0	4.5	2.00	4	B	B	C	B	C	C	B	B	B
1.a_IL	8.6	5	1.72	4	B	B	C	B	C	C	B	B	C

2.e_AN	10.9	12	0.90	4	C	B	C	C	C	C	C	C	C
6.a_CD	10.1	6.7	1.51	4	B	B	C	B	C	C	B	B	B
6.b_CD	11.5	3.7	3.11	4	B	B	C	B	B	B	B	B	B
1.a_AT	16.3	4	4.08	4	B	B	C	B	C	B	B	B	B
1.d_AS	8.8	6.5	1.35	4	B	B	C	C	C	C	B	B	B
6.b_AN	10.9	3.7	2.93	4	B	B	C	B	C	C	B	B	B
6.g_AN	8.1	2.8	2.89	4	B	B	C	B	C	C	B	B	B
2.b_AN	8.9	9.7	0.92	4	C	B	C	C	C	C	C	C	C
4.a_IL	7.5	2.3	3.26	5	B	B	C	B	B	B	B	B	B
6.a_AN	5.9	3.7	1.59	5	B	B	C	B	C	B	B	B	B
6.b_AS	9.6	3.7	2.59	5	B	B	C	B	C	B	B	B	B
2.d_AN	9.4	3.5	2.67	5	B	B	C	B	C	B	B	B	B
2.a_IL	5.3	4.9	1.08	5	B	B	C	C	C	C	B	B	B
3.b_IL	3.5	6.5	0.53	5	C	B	C	C	C	C	C	C	C
4.d_IL	4.1	4	1.03	5	B	B	C	C	C	C	B	B	B
7.a_IL	3.8	8.4	0.45	5	C	C	C	C	C	C	C	C	C
1.a_AS	9.2	3.4	2.71	5	B	B	C	B	B	B	B	B	B
1.b_AS	8.2	3.4	2.41	5	B	B	B	B	B	B	B	B	B
1.c_AS	9.1	6.5	1.40	5	B	B	C	C	C	C	B	B	B
6.c_AS	10.0	2.9	3.45	5	B	B	C	B	C	B	B	B	B
21.b_AS	8.3	5.2	1.60	5	B	B	C	B	C	B	B	B	B
6.c_AN	11.9	3.7	3.22	5	B	B	C	B	C	B	B	B	B
6.d_AN	11.0	3.7	2.97	5	B	B	C	B	C	B	B	B	B
6.e_AN	12.1	3.7	3.27	5	B	B	C	B	C	B	B	B	B

6.2 Earthquake Pedestrians' Evacuation Simulator: further notions about the employed tool

The Earthquake Pedestrians' Evacuation Simulator (EPES), developed and validated by previous works for historical city centers evacuation simulation [6], is used to perform evacuation simulations of Sections 4.2 and 4.3. EPES uses a combined ABM-SFM model to solve pedestrians-pedestrians and pedestrians-built environment interactions in emergency conditions.
In the ABM model, the Buil Environment (BE) is modelled like a specific agent, and so criteria for earthquake-induced modifications can be autonomously described. The original rules are based on a rough and discrete quantification of building debris according to building vulnerability and earthquake EMS-98 intensity. In the adopted EPES version, the building debris on urban paths d_{debris} [m] proposed by [39] is introduced to include continuous and experimentally-validated debris estimation criteria. For each building, the input values of the method are:

- buildings vulnerability V_F [-], determined according to [5];
- magnitude ratio R_M [-], that varies from 0 to 1 and is the ratio between the seismic event Moment Magnitude and the maximum expected Magnitude (equal to 9.5 according to the World seismic history);
- the ratio between building height and facing street geometry h/W [-].

The inputs are combined as shown by Equation A.1 to define the Modified Vulnerability index V_F^* [-], which includes three factors.

$$V_F^* = V_F \cdot R_M \cdot {}^{h}/_{W} \tag{A.1}$$

Finally, for each building, Equation A.2 calculates d_{debris} [m] as a function of V_F^* and the width W of the facing street [m]. Debris distribution is constant for all the building sides along the considered street.

$$d_{debris}^{pred} = \begin{cases} (213.09 \cdot V_F^*/100) \cdot W, & , V_F^* \leq 0.47 \\ W, & V_F^* > 0.47 \end{cases} \tag{A.2}$$

About the pedestrians' evacuation criteria, the motion of each simulated individual is influenced by the decisions of surrounding evacuees, debris, historical buildings, and path features. According to the SFM approach [141], each pedestrian moves in a "forces field" characterized by repulsive forces from obstacles $\overrightarrow{F_{rep,w}}$ [N] (i.e. obstacles and debris avoidance; keeping a safety distance from buildings and debris) and people $\overrightarrow{F_{rep,\iota}}$ [N] (i.e. avoid physical contact) and attractive forces from evacuation target $\overrightarrow{O_g(t)}$ (i.e. desire to reach an assembly area) and from other individuals $\sum \overrightarrow{F_{attr,\iota}(t)}$ (i.e. social attachment between evacuees in the same group) and phenomena. Synthetically, he/she tries to adequate its preferred speed to such forces. Equation A.3 resumes the SFM motion equation, where the

individual's acceleration $\frac{\overrightarrow{dv_i(t+dt)}}{dt}$ [m/s^2] at the instant of time t depends on the aforementioned forces resultants and on their random variation $\overrightarrow{\varepsilon(t)}$ [N]. Equation A.3 is solved for each simulated pedestrian at each simulation time.

$$m_i \frac{\overrightarrow{dv_i(t+dt)}}{dt} = \overrightarrow{O_g(t)} + \sum \overrightarrow{F_{rep,i}(t)} + \sum \overrightarrow{F_{rep,w}(t)} + \sum \overrightarrow{F_{attr,i}(t)} + \overrightarrow{\varepsilon(t)} \qquad \text{(A.3)}$$

Equation A.4 resumes the evacuation target attractive force, which depends on the individual's: mass m_i [kg]; preferred speed $v_{pref,i}(t)$ [m/s]; velocity at the next simulation step $\overrightarrow{v_i(t+dt)}$ [m/s]; reaction time τ_i [s]; dt [s] is the time difference between two consecutive calculation instants.

$$\overrightarrow{O_g} = \frac{m_i \left(v_{pref,i}(t)\overrightarrow{e_i(t)} - \overrightarrow{v_i(t+dt)} \right)}{\tau_i} \qquad \text{(A.4)}$$

About decisional rules included in the ABM, the evacuation path choice in "spontaneous" evacuation conditions (considering no wayfinding elements, so without any specified paths to be used) is influenced by the following non-dimensional parameters:

- paths geometry in terms of: $R_{W/h}$ - average W/h ratio along the path; d_s - ratio between geometric distances of shortest pedestrian's evacuation path and the considered path p;
- visible damage levels of the path in terms of: $A_{l,p}$ - ratio between the path area without debris and the total path area; L_p - ratio between p average width and the largest selectable path, by considering debris depth on them;
- social effects in terms of N_p - ratio between the number of people moving along p and the total number of visible surrounding pedestrians;
- the support of wayfinding elements (i.e.: the presence of rescuers or wayfinding signage or level of knowledge of the evacuation plan) by the term O_p (binary value: 0-no wayfinding support or 100-support presence). When no support of wayfinding elements is present in any path (i.e. in "spontaneous" conditions), $O_p=100$ for all the paths.
- level of knowledge of urban spaces, by considering M_p - memory effects on the considered path.

The evacuation direction choice is performed when the simulated individual is placed in an intersection between paths, i.e. crossroads and path plano-altimetric variations. A choice probability P_p [%] is calculated according to such parameters and expressed in percentage terms according to Equation A.5 (variable from 0% - the path will be not chosen to 100% - all the people will follow the path).

$$P_p = R_{W/h} \cdot d_s \cdot L_p \cdot A_{l,p} \cdot N_p \cdot O_p \cdot M_p \text{ [\%]} \qquad \text{(A.5)}$$

The pedestrian choice the path with the higher P_p values. Anyway, if more than one available path has the same P_p, the simulated pedestrian will randomly choose one of them. If the path from which the evacuees come from has a P_p greater than possible alternative ones, the individual can go back (for a maximum of 3 times). A stochastic error (10%) is introduced to describe behavioral differences between individuals about this selection path criteria. Finally, in simulations: $\tau_i = 0.5s$, dt=0.1s, m_i=80kg, M_p=*100* (considering people familiar with the urban layout) and attractive/repulsive forces are activated for elements within 3m of distance from the evaluated individual.

6.3 Key Performance Indicators (KPIs) definitions

In this Appendix Section the Key Performance Indicators (KPIs) introduced in Section 4.2.3 are defined to evaluate the outputs of the simulations performed in Sections 4.3.1 and 4.3.2. The following tables (i.e.: Table B 1, Table B 2 and Table B 3) provide the KPIs definitions respectively for each fundamental element of the emergency plan (i.e.: links, Assembly Areas (AA) and Spontaneous Assembly Areas (SAA)).

Table B 1. Key Performance Indicators for the link.

KPI (symbol) [unit of measurement] – KPI domain	**Computation procedure**	**Interpretation**
Link vulnerability V_{link} [-] – from 0 to 100	See Section 2.3.2	The higher V_{link}, the higher the possibility of debris generation.
Number of evacuees using a certain *link* to reach a certain AA ($N_{av,link}$) [pp] - ≥0 pp	Simulation output by tracking pedestrians' path; it is calculated as the average value for the performed simulations. It can be associated with $\%\sigma_{Nav,link}$ [%] which is the related percent standard deviation.	The higher this value, the higher the importance of the *link* in respect to the considered AA.
Link surface occupied by debris ($A_{debris,link}$) [m^2] - ≥0 m^2	Calculated according to the debris generation algorithm (see Santarelli et al. (2017))	Interferences with debris.
Effective AA surface ($A_{eff,link}$) [m^2] - ≥0 m^2	Difference between the *link* area (without considering courtyards and other not accessible areas) and $A_{debris,link}$	

Occupancy index for the given *link* (O_{link}) [-] – from 0 to 1	$O_{link} = min\left(\frac{A_{ruins,link} + N_{av,link} \cdot (1 + \%\sigma_{Nav,link}) \cdot dA_{ped,D}}{W_{link} \cdot L_{link}}; 1\right)$ where $A_{debris,link}$ [m^2] is the area of debris along the considered link (according to the debris generation algorithm Santarelli et al. (2017)) and is $dA_{ped,D}$ [m^2] the average moving pedestrian's area (fixed at 0.25 m^2) in Level of Service D conditions [115]	Describes the crowding conditions (including debris influence) by ideally considering all the pedestrians moving together.
Safety index for rescuers' access to the link of a defined access route ($S_{link,SAA}$) [-] – from 0 to 1	$S_{link,SAA} = \left(\frac{A_{debris,link}}{A_{eff,link} + A_{debris,link}}\right) \cdot \left(min\left(\frac{N_{av,link}}{\frac{A_{eff,link}}{dA_{ped,D}}}; 1\right)\right) \cdot \left(1 - \frac{pos_{link}}{n_{link,route}}\right)$ where pos_{link} is the position of the considered link inside the rescuers' path can be evaluated by considering the number $n_{link,route}$ of links composing the access path. The overall value is 1.0 for the link closer to the SAA.	The terms respectively consider: the debris influence, the evacuees' density conditions ($A_{eff,link}/dA_{ped,F}$ is the maximum reachable number of people along the link itself); the position of the link within the access path. The value can be normalized within the area $S_{link,SAA,norm}$ to define a priority list for interventions.

Table B 2. Key Performance Indicators for the AA.

KPI (symbol) [unit of measurement] – KPI domain	**Description and computation procedure**	**Interpretation**
Percentage of evacuees arrived at AA (J_{AA}) [%] – from 0% to 100%	The ratio between the total of $N_{av,link}$ and the total number of evacuees involved in the simulation	The higher this value, the higher the importance of the AA in the evacuation process, the higher the possibility to reach overcrowding conditions. Risk-reduction proposals should maximize the number of evacuees who arrived in a AA, by minimizing the number of AA to focus rescuers' actions.
Difference-in-path ratio (T) [-] – 0 to 2	Length ratio between the effective evacuation path and the ideal one; calculated as the average value for all the evacuees arrived at the AA. Values higher than 2 are arbitrarily considered equal to 2.	The higher T, the more winding is the path to reach AA, the higher the number of times in which the pedestrians change their direction (i.e. for pedestrians' and debris avoidance, for coming-and-going behaviors on the links)
Interference between evacuees moving towards the AA on the link (F_{link}) [-] – from 0 to 1	$F_{link} = \frac{N_{av,link}}{\sum_{link=1}^{n} N_{av,link}}$	it expresses the interferences between evacuees by considering how many people arrive in a certain AA by using the considered link

Safety index of a link to a AA ($S_{link,\ AA}$) [-] – from 0 to 1	Applied to a link that is placed along a rescuers' access route by multiplying O_{link} and F_{link}	It describes the possible interferences to the rescuers' access connected to evacuees and path debris interaction. The higher this value, the more sensible interferences are noticed in the link. The value can be normalized within the area $S_{link,AA,norm}$ to define a priority list for interventions.
AA surface occupied by debris (A_{debris}) [m^2] - ≥0 m^2	Calculated according to the debris generation algorithm (see Appendix D)	Interferences with debris.
Effective AA surface (A_{eff}) [m^2] - ≥0 m^2	Difference between the AA area (without considering courtyards and other not accessible areas) and A_{debris}	
Evacuation curve at the AA ([pp] versus [s])	Number of arrived people against the simulation time, through a graphical representation	Risk reduction proposals should minimize the evacuation time by maximizing evacuees' flows towards a few selected AA (i.e., increasing the curve slope).
Occupancy in the AA (LOS_{AA}) [m^2/pp] – >0 m^2/pp	The ratio between A_{eff} and the total of $N_{av,link}$; values <0.18 m^2/pp can be considered as unacceptable since they are connected to evacuees' densities > 5.3 pp/m^2 (physical contacts)	Risk reduction proposals should allow actions for areas management (i.e.: localization, evacuees' wayfinding support) aimed at limit LOS_{AA}≥0.3 m^2/pp (no physical interactions between individuals)
AA safety index S_{AA} [-] – from 0 to 1.73	$S_{AA} = \sqrt{J_{p,s}{}^2 + (T-1)^2 + \left(\sum_{link=1}^{n} S_{link,AA}\right)^2}$	It describes the safety of AA due to the number of arrived people and their interference in motion along the used *links*.

Table B 3. Key Performance Indicators for the SAA.

KPI (symbol) [unit of measurement] – KPI domain	**Description and computation procedure**	**Interpretation**
Percentage of evacuees spontaneously gathering in a SAA (J_{SAA}) [%] – from 0% to 100%	The ratio between the total of simulated individuals gathering near the same urban fabric area and the total number of evacuees not arrived in an assembly area. Since an error in path choice is introduced (10%) and simulation output differences could exist and be ≤10%, it is proposed that SAA are considered as effective if they collect at least the 5% of not arrived people to AAs	The higher this value, the higher the importance of the SAA in the evacuation process. Hence, significant SAA could be turned into AA and the number of evacuees who arrived in a AA should be maximized.
SAA surface occupied by debris ($A_{debris,SAA}$) [m^2] - ≥0 m^2	Calculated according to the debris generation algorithm (see Santarelli et al. (2017))	Interference with debris by including data on each facing building
Effective SAA surface ($A_{eff,SAA}$) [m^2] - ≥0 m^2	Difference between the SAA area (without considering courtyards and other not accessible areas) and $A_{debris,SAA}$	

Debris occupancy ($R_{b,SAA}$) [-] – from 0 to 1	$R_{b,SAA} = \sum_b \left(\frac{\frac{W_{SAA}}{2}}{W_{center,b}} \cdot \frac{d_{debris,b}}{W_{center,b}} \right)$ where b is the considered building facing the SAA, W_{SAA} [m] is the SAA width, $W_{center,b}$ [m] is the distance from the geometrical SAA center and the interfering building side, and $d_{debris,b}$ [m] is the debris average depth for the considered building	
SAA intrisic safety ($S_{area,SAA}$) [-] – from 0 to 1	$S_{area,SAA} = R_{b,SAA} \cdot \left(min \left(\frac{\frac{N_{av,SAA}}{A_{eff,SAA}}}{dA_{ped,D}}; 1 \right) \right) \cdot \left(\frac{1}{n_{acc}} \right)$ where n_{acc} [-] is the number of possible accesses to SAA (4 for a four roads crossroad and wide squares; 2 along a street; 1 for blind alley)	Data related to the SAA itself affect the possibility to wait in that SAA in safe conditions considering geometry versus damages and hosted individuals' density, and the possibility of access to the area. The higher the value, the more "dangerous" conditions can be noticed for the hosted evacuating pedestrians.

Safety index for rescuers' access route $S_{route,SAA}$ [-] – from 0 to 1	$S_{route,SAA} = \frac{\left(\sum_{n_{link}=1}^{n_{link}} S_{link,SAA}\right)}{n_{link}}$ where n_{link} represents the number of links composing the rescuers' access route.	The index considers all the number of links that compose the rescuers' access path. The higher the value, the more "dangerous" conditions for rescuers' access.
SAA safety index S_{SAA} [-] – from 0 to 1.73	$S_{SAA} = \sqrt{{J_{p,s}}^2 + {S_{path,SAA}}^2 + {S_{area,SAA}}^2}$	It describes the safety of SAA due to the number of arrived people; the access route conditions and the SAA conditions for evacuees' staying. The value can be normalized within the area S_{SAA} to define a priority list for interventions.

7 References

[1] P. Anbazhagan, S. Srinivas, D. Chandran, Classification of road damage due to earthquakes, Nat. Hazards. 60 (2012) 425–460. doi:10.1007/s11069-011-0025-0.

[2] R. Ferlito, A.G. Pizza, Modello di vulnerabilità di un centro urbano. Metodologia per la valutazione speditiva della vulnerabilità della viabilità d'emergenza, Ing. Sismica. 28 (2011) 31–49.

[3] S. Lagomarsino, S. Giovinazzi, Macroseismic and mechanical models for the vulnerability and damage assessment of current buildings, Bull. Earthq. Eng. 4 (2006) 415–443. doi:10.1007/s10518-006-9024-z.

[4] S. Santarelli, G. Bernardini, E. Quagliarini, M. D'Orazio, New indices for the existing city-centers streets network reliability and availability assessment in earthquake emergency, Int. J. Archit. Herit. 12 (2018) 153–168. doi:10.1080/15583058.2017.1328543.

[5] T.M. Ferreira, R. Vicente, H. Varum, R. Vicentea, H. Varum, Seismic vulnerability assessment of masonry facade walls: development, application and validation of a new scoring method, Struct. Eng. Mech. 50 (2014) 541–561. doi:10.12989/sem.2014.50.4.541.

[6] M. D'Orazio, E. Quagliarini, G. Bernardini, L. Spalazzi, EPES - Earthquake pedestrians' evacuation simulator: A tool for predicting earthquake pedestrians' evacuation in urban outdoor scenarios, Int. J. Disaster Risk Reduct. 10 (2014) 153–177. doi:10.1016/j.ijdrr.2014.08.002.

[7] G. Grünthal, European Macroseismic Scale 1998, 1998.

[8] M. Dilley, R.S. Chen, U. Deichmann, A.L. Lerner-Lam, M. Arnold, J. Agwe, P. Buys, O. Kjekstad, B. Lyon, Y. Gregory, Natural Disaster Hotspots A Global Risk, 2005. doi:10.1080/01944360902967228.

[9] P. Mouroux, B. Le Brun, B. Le Brun, Presentation of RISK-UE Project, Bull. Earthq. Eng. 4 (2006) 323–339. doi:10.1007/s10518-006-9020-3.

[10] A. D'Andrea, S. Cafiso, A. Condorelli, Methodological Considerations for the Evaluation of Seismic Risk on Road Network, Pure Appl. Geophys. 162 (2005) 767–782. doi:10.1007/s00024-004-2640-0.

[11] M. Pelling, The Vulnerability of Cities: Natural Disasters and Social Resilience, 2003. doi:10.1039/J19660001254.

[12] S. Lagomarsino, S. Podestà, S. Resemini, Observational and Mechanical Models for the Vulnerability Assessment of Monumental Buildings, Conf. World Vancouver,

Earthq. Eng. August, Canada. (2004).

[13] A. Formisano, N. Chieffo, M. Mosoarca, Seismic Vulnerability and Damage Speedy Estimation of an Urban Sector within the Municipality of San Potito Sannitico (Caserta, Italy), Open Civ. Eng. J. 11 (2017) 1106–1121. doi:10.2174/1874149501711011106.

[14] J.C. Villagràn De León, Vulnerability: A conceptual and methodological review, 2006.

[15] R.J. Delfino, T. Tjoa, D.L. Gillen, N. Staimer, A. Polidori, M. Arhami, L. Jamner, C. Sioutas, J. Longhurst, Traffic-related air pollution and blood pressure in elderly subjects with coronary artery disease, Epidemiology. 21 (2010) 396–404. doi:10.1097/EDE.0b013e3181d5e19b.

[16] M.W. Barrow, K.A. Clark, Heat-related illnesses, Am. Fam. Physician. 58 (1998) 749.

[17] E.E. Koks, B. Jongman, T.G. Husby, W.J.W. Botzen, Combining hazard, exposure and social vulnerability to provide lessons for flood risk management, Environ. Sci. Policy. 47 (2015) 42–52. doi:10.1016/j.envsci.2014.10.013.

[18] O.D. Cardona, M.K. Van Aalst, J. Birkmann, M. Fordham, G. Mc Gregor, P. Rosa, R.S. Pulwarty, E.L.F. Schipper, B.T. Sinh, H. Décamps, M. Keim, I. Davis, K.L. Ebi, A. Lavell, R. Mechler, V. Murray, M. Pelling, J. Pohl, A.O. Smith, F. Thomalla, Determinants of risk: Exposure and vulnerability, Manag. Risks Extrem. Events Disasters to Adv. Clim. Chang. Adapt. Spec. Rep. Intergov. Panel Clim. Chang. 9781107025 (2012) 65–108. doi:10.1017/CBO9781139177245.005.

[19] H.Y. Liu, K.C. Lauta, M.M. Maas, Governing Boring Apocalypses: A new typology of existential vulnerabilities and exposures for existential risk research, Futures. 102 (2018) 6–19. doi:10.1016/j.futures.2018.04.009.

[20] P.A. Wardhani, UNISDR Science and Technology Conference on the implementation of the Sendai Framework for Disaster Risk Reduction, Efikasi Diri Dan Pemahaman Konsep IPA Dengan Has. Belajar Ilmu Pengetah. Alam Siswa Sekol. Dasar Negeri Kota Bengkulu. 6 (2015) 1–5. doi:10.1017/CBO9781107415324.004.

[21] J. Teles, C. Mayhorn, F. Rebelo, E. Vilar, P. Noriega, The influence of environmental features on route selection in an emergency situation, Appl. Ergon. 44 (2013) 618–627. doi:10.1016/j.apergo.2012.12.002.

[22] J. Lin, R. Zhu, N. Li, B. Becerik-Gerber, How occupants respond to building emergencies: A systematic review of behavioral characteristics and behavioral theories, Saf. Sci. 122 (2020) 104540. doi:10.1016/j.ssci.2019.104540.

[23] G. Bernardini, E. Quagliarini, M. D'Orazio, Towards creating a combined database for earthquake pedestrians' evacuation models, Saf. Sci. 82 (2016) 77–94.

doi:10.1016/j.ssci.2015.09.001.

[24] C. Şahin, J. Rokne, R. Alhajj, Human behavior modeling for simulating evacuation of buildings during emergencies, Phys. A Stat. Mech. Its Appl. 528 (2019) 121432. doi:10.1016/j.physa.2019.121432.

[25] Y. Li, M. Chen, Z. Dou, X. Zheng, Y. Cheng, A. Mebarki, A review of cellular automata models for crowd evacuation, Phys. A Stat. Mech. Its Appl. 526 (2019) 120752. doi:10.1016/j.physa.2019.03.117.

[26] M.M. Sarabia, A. Kägi, A.C. Davison, N. Banwell, C. Montes, C. Aebischer, S. Hostettler, The challenges of impact evaluation: Attempting to measure the effectiveness of community-based disaster risk management, Int. J. Disaster Risk Reduct. (2020) 101732. doi:10.1016/j.ijdrr.2020.101732.

[27] T. Moore, BIP 2034:2008 - Disaster and Emergency Management Systems, British Standards Institution, London, UK, 2008.

[28] G. Bernardini, M. D'Orazio, E. Quagliarini, Towards a "behavioural design" approach for seismic risk reduction strategies of buildings and their environment, Saf. Sci. 86 (2016) 273–294. doi:10.1016/j.ssci.2016.03.010.

[29] A. Zlateski, M. Lucesoli, G. Bernardini, T.M. Ferreira, Integrating human behaviour and building vulnerability for the assessment and mitigation of seismic risk in historic centres: Proposal of a holistic human-centred simulation-based approach, Int. J. Disaster Risk Reduct. 43 (2019) 101392. doi:10.1016/j.ijdrr.2019.101392.

[30] M. Dolce, E. Speranza, F. Bocchi, C. Conte, Probabilistic assessment of structural operational efficiency in emergency limit conditions: the I.OPà.CLE method, Bull. Earthq. Eng. (2018). doi:10.1007/s10518-018-0327-7.

[31] E. Ronchi, D. Nilsson, Modelling total evacuation strategies for high-rise buildings, Build. Simul. 7 (2014) 73–87. doi:10.1007/s12273-013-0132-9.

[32] C. Casareale, G. Bernardini, A. Bartolucci, F. Marincioni, M. D'Orazio, Cruise ships like buildings: Wayfinding solutions to improve emergency evacuation, Build. Simul. 10 (2017) 989–1003. doi:10.1007/s12273-017-0381-0.

[33] W. O'Brien, I. Gaetani, S. Carlucci, P.-J. Hoes, J.L.M. Hensen, On occupant-centric building performance metrics, Build. Environ. 122 (2017) 373–385. doi:10.1016/j.buildenv.2017.06.028.

[34] B. Dong, D. Yan, Z. Li, Y. Jin, X. Feng, H. Fontenot, Modeling occupancy and behavior for better building design and operation—A critical review, Build. Simul. 11 (2018) 899–921. doi:10.1007/s12273-018-0452-x.

[35] F. Giuliani, A. De Falco, V. Cutini, The role of urban configuration during disasters. A scenario-based methodology for the post-earthquake emergency management of Italian historic centres, Saf. Sci. 127 (2020) 104700. doi:10.1016/j.ssci.2020.104700.

[36] S. Lagomarsino, S. Podestà, Analisi di vulnerabilità e rischio sismico degli edifici monumentali, (2002).

[37] S.R. Shrestha, R. Sliuzas, M. Kuffer, Open spaces and risk perception in post-earthquake Kathmandu city, Appl. Geogr. 93 (2018) 81–91. doi:10.1016/J.APGEOG.2018.02.016.

[38] M.B. Rojo, E. Beck, C. Lutoff, The street as an area of human exposure in an earthquake aftermath: the case of Lorca, Spain, 2011, Nat. Hazards Earth Syst. Sci. 17 (2017) 581–594. doi:10.5194/nhess-17-581-2017.

[39] E. Quagliarini, G. Bernardini, S. Santarelli, M. Lucesoli, Evacuation paths in historic city centres: a holistic methodology for assessing their seismic risk, Int. J. Disaster Risk Reduct. (2018). doi:10.1016/j.ijdrr.2018.07.010.

[40] E.L. French, S.J. Birchall, K. Landman, R.D. Brown, Designing public open space to support seismic resilience: A systematic review, Int. J. Disaster Risk Reduct. 34 (2019) 1–10. doi:10.1016/j.ijdrr.2018.11.001.

[41] M. Boukri, M.N. Farsi, A. Mebarki, M. Belazougui, M. Ait-Belkacem, N. Yousfi, N. Guessoum, D.A. Benamar, M. Naili, N. Mezouar, O. Amellal, Seismic vulnerability assessment at urban scale: Case of Algerian buildings, Int. J. Disaster Risk Reduct. 31 (2018) 555–575. doi:10.1016/j.ijdrr.2018.06.014.

[42] Z. Cagnan, M.B. Demircioglu, E. Durukal, M. Erdik, U. Hancilar, E. Harmandar, K. Sesetyan, C. Tuzun, C. Yenidogan, A.C. Zulfikar, Development of ELER (Earthquake Loss Estimation Routine) Methodology: Vulnerability Relationships, 2010.

[43] A. Preciado, A. Ramirez-Gaytan, R.A. Salido-Ruiz, J.L. Caro-Becerra, R. Lujan-Godinez, Earthquake risk assessment methods of unreinforced masonry structures: Hazard and vulnerability, Earthquakes Struct. 9 (2015) 719–733. doi:10.12989/eas.2015.9.4.719.

[44] T. Ferreira, R. Vicente, H. Varum, Seismic Vulnerability Assessment of Masonry Facade Walls, in: 14th Eur. Conf. Earthq. Eng., 2010: p. 583.

[45] A. Formisano, G. Florio, R. Landolfo, F.M. Mazzolani, Numerical calibration of an easy method for seismic behaviour assessment on large scale of masonry building aggregates, Adv. Eng. Softw. 80 (2015) 116–138. doi:10.1016/j.advengsoft.2014.09.013.

[46] E. Quagliarini, M. Lucesoli, G. Bernardini, Rapid tools for assessing building heritage's seismic vulnerability: a preliminary reliability analysis, J. Cult. Herit. (2019). doi:10.1016/j.culher.2019.03.008.

[47] J.J. Wang, Flood risk maps to cultural heritage: Measures and process, J. Cult. Herit. 16 (2015) 210–220. doi:10.1016/j.culher.2014.03.002.

[48] Italian technical commission for seismic micro-zoning, Handbook of analysis of emergency conditions in urban scenarios (Manuale per l'analisi della condizione limite dell'emergenza dell'insediamento urbano (CLE)), (2014).

[49] M.A. Zanini, F. Faleschini, P. Zampieri, C. Pellegrino, G. Gecchele, M. Gastaldi, R. Rossi, Post-quake urban road network functionality assessment for seismic emergency management in historical centres, Struct. Infrastruct. Eng. 13 (2016) 1117–1129. doi:10.1080/15732479.2016.1244211.

[50] G. Caiado, C. Oliveira, F. Sá, Assessing Urban Road Network Seismic Vulnerability : An Integrated Approach, in: Proc. Of15th WCEE, Lisboa, 2012.

[51] E. Quagliarini, G. Bernardini, C. Wazinski, L. Spalazzi, M. D'Orazio, Urban scenarios modifications due to the earthquake: ruins formation criteria and interactions with pedestrians' evacuation, Bull. Earthq. Eng. 14 (2016) 1071–1101. doi:10.1007/s10518-016-9872-0.

[52] A. Goretti, V. Sarli, Road Network and Damaged Buildings in Urban Areas: Short and Long-term Interaction, Bull. Earthq. Eng. 4 (2006) 159–175. doi:10.1007/s10518-006-9004-3.

[53] S. Adafer, M. Bensaibi, Seismic Vulnerability Index for Road Networks, in: Proc. 2015 Int. Conf. Ind. Technol. Manag. Sci., Atlantis Press, Paris, France, 2015. doi:10.2991/itms-15.2015.301.

[54] L. Xinpo, H. Siming, Seismically induced slope instabilities and the corresponding treatments: The case of a road in the Wenchuan earthquake hit region, J. Mt. Sci. 6 (2009) 96–100. doi:10.1007/s11629-009-0197-1.

[55] G. Tesoriere, G. Marinella, M. Russello, Analisi della Vulnerabilità delle Reti Stradali in Aree Soggette a Rischio Sismico, in: XI S.I.I.V, 2001: p. 12.

[56] F.T. Gizzi, N. Masini, Historical damage pattern and differential seismic effects in a town with ground cavities: A case study from Southern Italy, Eng. Geol. 88 (2006) 41–58. doi:10.1016/j.enggeo.2006.08.001.

[57] J. Coutinho-Rodrigues, N. Sousa, E. Natividade-Jesus, Design of evacuation plans for densely urbanised city centres, Proc. Inst. Civ. Eng. Eng. 169 (2015) 1–13. doi:10.1680/jmuen.15.00005.

[58] A. Cherubini, Progetto: SAVE - Strumenti Aggiornati per la Vulnerabilità sismica del patrimonio Edilizio e dei sistemi urbani, TASK 4 - Cap 2. (2003).

[59] G.M. Calvi, R. Pinho, G. Magenes, J.J. Bommer, H. Crowley, Development of seismic vulnerability assessment methodologies over the past 30 years, ISET J. {…}. 43 (2006) 75–104.

[60] E. Foerster, Y. Krien, S. Priest, S. Tapsell, G. Delmonaco, C. Margottini, C. Bonadonna, WP 1: State-of-the art on vulnerability types. Methodologies to assess

vulnerability of structural systems, (2009) 1–139. http://www.ensureproject.eu/ENSURE_Del1.1.1.pdf.

[61] A. Masi, Seismic vulnerability assessment of gravity load designed R/C frames, Bull. Earthq. Eng. 1 (2003) 371–395. doi:10.1023/B:BEEE.0000021426.31223.60.

[62] N. Khademi, B. Balaei, M. Shahri, M. Mirzaei, B. Sarrafi, M. Zahabiun, A.S. Mohaymany, Transportation network vulnerability analysis for the case of a catastrophic earthquake, Int. J. Disaster Risk Reduct. 12 (2015). doi:10.1016/j.ijdrr.2015.01.009.

[63] M.A. Zanini, F. Faleschini, C. Pellegrino, Probabilistic seismic risk forecasting of aging bridge networks, Eng. Struct. 136 (2017) 219–232. doi:10.1016/j.engstruct.2017.01.029.

[64] K. Pitilakis, H. Crowley, A.M. Kaynia, SYNER-G: Typology definition and fragility functions for physical elements at seismic risk, buildings, lifelines, transportation networks and critical facilities, Geotech., Springer Netherlands, 2014.

[65] A.M. Kaynia, Guidelines for deriving seismic fragility functions of elements at risk: Buildings, lifelines, transportation networks and critical facilities, SYNER-G Reference Report 4, 2013. doi:10.2788/19605.

[66] M. Dolce, E. Speranza, F. Bocchi, C. Conte, Probabilistic assessment of structural operational efficiency in emergency limit conditions: the I.OPà.CLE method, Bull. Earthq. Eng. 16 (2018) 3791–3818. doi:10.1007/s10518-018-0327-7.

[67] J.L.P. Aguado, T.M. Ferreira, P.B. Lourenço, The Use of a Large-Scale Seismic Vulnerability Assessment Approach for Masonry Façade Walls as an Effective Tool for Evaluating, Managing and Mitigating Seismic Risk in Historical Centers, Int. J. Archit. Herit. (2018) 1–17. doi:10.1080/15583058.2018.1503366.

[68] G. Bernardini, M. Lucesoli, E. Quagliarini, Sustainable planning of seismic emergency in historic centres through semeiotic tools: comparison of different existing methods through real case studies, Sustain. Cities Soc. SCS_101834 (2019) in press. doi:10.1016/j.scs.2019.101834.

[69] F. Giuliani, A. De Falco, G. Sevieri, Managing emergency into historic centres in Italy: seismic vulnerability evaluation at urban scale, 7th ECCOMAS Themat. Conf. Comput. Methods Struct. Dyn. Earthq. Eng. (2019).

[70] S. Santarelli, G. Bernardini, E. Quagliarini, Earthquake building debris estimation in historic city centres: From real world data to experimental-based criteria, Int. J. Disaster Risk Reduct. 31 (2018) 281–291. doi:10.1016/j.ijdrr.2018.05.017.

[71] M. Francini, S. Artese, S. Gaudio, A. Palermo, M.F. Viapiana, To support urban emergency planning: A GIS instrument for the choice of optimal routes based on seismic hazards, Int. J. Disaster Risk Reduct. 31 (2018) 121–134. doi:10.1016/j.ijdrr.2018.04.020.

[72] S. Artese, V. Achilli, A gis tool for the management of seismic emergencies in historical centers: How to choose the optimal routes for civil protection interventions, ISPRS Ann. Photogramm. Remote Sens. Spat. Inf. Sci. 42 (2019) 99–106. doi:10.5194/isprs-Archives-XLII-2-W11-99-2019.

[73] S. Argyroudis, J. Selva, P. Gehl, K. Pitilakis, Systemic Seismic Risk Assessment of Road Networks Considering Interactions with the Built Environment, Comput. Civ. Infrastruct. Eng. 30 (2015) 524–540. doi:10.1111/mice.12136.

[74] M. Fox, S. Goodhew, P. De Wilde, Building defect detection: External versus internal thermography, Build. Environ. 105 (2016) 317–331. doi:10.1016/j.buildenv.2016.06.011.

[75] D. Roca, S. Lagüela, L. Díaz-Vilariño, J. Armesto, P. Arias, Low-cost aerial unit for outdoor inspection of building façades, Autom. Constr. 36 (2013) 128–135. doi:10.1016/j.autcon.2013.08.020.

[76] V. Baiocchi, V. Giammarresi, R. Ialongo, C. Piccaro, M. Allegra, D. Dominicic, The survey of the basilica di collemaggio in L'Aquila with a system of terrestrial imaging and most proven techniques, Eur. J. Remote Sens. 50 (2017) 237–253. doi:10.1080/22797254.2017.1316523.

[77] T.M. Ferreira, R. Maio, A.A. Costa, R. Vicente, Seismic vulnerability assessment of stone masonry façade walls: Calibration using fragility-based results and observed damage, Soil Dyn. Earthq. Eng. 103 (2017) 21–37. doi:10.1016/j.soildyn.2017.09.006.

[78] P. Mazzotti, Valutazione speditiva della vulnerabilità dell'aggregato. In: Prevenzione del rischio sismico nei Centri Storici marchigiani: il caso di studio di Offida (AP)., Ancona, Italy: Regione Marche Servizio Cultura, Turismo e Commercio P.F. "Beni culturali e Programmi di Recupero"- Dipartimento per le politiche integrate di sicurezza e per la protezione civile S.I.S.M.A. System Integrated for Security Management Activit, 2008.

[79] J. Lee Rodgers, W. Alan Nice Wander, Thirteen ways to look at the correlation coefficient, Am. Stat. 42 (1988) 59–66. doi:10.1080/00031305.1988.10475524.

[80] R.R. Pagano, Understanding Statistics in the Behavioral Sciences, Cengage Learning, 2012. https://books.google.it/books?id=SqecbrxfQwwC.

[81] G. Bernardini, S. Santarelli, E. Quagliarini, M. D'Orazio, Dynamic guidance tool for a safer earthquake pedestrian evacuation in urban systems, Comput. Environ. Urban Syst. 65 (2017) 150–161. doi:10.1016/j.compenvurbsys.2017.07.001.

[82] T.L. Saaty, The Analytic Hierarchy Process: Planning, Priority Setting, Resource Allocation, McGraw-Hill, 1980. https://books.google.it/books?id=Xxi7AAAAIAAJ.

[83] A. Galanis, G. Botzoris, N. Eliou, Pedestrian road safety in relation to urban road

type and traffic flow, Transp. Res. Procedia. 24 (2017) 220–227. doi:10.1016/j.trpro.2017.05.111.

[84] S. Menoni, F. Pergalani, M.P. Boni, V. Petrini, Lifelines earthquake vulnerability assessment: a systemic approach, Soil Dyn. Earthq. Eng. 22 (2002) 1199–1208. doi:10.1016/S0267-7261(02)00148-3.

[85] J. Azevedo, L. Guerreiro, R. Bento, J.M. Proenca, Seismic Impact on lifelines in the great Lisbon area, (2004).

[86] K. Pitilakis, M. Alexoudi, S. Argyroudis, O. Monge, C. Martin, Earthquake risk assessment of lifelines, Bull. Earthq. Eng. 4 (2006) 365–390. doi:10.1007/s10518-006-9022-1.

[87] European Commitee for Standardization, Eurocode 8: Design of structures for earthquake resistance - Part 1 : General rules, seismic actions and rules for buildings, Eur. Comm. Stand. 1 (2004) 231. doi:[Authority: The European Union per Regulation 305/2011, Directive 98/34/EC, Directive 2004/18/EC].

[88] Italian Ministry of Infrastructure and Transport, NTC 2008 - Italian Building Code. D.M. 14/01/2008, (2008). doi:10.1515/9783110247190.153.

[89] F. Bramerini, G. di Pasquale, G. Naso, M. Severino, Indirizzi per la microzinazione sismica, Parti I e II, Conf. Delle Reg. e Prov. Auton. Della Prot. Civile, Roma. 3 (2008).

[90] T. Kalman Šipoš, M. Hadzima-Nyarko, Rapid seismic risk assessment, Int. J. Disaster Risk Reduct. 24 (2017) 348–360. doi:10.1016/j.ijdrr.2017.06.025.

[91] K.J. Wilson, An investigation of dependence in expert judgement studies with multiple experts, Int. J. Forecast. 33 (2017) 325–336. doi:10.1016/j.ijforecast.2015.11.014.

[92] S. Adafer, M. Bensaibi, Seismic vulnerability classification of roads, Energy Procedia. 139 (2017) 624–630. doi:10.1016/j.egypro.2017.11.263.

[93] D. Alder, C.J.F.P. Jones, J. Lamont-Black, C. White, S. Glendinning, D. Huntley, Design principles and construction insight regarding the use of electrokinetic techniques for slope stabilisation, Proc. XVI ECSMGE. (2015) 1531–1536. doi:10.1680/ecsmge.60678.

[94] E. Anglade, A.M. Giatreli, A. Blyth, B. Di Napoli, F. Parisse, Z. Namourah, H. Rodrigues, T.M. Ferreira, Seismic damage scenarios for the Historic City Center of Leiria, Portugal: Analysis of the impact of different seismic retrofitting strategies on emergency planning, Int. J. Disaster Risk Reduct. 44 (2020) 101432. doi:10.1016/j.ijdrr.2019.101432.

[95] R. Hassanzadeh, Earthquake population loss estimation using spatial modelling and survey data: The Bam earthquake, 2003, Iran, Soil Dyn. Earthq. Eng. 116 (2019)

421–435. doi:10.1016/j.soildyn.2018.09.023.

[96] R. Lovreglio, V. Gonzalez, Z. Feng, R. Amor, M. Spearpoint, J. Thomas, M. Trotter, R. Sacks, Prototyping virtual reality serious games for building earthquake preparedness: The Auckland City Hospital case study, Adv. Eng. Informatics. 38 (2018) 670–682. doi:10.1016/j.aei.2018.08.018.

[97] G. Bernardini, R. Lovreglio, E. Quagliarini, Proposing behavior-oriented strategies for earthquake emergency evacuation: A behavioral data analysis from New Zealand, Italy and Japan, Saf. Sci. 116 (2019) 295–309. doi:10.1016/j.ssci.2019.03.023.

[98] PreventionWeb - UNDRR, https://www.preventionweb.net/terminology#D, (n.d.).

[99] X. Yang, Z. Wu, Y. Li, Difference between real-life escape panic and mimic exercises in simulated situation with implications to the statistical physics models of emergency evacuation: The 2008 Wenchuan earthquake, Phys. A Stat. Mech. Its Appl. 390 (2011) 2375–2380. doi:10.1016/j.physa.2010.10.019.

[100] E. Quagliarini, M. Lucesoli, G. Bernardini, Understanding Human Behaviors in Earthquakes to Improve Safety in Built Environment: A State of the Art on Sustainable and Validated Investigation Tools, in: J. Littlewood, R.J. Howlett, L.C. Jain (Eds.), Sustain. Energy Build. 2020, Springer Singapore, Singapore, 2021: pp. 297–307.

[101] J. Zhou, S. Li, G. Nie, X. Fan, J. Tan, L. Meng, C. Xia, Q. Zhou, Research on earthquake emergency response modes of individuals based on social surveillance video, Int. J. Disaster Risk Reduct. 28 (2018) 350–362. doi:10.1016/j.ijdrr.2018.03.015.

[102] N. Shiwakoti, Understanding differences in emergency escape and experimental pedestrian crowd egress through quantitative comparison, Int. J. Disaster Risk Reduct. 20 (2016) 129–137. doi:10.1016/j.ijdrr.2016.11.002.

[103] S. Li, X. Yu, Y. Zhang, C. Zhai, A numerical simulation strategy on occupant evacuation behaviors and casualty prediction in a building during earthquakes, Phys. A Stat. Mech. Its Appl. 490 (2018) 1238–1250. doi:10.1016/j.physa.2017.08.058.

[104] Sukirman, R.A. Wibisono, Sujalwo, Self-evacuation drills by mobile virtual reality application to enhance earthquake preparedness, Procedia Comput. Sci. 157 (2019) 247–254. doi:10.1016/j.procs.2019.08.164.

[105] L. Chittaro, R. Sioni, Serious games for emergency preparedness: Evaluation of an interactive vs. a non-interactive simulation of a terror attack, Comput. Human Behav. 50 (2015) 508–519. doi:10.1016/j.chb.2015.03.074.

[106] M. Moussaïd, V.R. Schinazi, M. Kapadia, T. Thrash, Virtual sensing and virtual reality: How new technologies can boost research on crowd dynamics, Front. Robot. AI. 5 (2018) 1–14. doi:10.3389/frobt.2018.00082.

[107] M. D'Orazio, L. Spalazzi, E. Quagliarini, G. Bernardini, M. D'Orazio, L. Spalazzi, E. Quagliarini, G. Bernardini, Agent-based model for earthquake pedestrians' evacuation in urban outdoor scenarios: Behavioural patterns definition and evacuation paths choice, Saf. Sci. 62 (2014) 450–465. doi:10.1016/j.ssci.2013.09.014.

[108] H. Zhang, H. Liu, X. Qin, B. Liu, Modified two-layer social force model for emergency earthquake evacuation, Phys. A Stat. Mech. Its Appl. 492 (2018) 1107–1119. doi:10.1016/j.physa.2017.11.041.

[109] M. Li, Y. Zhao, L. He, W. Chen, X. Xu, The parameter calibration and optimization of social force model for the real-life 2013 Ya'an earthquake evacuation in China, Saf. Sci. 79 (2015) 243–253. doi:10.1016/j.ssci.2015.06.018.

[110] S. Shapira, L. Aharonson-Daniel, I.M. Shohet, C. Peek-Asa, Y. Bar-Dayan, Integrating epidemiological and engineering approaches in the assessment of human casualties in earthquakes, Nat. Hazards. 78 (2015) 1447–1462. doi:10.1007/s11069-015-1780-0.

[111] N. Emori, T. Izumi, Y. Nakatani, A Support System for Developing Tourist Evacuation Guidance, in: H.K. Kim, M.A. Amouzegar, S. Ao (Eds.), Trans. Eng. Technol., Springer Singapore, Singapore, 2016: pp. 15–28. doi:10.1007/978-981-10-0551-0_2.

[112] M. Haghani, M. Sarvi, Crowd behaviour and motion: Empirical methods, Transp. Res. Part B Methodol. 107 (2018) 253–294. doi:10.1016/j.trb.2017.06.017.

[113] Federal Emergency Management Agency (FEMA), Developing and maintaining emergency operations plans, Compr. Prep. Guid. 101. (2010) 1–124. papers2://publication/uuid/AAE7FC8F-3336-4DE7-ABD8-8CAA6137703D.

[114] M. Mori, H. Tsukaguchi, A new method for evaluation of level of service in pedestrian facilities, Transp. Res. 21A(3) (1987) 223–234.

[115] T. Klüpfel, H. Meyer-König, PedGo Guardian: an assistant for evacuation decision making, in: U. Weidmann, U. Kirsch, M. Schreckenberg (Eds.), Pedestr. Evacuation Dyn. 2012, Springer International Publishing, 2014: pp. 445–454.

[116] G. Bernardini, E. Quagliarini, M. D'Orazio, STRUMENTI PER LA GESTIONE DELL'EMERGENZA NEI CENTRI STORICI, Edicom edizioni, Monfalcone (Gorizia), 2018.

[117] G. Bernardini, M. D'Orazio, E. Quagliarini, L. Spalazzi, M. D'Orazio, E. Quagliarini, L. Spalazzi, An Agent-based Model for Earthquake Pedestrians' Evacuation Simulation in Urban Scenarios, Transp. Res. PROCEDIA. 2 (2014) 255–263. doi:10.1016/j.trpro.2014.09.050.

[118] R. Becker, Fundamentals of performance-based building design, Build. Simul. 1 (2008) 356–371. doi:10.1007/s12273-008-8527-8.

[119] T.M. Ferreira, R. Vicente, J.A. Raimundo Mendes da Silva, H. Varum, A. Costa, R. Maio, Urban fire risk: Evaluation and emergency planning, J. Cult. Herit. 20 (2016) 739–745. doi:10.1016/j.culher.2016.01.011.

[120] G. Cerè, Y. Rezgui, W. Zhao, Critical review of existing built environment resilience frameworks: Directions for future research, Int. J. Disaster Risk Reduct. 25 (2017) 173–189. doi:10.1016/j.ijdrr.2017.09.018.

[121] R. Spence, Risk and regulation: can improved government action reduce the impacts of natural disasters?, Build. Res. Inf. 32 (2004) 391–402. doi:10.1080/0961321042000221043.

[122] G. Lämmel, D. Grether, K. Nagel, The representation and implementation of time-dependent inundation in large-scale microscopic evacuation simulations, Transp. Res. Part C Emerg. Technol. 18 (2010) 84–98. doi:10.1016/j.trc.2009.04.020.

[123] S. Hubbard, K. Stewart, J. Fan, Modeling spatiotemporal patterns of building vulnerability and content evacuations before a riverine flood disaster, Appl. Geogr. 52 (2014) 172–181. doi:10.1016/j.apgeog.2014.05.006.

[124] N. Hirokawa, T. Osaragi, Earthquake disaster simulation system : Integration of models for building collapse, road blockage, and fire spread, J. Disaster Res. 11 (2016) 175–187. doi:10.20965/jdr.2016.p0175.

[125] R. Robat Mili, K. Amini Hosseini, Y.O. Izadkhah, Developing a holistic model for earthquake risk assessment and disaster management interventions in urban fabrics, Int. J. Disaster Risk Reduct. 27 (2018) 355–365. doi:10.1016/j.ijdrr.2017.10.022.

[126] T.M. Ferreira, R. Maio, R. Vicente, Analysis of the impact of large scale seismic retrofitting strategies through the application of a vulnerability-based approach on traditional masonry buildings, Earthq. Eng. Eng. Vib. 16 (2017) 329–348. doi:10.1007/s11803-017-0385-x.

[127] T.K. Egbelakin, S. Wilkinson, R. Potangaroa, J. Ingham, Challenges to successful seismic retrofit implementation: a socio-behavioural perspective, Build. Res. Inf. 39 (2011) 286–300. doi:10.1080/09613218.2011.552264.

[128] O. Filippova, Y. Xiao, M. Rehm, J. Ingham, Economic effects of regulating the seismic strengthening of older buildings, Build. Res. Inf. 46 (2018) 711–724. doi:10.1080/09613218.2017.1357318.

[129] C.-A. Tai, Y.-L. Lee, C.-Y. Lin, Urban Disaster Prevention Shelter Location and Evacuation Behavior Analysis, J. Asian Archit. Build. Eng. 9 (2010) 215–220. doi:10.3130/jaabe.9.215.

[130] A.H. Barbat, M.L. Carreno, L.G. Pujades, N. Lantada, O.D. Cardona, M.C. Marulanda, Seismic vulnerability and risk evaluation methods for urban areas. A review with application to a pilot area, Struct. Infrastruct. Eng. 6 (2010) 17–38. doi:10.1080/15732470802663763.

[131] T.M. Ferreira, A.A. Costa, A. Costa, Analysis of the Out-Of-Plane Seismic Behavior of Unreinforced Masonry: A Literature Review, Int. J. Archit. Herit. 9 (2015). doi:10.1080/15583058.2014.885996.

[132] G. Lombardo, C. Cicero, Analysis of seismic vulnerability for urban centres, Int. J. Des. Sci. Technol. 1 (2015) 39–58.

[133] A. Kimms, M. Maiwald, Bi-objective safe and resilient urban evacuation planning, Eur. J. Oper. Res. 269 (2018) 1122–1136. doi:10.1016/j.ejor.2018.02.050.

[134] D.R. Parisi, C.O. Dorso, Microscopic dynamics of pedestrian evacuation, Phys. A Stat. Mech. Its Appl. 354 (2005) 606–618. doi:10.1016/j.physa.2005.02.040.

[135] T. Oki, T. Osaragi, Urban Improvement Policies for Reducing Human Damage in a Large Earthquake by Using Wide-Area Evacuation Simulation Incorporating Rescue and Firefighting by Local Residents, in: S. Geertman, A. Allan, C. Pettit, J. Stillwell (Eds.), Plan. Support Sci. Smarter Urban Futur., Springer International Publishing, Cham, 2017: pp. 449–468. doi:10.1007/978-3-319-57819-4_25.

[136] M. Hashemi, A.A. Alesheikh, GIS: agent-based modeling and evaluation of an earthquake-stricken area with a case study in Tehran, Iran, Nat. Hazards. 69 (2013) 1–23. doi:10.1007/s11069-013-0784-x.

[137] L. Bourdic, S. Salat, C. Nowacki, Assessing cities: a new system of cross-scale spatial indicators, Build. Res. Inf. 40 (2012) 592–605. doi:10.1080/09613218.2012.703488.

[138] E.D. Kuligowski, Computer Evacuation Models for Buildings, in: SFPE Handb. Fire Prot. Eng., Springer New York, New York, NY, 2016: pp. 2152–2180. doi:10.1007/978-1-4939-2565-0_60.

[139] A. Schadschneider, W. Klingsch, H. Klüpfel, T. Kretz, C. Rogsch, A. Seyfried, Evacuation Dynamics: Empirical Results, Modeling and Applications, Encycl. Complex. Syst. Sci. (2009) 3142-3176 LA-English. doi:10.1007/978-0-387-30440-3_187.

[140] P. Thompson, D. Nilsson, K. Boyce, D. McGrath, Evacuation models are running out of time, Fire Saf. J. 78 (2015) 251–261. doi:10.1016/j.firesaf.2015.09.004.

[141] D. Helbing, A.F. Johansson, Pedestrian, Crowd and Evacuation Dynamics, Encycl. Complex. Syst. Sci. 16 (2010) 6476–6495.

[142] C.M. MacAl, M.J. North, Tutorial on agent-based modelling and simulation, J. Simul. 4 (2010) 151–162. doi:10.1057/jos.2010.3.

[143] M.-L. Xiao, Y. Chen, M.-J. Yan, L.-Y. Ye, B.-Y. Liu, Simulation of household evacuation in the 2014 Ludian earthquake, Bull. Earthq. Eng. 14 (2016) 1757–1769. doi:10.1007/s10518-016-9887-6.

[144] X. Lu, Z. Yang, G.P. Cimellaro, Z. Xu, Pedestrian evacuation simulation under the

scenario with earthquake-induced falling debris, Saf. Sci. 114 (2019) 61–71. doi:10.1016/J.SSCI.2018.12.028.

[145] T. Egbelakin, S. Wilkinson, R. Potangaroa, J. Rotimi, Stakeholders' practices: a challenge to earthquake risk mitigation decisions, Int. J. Strateg. Prop. Manag. 19 (2015) 395–408. doi:10.3846/1648715X.2015.1101029.

[146] K.A. Hosseini, M.K. Jafari, M. Hosseini, B. Mansouri, S. Hosseinioon, Development of urban planning guidelines for improving emergency response capacities in seismic areas of Iran, Disasters. 33 (2009) 645–664. doi:10.1111/j.1467-7717.2008.01092.x.

[147] R. Maio, T.M. Ferreira, R. Vicente, A critical discussion on the earthquake risk mitigation of urban cultural heritage assets, Int. J. Disaster Risk Reduct. 27 (2018) 239–247. doi:10.1016/j.ijdrr.2017.10.010.

[148] R. Vicente, T.M. Ferreira, J.A.R. Mendes da Silva, Supporting urban regeneration and building refurbishment. Strategies for building appraisal and inspection of old building stock in city centres, J. Cult. Herit. 16 (2015) 1–14. doi:10.1016/j.culher.2014.03.004.

[149] R. Vicente, S. Parodi, S. Lagomarsino, H. Varum, J.A.R. da Silva, Seismic vulnerability and risk assessment: case study of the historic city centre of Coimbra, Portugal, Bull. Earthq. Eng. 9 (2010) 1067–1096. doi:10.1007/s10518-010-9233-3.

[150] A. Campos Costa, M.L. Sousa, A. Carvalho, Seismic Zonation for Portuguese National Annex of Eurocode 8, Proc. 14th World Conf. Earthq. Eng. Beijing, China. (2008) 8–15.